Analysis of functional impairments of the human $P2Y_{11}$ nucleotide receptor with the Alanine-87-Threonine mutation, and development of novel agonists specific for the human $P2Y_{11}$ and $P2Y_6$ receptors

Dissertation

zur Erlangung des akademischen Grades

doctor rerum naturalium

(Dr. rer. nat.)

genehmigt durch die Fakultät für Naturwissenschaften

der Otto-von-Guericke-Universität Magdeburg

von Dipl.-Biol. Michael Haas

geb. am 13.12.1979 in Mittweida

Gutachter:

Prof. Dr. Georg Reiser

Prof. Dr. Günter Schmalzing

Eingereicht am: 30. September 2014

Verteidigt am: 1. Juni 2015

Danksagung

Table of content

Figures

Tables

1. Introduction

1.1 Important physiological nucleotides in human

Nucleotides fulfill a wide range of tasks in physiological processes of the human organism. They are the monomeric subunits of the nucleic acid polymers deoxyribonucleic acid (DNA) and ribonucleic acid (RNA) (Berg *et al.*, 2002). Furthermore, in biology in general ATP (adenosine 5'-triphosphate) plays a fundamental role as a main storage of chemical energy. Importantly, several types of nucleotides serve as intracellular or extracellular regulatory or signaling molecules.

Nucleotides contain purine (adenine, A; guanine, G) or pyrimidine (cytosine, C; uracil, U; thymine, T) nucleobase moieties (Figure 1). This nucleobase is bound to a pentose sugar (ribose or 2-deoxyribose) via a *N*-glycosidic linkage, thus forming a glycosylamine or a so called nucleoside. The nitrogen (N) at position 9 of a purine base and the N at position 1 of a pyrimidine base, respectively, are connected to the carbon (C) at position 1' of the pentose. A phosphate moiety (α-phosphate) is usually connected to the C5' of the sugar via an ester bond, forming a nucleotide or a nucleoside monophosphate. Additional phosphates (β, γ, ...) are bound to the α-phosphate via acid anhydride bonds.
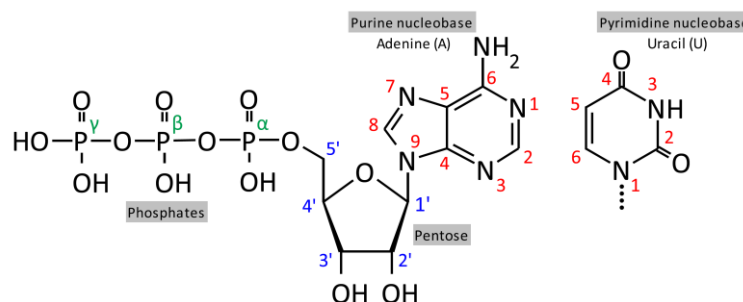
Figure 1: *Structures and nomenclature of the purine nucleotide adenosine 5'-triphosphate (ATP) and the pyrimidine nucleotide uridine 5'-triphosphate (UTP).*

Important naturally occurring nucleotides other than ATP are ADP (adenosine 5'-diphosphate), UTP (uridine 5'-triphosphate), UDP (uridine 5'-diphosphate), and UDP-sugars like UDP-glucose (Jacobson *et al.*, 2009). Also, several di-nucleotides with an interconnecting C5'-C5'' phosphate chain of varying length (n = 2-7) have been characterized: Ap$_n$A (diadenosine polyphosphates; Guzmán-Aranguez *et al.*, 2007; Carracedo *et al.*, 2013), Ap$_4$U (adenosine 5'-tetraphosphate 5''-uridine; Jankowski *et al.*, 2005) and the well-known elements of many redox reactions in cells NAD (nicotinamide adenine dinucleotide), its C2' phosphorylated form NADP, and FAD (flavin adenine dinucleotide) (Guzmán-Aranguez *et al.*, 2007).

The cyclic nucleotides cAMP (3'-5'-cyclic adenosine monophosphate) and cGMP (3'-5'-cyclic guanosine monophosphate) are well established second messengers (Sassone-Corsi, 2012; Hoffmann, 2005). They are synthesized by adenylyl cyclase (AC) and guanylyl cyclase (GC), respectively, by esterification of the 5' phosphate with the C3' of the ribose. cCMP (3'-5'-cyclic cytosine monophosphate)

and cUMP (3'-5'-cyclic uridine monophosphate) have also been indentified, but their specific roles are less well understood (Wolters *et al.*, 2011).

1.2 The human P1 and P2 nucleotide receptors

The human P1 adenosine receptor family.

      A range of nucleotide and nucleoside receptors, classified as P1 and P2 receptors, are used by cells to sense nucleotides and their metabolites. The P1 receptor family includes the four metabotropic (G protein-coupled) seven-transmembrane receptors (7TMR) A_1, A_{2A}, A_{2B}, and A_3 (Fredholm *et al.*, 2001 and 2011). All P1 receptors can be activated by adenosine, which either is a product of the extracellular hydrolysis of adenine nucleotides or is released by cells directly (King *et al.*, 2006). A_1 and A_3 receptors are coupled to G_i signaling, which results in the inhibition of ACs. Conversely, the A_{2A} and A_{2B} receptors are coupled to the G_s pathway and induce AC activation. However, coupling of P1 receptors to other G proteins has also been reported.

The human P2 nucleotide receptor family.

      The group of P2 receptors includes the P2X and P2Y receptor families. The $P2X_{1-7}$ receptors are cation channels activated by ATP. The family of P2Y receptors in human consists of eight proteins, the $P2Y_1$, $P2Y_2$, $P2Y_4$, $P2Y_6$, and $P2Y_{11-14}$ receptors. Those are mainly coupled to the G_i, G_s, and/or G_q signaling pathways and show overlapping activation patterns by adenine and uridine nucleotides (Abbrachio *et al.*, 2006). P2Y receptors are heptahelical transmembrane receptors coupled to intracellular G protein signaling. They are assigned to the δ-subfamily of the rhodopsin-related (Class A) G protein-coupled receptors (GPCRs; Ralevic *et al.*, 1998; Latek *et al.*, 2012). The seven transmembrane helices are interconnected by 3 extracellular loops (EL) and 3 cytoplasmic loops (Palczewski *et al.*, 2000). The EL and TM regions constitute the nucleotide ligand binding pocket, which faces towards the extracellular space. The N-terminus of the receptor protein is located at the extracellular side of the protein, while the C-terminus is exposed to the cytoplasm.

      The group of the eight purinergic human P2Y receptors can be divided into either adenine or uridine nucleotide-preferring receptors (Abbrachio *et al.*, 2006). While the $P2Y_1$, $P2Y_{11}$, $P2Y_{12}$, and $P2Y_{13}$ receptors belong to the adenine nucleotide-preferring group, the $P2Y_4$, $P2Y_6$, and $P2Y_{14}$ receptors can be activated by uridine nucleotides. The human $P2Y_2$ receptor equally accepts ATP and UTP. However, there are differences regarding the preference for nucleoside di- or triphosphates. At the $P2Y_1$ receptor, ADP shows greater potency than ATP. On the other hand, the $P2Y_{11}$ receptor prefers ATP over ADP. Both the $P2Y_2$ and $P2Y_4$ receptors are UTP-preferring receptors, while the $P2Y_6$ receptor is selective for UDP. The $P2Y_{12}$ and $P2Y_{13}$ receptors are selective for ADP, and the $P2Y_{14}$ receptor can be activated by UDP and UDP-glucose (Chambers *et al.*, 2000; Carter *et al.*, 2009).

P2Y receptor-mediated intracellular signaling.

      The classification of P2Y receptors based on ligand preferences offers a convenient way to discriminate individual receptors. However, this does not reflect the phylogenetic relationship of two distinct phylogenetic branches (Constanzi *et al.*, 2004). The $P2Y_1$, $P2Y_2$, $P2Y_4$, $P2Y_6$, and $P2Y_{11}$ receptors represent one branch, activating the G_q/G_{11} signaling pathway. The $P2Y_{12}$, $P2Y_{13}$, and $P2Y_{14}$ receptors in the second phylogenetic branch are coupled to the G_i pathway. The $P2Y_2$ and $P2Y_4$ receptors were found to be additionally linked to G_i signaling (Murthy *et al.*, 1998; Communi *et al.*, 1996).

The activation of the G_q pathway leads to activation of phospholipase C (PLC) and consequently to the production of the soluble inositol 1,4,5-trisphosphate (IP_3). This eventually triggers the elevation of the intracellular Ca^{2+} concentration ($[Ca^{2+}]_i$) via Ca^{2+} release from intracellular stores. At the same time, the membrane-bound second messenger diacylglycerol is generated and activates protein kinase C (PKC).

The activation of the G_i signaling pathway leads to the inhibition of AC, thus the inhibition of cAMP synthesis. The $P2Y_{11}$ receptor is the only P2Y receptor, which triggers the G_s signal transduction pathway and therefore the activation of AC. cAMP subsequently activates the cAMP-dependent protein kinases (protein kinase A; PKA) which in turn can phosphorylate a wide range of target proteins. Another way of P2Y receptor signaling works via β-arrestin recruitment following the phosphorylation of the receptor by G protein-coupled receptor kinases (GRKs). These steps mediate the nucleotide-induced P2Y receptor internalization (Hoffman *et al.*, 2008b). Additionally, β-arrestin recruitment can facilitate signaling via mitogen-activated protein kinases (MAPK) and other intracellular pathways (Ferguson 2001; Lefkowitz *et al.*, 2005). The translocation of β-arrestin1 or β-arrestin2 to the plasma membrane upon P2Y receptor activation defines whether a rapid receptor recycling to the cell surface takes place, or the receptor is recycled only slowly, or even degraded inside the endosomes.

P2Y receptors are major drug targets.

Because P2Y receptors are widely expressed and contribute to the important purinergic signaling (chapter 1.5) in all human tissues, these receptors are considered to be major drug targets. For this reason, many different nucleotide and non-nucleotide compounds have been investigated in functional assays in order to determine their agonist or antagonist potential. The development of potent agonists and antagonists, which are highly resistant to hydrolysis, is mandatory for drug development. Furthermore, the selectivity of synthetic ligands for a certain P2Y receptor is needed for the investigation of physiological P2Y receptor functions, since several of the P2Y receptors can be activated by adenine and uridine nucleotide derivatives.

Concentration-response experiments are a common way to evaluate whether a receptor ligand has the ability to activate a specific receptor-mediated downstream signaling pathway. This method involves the application of a range of concentrations of the ligand to cells expressing the P2Y receptor of interest. The determination of the amplitudes of the concentration-dependent downstream responses allows for the calculation of the EC_{50} value. The latter gives the concentration of the ligand at which a half-maximal downstream response is achieved. The EC_{50} value helps to assess the so-called ligand efficacy which describes the consequences of the ligand binding to the receptor and the downstream signaling pathways (Strange, 2008). The EC_{50} value also is referred to as the 'potency of a ligand'. A low EC_{50} value represents a high potency to induce a specific downstream signaling pathway. Determination of the EC_{50} value of an agonist can also be used to evaluate how receptor mutations affect the receptor signaling or activation. Importantly, the EC_{50} value of a ligand at a certain receptor depends on the investigated downstream signaling pathway, since different downstream signaling components are involved. Moreover, the efficacy of a ligand should not be mistaken for its affinity, which only describes the dissociation constant of the ligand bound to the receptor (Strange, 2008). The receptor affinity to a ligand can dramatically change as a consequence of the ligand binding and of G protein-coupling to

GPCRs. Thus, the EC_{50} value of a GPCR is a functional parameter of the ternary complex of ligand-receptor-G protein.

In the present study, concentration-response experiments were performed in order to assess the potency of novel $P2Y_{11}$ and $P2Y_6$ receptor agonists featuring several molecular substitutions. Additionally, the functional consequences of an amino acid shift in the $P2Y_{11}$ receptor protein on the efficacy of several nucleotides was investigated this way.

1.3 The human $P2Y_{11}$ receptor

The human $P2Y_{11}$ receptor was first characterized by Communi and coworkers in 1997. The gene was found to be the only P2Y receptor gene containing an intron which separates the first 18 codons from the rest of the coding sequence. The *P2RY11* gene is located on chromosome 19p31 upstream of the human ortholog of the yeast *SSF1* gene. In human, *SSF1* mRNA can be detected in many tissues (Suarez-Huerta *et al.*, 2000). Intergenic splicing was reported to lead to the formation of a $SSF1$-$P2Y_{11}$ receptor fusion protein. The first three codons which were initially reported for the *P2RY11* gene in fact were coming from the *SSF1* part of the *SSF1-$P2Y_{11}$* fusion cDNA (Communi *et al.*, 2001).

The presence of *P2RY11* mRNA was detected in virtually all human tissues. It is most abundant in brain, pituitary, lymphocytes, and spleen. It was also found at significant levels in macrophages, dendritic cells (DC), neutrophils, platelets, and mast cells (Berchtold *et al.*, 1999; Moore *et al.*, 2001; Schnurr *et al.*, 2003; Feng *et al.*, 2004). However, Wang *et al.* (2003) found no *P2RY11* mRNA in human platelets. In the human heart, the *P2RY11* mRNA was found to some extent as well (Wihlborg *et al.*, 2006).

The $P2Y_{11}$ receptor has been reported to interact with the $P2Y_1$ receptor (Ecke *et al.*, 2008a). This interaction results in distinct changes of pharmacological and functional properties of the receptors. The $P2Y_{11}$ receptor, for instance, is not able to undergo nucleotide-induced internalization unless the $P2Y_1$ receptor is co-expressed. The latter receptor undergoes nucleotide-induced, clathrin-dependent internalization on its own (Mundell *et al.*, 2006). In HEK293 cells, which endogenously express the $P2Y_1$ receptor, the potent $P2Y_1$ receptor agonist 2-MeS-ADP (2-methlythio-adenosine 5'-diphosphate) induces strong internalization of the $P2Y_{11}$ receptor. Importantly, the $P2Y_{11}$ receptor-specific antagonist NF157 was unable to block the internalization of the $P2Y_{11}$ receptor in HEK293 cells. Only the $P2Y_1$ receptor-specific antagonist MRS2179 (N^6-methyl-2'-deoxyadenosine 3',5'-diphosphate) was able to completely inhibit nucleotide-induced $P2Y_{11}$ receptor internalization. The formation of $P2Y_1$-$P2Y_{11}$ receptor oligomers explains why a $P2Y_1$ but not a $P2Y_{11}$ receptor-specific antagonist was able to inhibit the internalization of the $P2Y_{11}$ receptor.

Structure-activity relationships of agonists and antagonists of the human $P2Y_{11}$ receptor.

The quest for potent, selective, and stable agonists and antagonists lead to significant findings about the $P2Y_{11}$ receptor structure including the nucleotide binding pocket and structure-activity relationships of ligands (Jacobson *et al.*, 2012). Within the P2Y receptor family, the $P2Y_1$ and $P2Y_{11}$ receptors are the closest homologues with 38% sequence identity and 72% similarity of the TM domains (Zylberg *et al.*, 2007). This results in 33% overall amino acid identity (Communi *et al.*, 1999). The $P2Y_{11}$ receptor has the largest EL2 and EL3 regions within the human P2Y receptor family. Due to their flexibility, the spatial organization of the extracellular loops can hardly be modeled. However, for the $P2Y_1$

receptor the EL2 and EL3 were reported to contribute to ligand binding and recognition (Moro *et al.*, 1999; Hoffmann et al., 1999). This could indicate that the EL2 and EL3 of the $P2Y_{11}$ receptor contribute to the distinct activation pattern of the receptor, when compared to other P2Y receptors. Zylberg *et al.* (2007) presented a computational model of the TM regions of the $P2Y_{11}$ receptor which was verified by mutational analysis. In this study, the secondary structure of the $P2Y_{11}$ receptor was derived from a $P2Y_1$ receptor homology model published by Major *et al.* (2004a). The $P2Y_1$ receptor structure itself is based on the crystal structure of bovine rhodopsin (Okada *et al.*, 2002), the first crystallized GPCR (Palczewski *et al.*, 2000). The so-called homology modeling is a valuable method for the deduction of protein structures from the crystal structure of a closely related protein. The receptor model can be used for the investigation of the parameters of ligand-receptor binding. Thus, it is an important tool for computational fitting analysis of hypothetical ligand structures interacting with the receptor binding pocket.

With the help of the $P2Y_{11}$ receptor model, residues Arg106, Phe109, Ser206, Arg268, Arg307, and Met310 were identified to be directly involved in nucleotide binding. Furthermore, the nucleotide binding pocket of the $P2Y_{11}$ receptor was found to be very similar to that of the $P2Y_1$ receptor.

The model further revealed a hydrophobic pocket within the receptor. The carbon atom C2 of the nucleobase of an adenine nucleotide (Figure 1) bound to the receptor would be located near this hydrophobic pocket. This consequently led to the hypothesis that substitutions at the C2 position of nucleotides could possibly improve nucleotide potency at the $P2Y_{11}$ receptor. Experimental results show that 2-Cl-ATP (2-chloro-adenosine 5'-triphosphate) and 2-MeS-ATP (2-methlythio-adenosine 5'-triphosphate), with rather small C2 substitutions, are poor agonists of the $P2Y_{11}$ receptor. However, AR-C67085 (2-propylthio-ATP-β,γ-dichloromethylene), which carries a larger 2-propylthio substitution at position C2, is a very potent agonist.

The following rank order of nucleotide potencies for the $[Ca^{2+}]_i$ elevation was reported by Communi *et al.* (1999): AR-C67085 > BzATP (2'(3')-O-(4-Benzoylbenzoyl)adenosine 5'-triphosphate) > ATP-γS (adenosine 5'-triphosphate-γ-thio) > dATP (2'-deoxyadenosine 5'-triphosphate) > ATP > ATP-βS (adenosine 5'-triphosphate-β-thio) > 2-MeS-ATP. The same rank order applies for the nucleotide-induced accumulation of cAMP with the only difference that ATP-γS was slightly more potent than BzATP. Meis *et al.* (2010) reported that the non-nucleotide compound NF546, a suramin derivative, is a specific agonist of the $P2Y_{11}$ receptor. Interestingly, suramin, a symmetrical, polysulfonated derivative of urea containing eight benzene rings, is an unspecific antagonist for P2 receptors. It was also used as basis for the development of the specific $P2Y_{11}$ receptor antagonist NF157 (Ullmann *et al.*, 2005). ADP, AMP (adenosine 5'-monophosphate), adenosine, UTP, UDP, GTP (guanosine 5'-triphosphate), CTP (cytidine 5'-triphosphate), TTP (thymidine 5'-triphosphate), ITP (inosine 5'-triphosphate), as well as the di-adenosine nucleotides Ap_4A, Ap_5A, and Ap_6A all turned out to be inactive at the human $P2Y_{11}$ receptor (Communi *et al.*, 1997).

The $P2Y_{11}$ receptor diastereoselectivity is opposite to that of the $P2Y_1$ receptor (Ecke *et al.*, 2006). For this study, a new chiral center was added to several nucleotides by substituting a non-bridging oxygen of the α-phosphate with a borano or thio group. The $P2Y_{11}$ receptor clearly preferred the S*p*-isomers of ATP-αB (adenosine 5'-triphosphate-α-borano), 2-MeS-ATP-αB (2-methylthio-adenosine 5'-triphosphate-α-borano), and 2-Cl-ATP-αB (2-chloro-adenosine 5'-triphosphate-α-borano) over the respective R*p*-isomers. In contrast, the $P2Y_1$ receptor preferred the R*p*-isomers of these nucleotides.

Additionally, it was found that Pα-substitutions in most cases helped to improve nucleotide potencies at both receptors, with the preferred isomers showing the greatest improvements. At the $P2Y_{11}$ receptor, the EC_{50} value for ATP-αB (Sp) was 0.34 µM compared to 2.83 µM for ATP. 2-MeS-ATP-αB (Sp) had an EC_{50} value of 0.26 µM compared to 13.8 µM for 2-MeS-ATP. 2-Cl-ATP-αB (Sp) showed an EC_{50} of 0.47 µM, while the parent compound 2-Cl-ATP was a very weak agonist of the $P2Y_{11}$ receptor with an EC_{50} value higher than 30 µM. The residue responsible for the stereospecific recognition of nucleotides is Arg268 located in TM6. This arginine is part of the group of amino acids, which compose the binding pocket, and it interacts with the triphosphate chain of bound nucleotides (Ecke *et al.*, 2008b). The mutation of Glu186, located in EL2 and not directly involved in nucleotide binding, further increased the degree of stereospecificity.

The human $P2Y_{11}$ receptor has a strong connection to immune cell functions.

The $P2Y_{11}$ receptor mediates the maturation of DCs after stimulation with extracellular ATP (Wilkin *et al.*, 2001). The migration of DCs (Schnurr *et al.*, 2003), the release of Interleukin (IL)-8 (Meis *et al.*, 2010) and IL-12, as well as stimulation of IL-10 production (Wilkin *et al.*, 2002) are also regulated by the $P2Y_{11}$ receptor. Another connection of the $P2Y_{11}$ receptor to immune system responses was found with the ATP-induced inhibition of the constitutive apoptosis of neutrophils, which is important for the balance between the perpetuation of inflammation and its down-regulation after successful clearance of the pathogens (Vaughan *et al.*, 2007). ATP released by endothelial cells can inhibit chemotaxis and cytotoxicity of natural killer cells via activation of the $P2Y_{11}$ receptor (Gorini *et al.*, 2010). This receptor also regulates the lipopolysaccharid-induced activation of THP-1 cells via autocrine ATP signaling and release of IL-6 (Sakaki *et al.*, 2013). The expression levels of the *P2RY11* mRNA in natural killer cells and CD8+ T-lymphocytes are reduced as a consequence of a single-nucleotide polymorphism (SNP) in the 3'-untranslated region of the *P2RY11* gene (rs2305795; Kornum *et al.*, 2011). The $P2Y_{11}$ receptor-mediated protection against ATP-induced cell death is also decreased. This $P2Y_{11}$ receptor mutation is associated with narcolepsy with cataplexy, an auto-immune disease involving the loss of hypocretin-producing neurons in the hypothalamus.

The dataset of the Malmö diet and cancer study revealed that the SNP rs3745601, which is located in the coding region of the *P2RY11* gene, was present in 22.9% of patients with acute myocardial infarction (AMI; Amisten *et al.*, 2007). It was found in only 19.8% of the individuals of the control group. The SNP results in the incorporation of a threonine instead of an alanine at position 87 (Ala-87-Thr, A87T), near the extracellular end of TM2, of the $P2Y_{11}$ receptor protein. Early onset AMI of homozygous individuals showed the strongest correlation to the SNP. Additionally, individuals with this SNP were found to have increased concentrations of C-reactive protein, an acute phase protein and a general marker for inflammatory processes. A main cause for AMI is atherosclerosis (Tabas, 2010). Dendritic cells, macrophages, and mast cells contribute to the development of atherosclerosis. These cells are known for co-expression of the $P2Y_{11}$ and the $P2Y_1$ receptor. Considering the formation of oligomers of the $P2Y_{11}$ and $P2Y_1$ receptors, the question arises whether the aforementioned resulting alteration of the receptor function has a pathological relevance. Thus, the impact of the A87T amino acid shift in the human $P2Y_{11}$ receptor on the activity of cells which co-express both receptors is of special interest.

1.4 The human P2Y$_6$ receptor

The human P2Y$_6$ receptor was first described by Communi *et al.* in 1996. The *P2RY$_6$* receptor gene is located on chromosome 11q13.5, and the corresponding messenger RNA was detected in the spleen, placenta, thymus, small intestine, as well as in neutrophils, lymphocytes, and monocytes (Jin *et al.*, 1998). A number of reports addressed pharmacology and physiological roles of the human P2Y$_6$ receptor. Several studies showed a clear link to immune system-related processes. In monocytes, UDP mediates the release of the pro-inflammatory IL-8 (also called CXCL8) via activation of the P2Y$_6$ receptor (Warny *et al.*, 2001). IL-8 is a powerful attractant of neutrophils, macrophages, and dendritic cells to a site of inflammation. In the same study, the known lipopolysaccharid-induced secretion of IL-8 by THP-1 monocytes was described to function via the autocrine activation of P2Y$_6$ receptors by nucleotides. The UDP-induced release of the pro-inflammatory cytokines IL-8, tumor necrosis factor-α (TNF-α), Interferon gamma-induced protein (IP)-10, and monocyte chemotactic protein (MCP)-1 via the P2Y$_6$ receptor signaling was later demonstrated for the human promonocytic cell line U937 (Cox *et al.*, 2005). However, in 1321N1 astrocytoma cells expressing the P2Y$_6$ receptor a UDP-dependent secretion of TNF-α could not be detected. This indicates that cell type-specific, subcellular mechanisms are necessary for the P2Y$_6$ receptor-mediated release of TNF-α, which seem to be present in monocytic cells, but not in the 1321N1 cell line.

The TNF-α-induced secretion of IL-8 was triggered by UDP in an ERK-dependent fashion in human ARPE-19 (american retinal pigment epithelium type 19) cells, probably regulated by the P2Y$_6$ receptor (Relvas *et al.*, 2009). RPE cells form the blood-retinal-barrier. In auto-immune uveitis, these cells recruit inflammatory cells into the eye. This may result in permanent loss of vision.

It was shown that T cells infiltrating sites of intestinal inflammation express the P2Y$_6$ receptor (Somers *et al.*, 1998). Furthermore, the P2Y$_6$ receptor is also expressed by the human intestinal epithelial cells, which release IL-8 upon receptor activation by UDP (Grbic *et al.*, 2012).

In human lung epithelial cells, human neutrophil peptide (HNP)-induced production of IL-8 was also shown to be dependent on P2Y$_6$ receptor activity (Khine *et al.*, 2006). HNPs are produced and released by neutrophils, which play a crucial role in the innate immune system (Mantovani *et al.*, 2011).

In human mast cell lines, it was demonstrated that the P2Y$_6$ receptor interacts with the cysteinyl leukotriene receptor 1 (CysLT$_1$R) to promote chemokine secretion (Jiang *et al.*, 2009). In this study, also mouse bone marrow-derived mast cells (mBMMC) were used to demonstrate cytoprotection mediated by both receptors together. Cysteinyl leukotrienes are secreted by cells of the innate immune system and are potent mediators of immune responses. The CysLT$_1$ receptor is known for its contribution to the development of asthma (Camargo *et al.*, 2002). Hence, there are strong indications for an important contribution of the P2Y$_6$ receptor to the innate immune response.

Other reports link the P2Y$_6$ receptor to processes outside the immune system functions. The activation of P2Y$_6$ receptors by the potent agonist UTPβS (uridine 5'-triphosphate-β-thio) induced contractions of human cerebral arteries. This offers a possible way to treat cerebral vasospasm via P2Y$_6$ receptor inhibition (Malmsjö *et al.*, 2003). The receptor was further found to be involved in the regulation of fluid and electrolyte transport in human bronchial epithelial cell lines (Wong *et al.*, 2008).

The rank order of nucleotide potencies at the P2Y$_6$ receptor as reported by Communi *et al.* in 1996 is UDP > 5-Br-UTP (5-bromo-uridine 5'-triphosphate) > UTP > ADP > 2-MeS-ATP. Several nucleotide derivatives based on the non-selective physiological P2Y$_6$ receptor agonist UDP were developed (Jacobson *et al.*, 2009 and 2012). UDP-βS, which carries a thio-substitution of a non-bridging oxygen at the β-phosphate, was found to be 6-fold more potent than UDP. Modifications at the uracil ring, however, did not result in derivatives that were much more potent in activating the P2Y$_6$ receptor than UDP. A modification at position 3 of the uracil ring of UDP made 3-phenylacyl-UDP, which was only slightly more potent than its parent compound (El-Tayeb *et al.*, 2006). 5-Br-UDP and 5-I-UDP (5-iodo-uridine 5'-triphosphate) were equipotent with UDP (Nicholas *et al.*, 1996; Besada *et al.*, 2006). The synthesis of UDP-α,β-CH$_2$ and 5-bromo-UTP-β,γ-CCl$_2$ (Ko *et al.*, 2008) yielded enzymatically stable nucleotides. The latter combines substitutions at the phosphate chain and the uracil nucleobase. The di-uridine nucleotide Up$_3$U (uridine 5'-triphosphate 5''-uridine) was also equipotent with UDP. INS48823, an Up$_3$U derivative, was slightly more potent than UDP, and experimental data indicated greater hydrolytic stability (Korcok *et al.*, 2005). The CDP (cytidine 5'-diphosphate) derivatives N^4-benzyloxy-CDP (MRS2964), N^4-methoxy-CDP, and N^4-methoxy-Cp$_3$U (MRS2957) were reported to activate the P2Y$_6$ receptor with higher potency than the standard agonist UDP (Maruoka *et al.*, 2010). These analogs were also selective for the P2Y$_6$ receptor over the P2Y$_2$ and P2Y$_4$ receptors and showed hydrolytic stability. With the help of homology modeling of the P2Y$_6$ receptor structure, it was shown that the P2Y$_6$ receptor is preferentially activated by UDP derivatives with a South (*S*)-conformation of the ribose ring: (*N*)-methanocarba-UDP was completely inactive, but (*S*)-methanocarba-UDP was more potent than UDP (Costanzi *et al.*, 2005; Besada *et al.*, 2006).

To date, the only known specific P2Y$_6$ receptor antagonist is MRS2578, a di-isocyanate derivative (Mamedova *et al.*, 2004). However, this compound inhibits the P2Y$_6$ receptor activity in an irreversible manner.

1.5 Purinergic signaling: the role of extracellular nucleosides and nucleotides in cell-to-cell communication

In the extracellular space, adenosine and nucleotides such as ATP, ADP, UTP, and UDP can act as autocrine or paracrine signaling molecules. They regulate numerous physiological functions depending on cell type and tissue (Abbracchio *et al.*, 2006; Burnstock, 2006; Corriden and Insel, 2010). Several human cell lines have been shown to constitutively release ATP and UTP in the resting state (Lazarowski *et al.*, 2000). Nucleotide release is balanced by extracellular nucleotide hydrolysis and transphosphorylation. Resting nucleotide concentrations are observed only in the nanomolar range. They are lower than the mere dilution by diffusion of molecules in a medium, with increasing distance from the secreting cells, would suggest. This can be explained with the activity of extracellular nucleotide-hydrolyzing enzymes (Joseph *et al.*, 2003). However, depending on cell type and stimulus, the transient local concentration of secreted nucleotides in close proximity to a cell surface can be high enough to be able to activate membrane-localized nucleotide receptors (Ostrom *et al.*, 2000). Such signals serve as a means for several specialized physiological cell-to-cell communications.

There is solid evidence that ATP and its break-down product adenosine can act as a neural transmitter or co-transmitter in the central and peripheral nervous system (Burnstock, 2007 and 2008).

Together with glutamate, γ-aminobutyric acid and glycine, ATP is an integral part of the inter-glial and neuron-to-glia cell communication. Also, di-adenosine polyphosphates play a role, since high concentrations have been detected in synaptic terminals (Guzmán-Aranguez *et al.*, 2007). ATP was shown to play a key role in nociception, to affect neuronal and non-neuronal cell growth and differentiation, and was found to be involved in several disorders of the central nervous system (Burnstock, 2007 and 2008; Giniatullin *et al.*, 2013). In neurons, ATP, like other nucleotides, is stored in synaptic vesicles. Also, nucleotides and nucleosides are released from injured or dying neuronal and non-neuronal cells. In brain, microglia perceive these signals, migrate towards their source and eventually engulf the dead cells (Koizumi *et al.*, 2013).

As a result of the typical intracellular ATP concentration of 3 – 10 mM, cell lysis results in high concentrations of ATP in the extracellular space. This has been well documented to affect a series of immune cell responses, ranging from chemotaxis to cytokine release, and to the promotion of inflammation (Bours *et al.*, 2006; Jacob *et al.*, 2013). This way, extracellular ATP at very high concentrations acts as a danger signal. At the same time, extracellular ATP is also an important modulator of immune responses (Trautmann, 2009), which balances inflammation and immune-tolerance (Di Virgilio *et al.*, 2009; Vitiello *et al.*, 2012).

Cell death does, however, not necessarily involve cell lysis and the accompanying leakage of cytoplasmic content into the extracellular space. During the tightly controlled process of apoptosis, the cytoplasmic contents, including the high concentrations of intracellular nucleotides, are kept enclosed within the dying cells. This process allows for the removal of aged, damaged, or redundant cells without promoting inflammation. Apoptotic cells release ATP and UTP at nanomolar concentrations which both act as 'find-me' signals for phagocytes (Elliott *et al.*, 2009). These phagocytes, mainly macrophages and dendritic cells, are responsible for the following clearance of the apoptotic cells.

Nucleotides can further serve as signaling molecules in numerous physiological processes beyond the realms of the immune and nervous systems. In the vascular system for example, erythrocytes subjected to metabolic and mechanical stimuli release ATP, which is subsequently detected by P2Y nucleotide receptors of the vascular endothelial cells (Sprague *et al.*, 1996; González-Alonso *et al.*, 2002; Kalsi *et al.*, 2012; González-Alonso, 2012). This eventually leads to the activation of nitric oxide (NO) synthases and vasodilatation.

ADP release from platelets promotes thrombus formation by activating additional platelets, but increased concentrations of extracellular ADP trigger the production and the release of NO from platelets. This inhibits further recruitment of platelets, balancing the thrombus size (Lüthje *et al.*, 1984; Freedman *et al.*, 1997; Ku *et al.*, 2007; Carroll *et al.*, 2007).

Mechanisms of nucleotide release.

The release of nucleotides from intracellular vesicles is not restricted to neuronal cells. It can also be observed in several non-neuronal cells, like mast cells, platelets, and many epithelial cell types, like urothelial cells, vascular epithelial cells, and the biliary secreting cholangiocyte cells (Osipchuk and Cahalan, 1992; Guzmán-Aranguez *et al.*, 2007; Taylor *et al.*, 1998; Bodin and Burnstock, 2001; Knight *et al.*, 2002; Gatof *et al.*, 2003). In platelets, nucleotides like ATP, ADP, and the di-adenosine polyphosphates Ap_3A, Ap_4A, Ap_5A, and Ap_6A are stored in dense granules (Lüthje *et al.*, 1983; Schlüter *et al.* 1994). In dense secretory granules of adrenal medullary chromaffin cells, the nucleotides ATP, ADP,

and AMP, as well as Ap$_4$A, Ap$_5$A, and Ap$_6$A were detected (Rodriguez del Castillo *et al.*, 1988; Pintor *et al.*, 1992c). The accumulation of ATP in vesicles was shown to rely on the vesicular nucleotide transporter (VNUT) SLC17A9 (Sawada *et al.*, 2008). Furthermore, exocytosis of ATP-containing lysosomes appears to be important for calcium (Ca^{2+}) wave propagation between astrocytes (Zhang *et al.*, 2007).

Non-vesicular nucleotide release can be caused by mechanical stimulation, hypoxia, or receptor stimulation in many cell types (Forrester and Lind, 1969; Lazarowski *et al.*, 1997b; Gerasimovskaya *et al.*, 2002; Abbrachio *et al.*, 2006). Pannexin and connexin hemichannels were found to mediate ATP efflux (Figure 2; Kang *et al.*, 2008; Huang *et al.*, 2007). In concert with the subsequent autocrine or paracrine activation of P2 receptors, the non-vesicular nucleotide release is recognized as an important contributor to pro- and anti-inflammatory pathways, apoptosis, tissue regeneration, and stem cell differentiation, as well as ischemia, atherosclerosis, and even HIV infection (Adamson *et al.*, 2014; Marenkova *et al.*, 2014; Velasquez *et al.*, 2014).

Recent studies have extended the list of ATP-releasing membrane channels to volume-regulated anion channels (Hisadome *et al.*, 2002) and voltage-dependent anion channels (Bell *et al.*, 2003; Liu *et al.*, 2008). The P2X$_7$ receptor, an ATP-activated cation channel, can mediate the release of ATP through pannexin-1 channels (Pelegrin *et al.*, 2006; Adamson *et al.*, 2014) but not Connexin-43 hemichannels (Suadicani *et al.*, 2008).
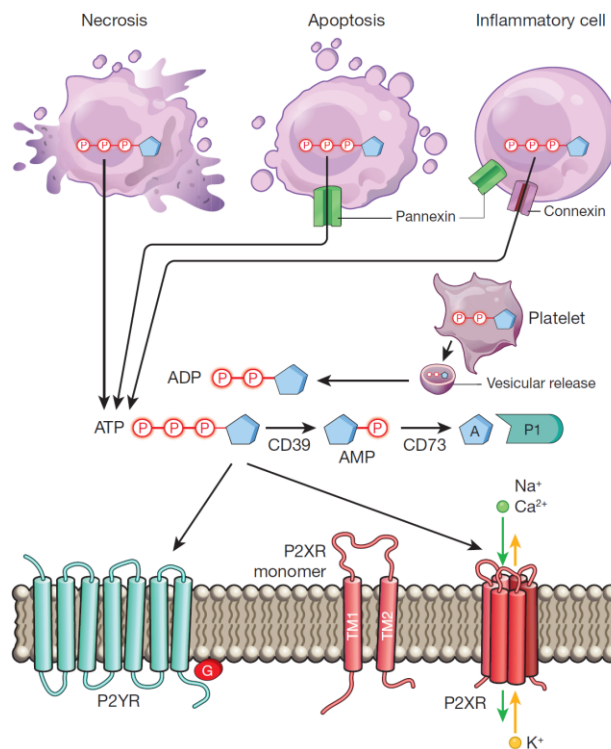
Figure 2: *Nucleotide release and signaling during apoptosis and inflammation* (Idzko *et al.*, 2014). CD39 = E-NTPDase 1; CD73 = ecto-5'-nucleotidase.

Modulation of purinergic signaling by hydrolyzing and converting enzymes.

The aforementioned enzymatic hydrolysis or conversion of extracellular nucleotides contributes to extracellular nucleotide signaling to the same degree as the nucleotide secretion itself. Rapid degradation of nucleotides can switch off signals and may additionally initiate other signaling pathways by creating new receptor-specific ligands (Figure 3). This also can locally restrict the occurrence of extracellular nucleotides (Joseph *et al.*, 2003). This important modulation of the extracellular nucleotide signaling is realized by several groups of ecto-nucleotidases (Zimmermann *et al.*, 2000).
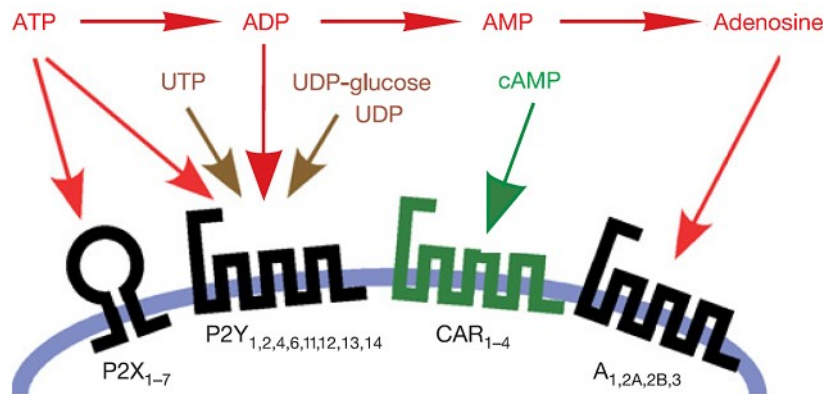
Figure 3: *Schematic overview of nucleotide receptors and signal modulation via activity of nucleotide hydrolyzing enzymes* (modified from Khakh *et al.*, 2006). P2X = ionotrophic P2 nucleotide receptors; P2Y = metabotropic, G protein-coupled P2 nucleotide receptors; CAR = cAMP receptors; A = metabotropic, G protein-coupled P1 adenosine receptors.

These enzymes, which are either soluble or membrane localized, are present in virtually every human tissue and may have a large spectrum of cell type-dependent physiological functions. Ecto-nucleoside triphosphate diphosphohydrolases (E-NTPDases) hydrolyze nucleoside di- or triphosphates. E-NTPDase1, 2, 3, and 8 are membrane-localized, and have an extracellular catalytic activity. E-NTPDase4 - 7 activity is localized intracellularly (Robson *et al.*, 2006). Ecto-nucleotide pyrophosphatase/phosphodiesterases (E-NPPs) can hydrolyze phosphodiester bonds and pyrophosphate (PP_i) and exist in membrane localized and soluble forms (Goding *et al.*, 2003). E-NPP1 - 3 convert ATP and ADP to AMP, PP_i, and eventually ortho-phosphate (P_i), but they degrade also NAD^+ to nicotinamide mononucleotide. Additionally, cAMP can be processed to AMP. E-NPP4 recently was found to hydrolyze the di-nucleotide Ap_3A to AMP and ADP and Ap_4A to AMP and ATP (Albright *et al.*, 2012).

The ecto-5'-nucleotidases are considered to be a major source for the production of extracellular adenosine as they are actively cleaving nucleoside monophosphates into nucleosides and P_i (Zimmermann at al., 1992). The enzymes of the alkaline phosphatase family are able to perform the complete hydrolysis of nucleoside triphosphates into the corresponding nucleosides and phosphates without further contribution of other nucleotidases.

In contrast to the nucleotide-hydrolyzing enzymes, nucleoside diphosphokinases and alkaline kinases elevate the concentration of nucleotides via transphosphorylation reactions (Lazarowski *et al.*, 1997a; Yegutkin *et al.*, 2001). These enzymes catalyze the conversion of ATP plus UDP to ADP plus UTP or two molecules of ADP to ATP and AMP, respectively.

1.6 Aims of the project

1.   Characterization of the human P2Y$_{11}$ receptor carrying the Ala-87-Thr mutation.

Naturally occurring genetic polymorphisms of P2Y receptor genes may change functional characteristics of the receptors and thus provide an excellent opportunity to study the biochemical parameters of physiological and pathological nucleotide signaling. Here, we characterized a nucleotide polymorphism in the human *P2RY11* gene, which results in an Ala-87-Thr amino acid change in the P2Y$_{11}$ receptor protein. The impact of this mutation on P2Y$_{11}$ receptor activity, as well as its mechanistic connection to the development of AMI, has been unknown so far. Therefore, this study should provide first functional insights.

1.1 Investigation of nucleotide-induced P2Y$_{11}$A87T receptor-mediated intracellular responses in comparison to the wildtype P2Y$_{11}$ receptor.

The P2Y$_{11}$A87T receptor was expressed in 1321N1 astrocytoma and in HEK293 cells. In these cells, nucleotide-induced intracellular Ca^{2+} mobilization, cAMP generation, receptor internalization, as well as de- and resensitization of Ca^{2+} responses were investigated. The data were compared to those from the wildtype P2Y$_{11}$ receptor.

1.2 Generation of the P2Y$_{11}$A87S and P2Y$_{11}$A87Y receptors and investigation of intracellular responses in comparison to the P2Y$_{11}$A87T receptor.

The P2Y$_{11}$A87S and P2Y$_{11}$A87Y mutant receptors were generated additionally. We investigated nucleotide-induced intracellular Ca^{2+} responses, receptor internalization, and de- and resensitization of Ca^{2+} responses. This should help to elucidate whether the polarity of the amino acid at position 87 of the protein might be the cause for a putative change in receptor activity.

1.3 Co-expression of the P2Y$_{11}$A87T receptor with the P2Y$_1$ receptor in the P2Y receptor-null background of 1321N1 astrocytoma cells.

HEK293 cells endogenously express the P2Y$_1$ receptor, which was reported to form functionally unique oligomers with the P2Y$_{11}$ receptor. 1321N1 astrocytoma cells provide a P2Y receptor-null background and therefore are predestined for the analysis of isolated P2Y receptor functions and signaling. The co-expression of the P2Y$_1$ and P2Y$_{11}$A87T receptors in 1321N1 astrocytoma cells was used to confirm the results achieved with HEK293 cells.

2.   Evaluation of potency and receptor selectivity of novel synthetic nucleotides as agonists of the human P2Y$_{11}$ and P2Y$_6$ receptors.

Human P2Y receptors are interesting targets for drug development since they are connected to many physiological and pathological processes. Thus, the next aim was to gain new insights into structure-activity relationships of novel synthetic ATP-derived nucleotides as agonists of the human P2Y$_{11}$ receptor. In addition, UDP-derived nucleotide analogs were evaluated as agonists of the human P2Y$_6$ receptor. The novel nucleotide compounds were synthesized in our collaborators laboratory (Prof. Bilha Fischer, Department of Chemistry, Gonda-Goldschmied Medical Research Center, Bar-Ilan University, Ramat-Gan, Israel). The nucleotides were tested on 1321N1 astrocytoma cells expressing these receptors mostly as C-terminal GFP-fusion proteins. GFP-labeled P2Y receptors have successfully been used before in several physiological and pharmacological studies (Tulapurkar *et al.*, 2004; Ecke *et al.*, 2006;

Tulapurkar *et al.*, 2006; Zylberg *et al.*, 2007). Nucleotide potency at the $P2Y_{11}$ and $P2Y_6$ receptors was analyzed by measuring the nucleotide-induced rise of intracellular Ca^{2+}. Since the human $P2Y_{11}$ receptor is coupled to G_s signaling, the $P2Y_{11}$ receptor-mediated elevation of cAMP levels was investigated for selected ATP analogs.

2.1 Investigation of 2-propylthio-substituted analogs of ATP at the human $P2Y_{11}$ receptor.

The novel $P2Y_{11}$ receptor agonists investigated here were based on the structure of the very potent $P2Y_{11}$ receptor agonist AR-C67085 (Communi *et al.*, 1999). This ATP derivative features a propylthio-group at the C2 position of the adenine nucleobase and a CCl_2 group between the β- and the γ-phosphate. By introducing an additional borano or thio substitution of a non-bridging oxygen at the α-phosphate, we created a new chiral center. This should increase nucleotide selectivity since the stereoselectivity of the $P2Y_{11}$ receptor is opposite to that of the closest homolog, the adenine nucleotide-preferring $P2Y_1$ receptor. Furthermore, we expected a beneficial effect on hydrolytic stability and nucleotide potency, as these effects have been reported before for several other nucleotide analogs.

2.2 Investigation of 5-OMe-substituted analogs of UDP at the human $P2Y_6$ receptor.

On the $P2Y_6$ receptor, a series of mono- and di-nucleotide analogs of UDP, which carried an OMe-substitution at the C5 position of the nucleobase, was tested regarding nucleotide selectivity and potency. Additionally, several of the tested analogs featured Pα-substitutions. This should increase hydrolytic stability and nucleotide potency, despite the fact that a diastereoselectivity has not been reported before for the $P2Y_6$ receptor.

2. Materials and methods

2.1 Materials

2.1.1 Expression vectors

For C-terminal GFP-fusion protein expression in mammal cell lines, the 4.7 kb pEGFP-N1 vector (Clontech Laboratories Inc., Palo Alto, CA, USA) with a kanamycin/neomycin resistance cassette was used. The 5.5 kb pcDNA 3.1/myc-His vector (Life Technologies Corporation, Carlsbad, CA, USA) with an ampicillin/neomycin resistance cassette was used for expression of proteins with a C-terminal myc-His tag in mammal cell lines.

2.1.2 Chemicals, reagents, and enzymes

Penicillin and streptomycin were used to supplement cell culture media and were purchased from Biochrom AG (Berlin, Germany). G418 (geneticine) was used for culturing of mammal cell lines transfected with the pEGFP-N1 expression vector and was obtained from Merck Chemicals GmbH (Schwalbach/Ts., Germany). Fura 2/AM for single-cell Ca^{2+} measurements was supplied by Life Technologies Corporation (Carlsbad, CA, USA). For the lipofection of mammal cell lines, FuGENE 6 Transfection Reagent and DOTAP by Roche Diagnostics GmbH (Mannheim, Germany) were used. MATra-A nanoparticles for magnet-assisted transfection were obtained from Iba GmbH (Göttingen, Germany). Para-formaldehyde used for cell fixation and the nucleotides used for P2Y receptor activation (ATP, UDP, UTP, 2-MeS-ADP, and BzATP) were supplied by Sigma-Aldrich (St. Louis, MO, USA). The $P2Y_1$ receptor antagonist MRS2179 and the $P2Y_6$ receptor antagonist MRS2578 were produced by Sigma-Aldrich and Tocris Bioscience (Bristol, UK). The Pfu polymerase, the restriction enzymes DpnI, HindIII, and BamHI, as well as the mouse monoclonal α-Myc and Alexa555 goat anti–mouse antibodies used for immunocytochemistry were supplied by Thermo Fisher Scientific Inc. (Waltham, MA, USA). All other chemicals used for cell culture and single-cell Ca^{2+} measurements were obtained from Carl Roth GmbH (Karlsruhe, Germany).

2.1.3 Primers for site-directed mutagenesis

MHP2Y11GFPA87Tup: 5'-CTG CCC CCG CTG GCC <u>ACC</u> TAC CTC TAT CCC-3'

MHP2Y11GFPA87Tlow: 5'-GGG ATA GAG GTA GCT <u>GGT</u> CAG CGG GGG CAG-3'

MHP2Y11GFPA87Sup: 5'-CTG CCC CCG CTG GCC <u>AGC</u> TAC CTC TAT CCC-3'

MHP2Y11GFPA87Slow: 5'-GGG ATA GAG GTA GCT <u>GGC</u> CAG CGG GGG CAG-3'

MHP2Y11GFPA87Yup: 5'-CTG CCC CCG CTG GCC <u>TAT</u> TAC CTC TAT CCC-3'

MHP2Y11GFPA87Ylow: 5'-GGG ATA GAG GTA GCT <u>ATA</u> CAG CGG GGG CAG-3'

19

2.1.4 Sequencing primers

THP2Y11FW1:   5'-ACC TGC ATC AGC CTC AAC CGC-3'

THP2Y11FW2:   5'-TGG CCC TCT ACG CCA GCT CCT A-3'

THP2Y11FW3:   5'-TGT GTC CAC CCT CTA CTC TAC A-3'

THP2Y11RV1:   5'-AGC GGT TGA GGC TGA TGC AGG T-3'

THP2Y11RV2:   5'-TAG GAG CTG GCG TAG AGG GCC A-3'

THP2Y11RV3:   5'-TGT AGA GTA GAG GGT GGA CAC A-3'

2.2 Cell media

Dulbecco's modified Eagle's medium (DMEM) for 1321N1 astrocytoma cell culture:

DMEM (Biochrom AG, Berlin, Germany) was supplemented with 10% (v/v) fetal calf serum (FCS; PAA Laboratories GmbH, Pasching, Austria), 100 U/ml penicillin, and 100 U/ml streptomycin.

DMEM/Ham's F-12 (1:1) for HEK293 cell culture:

Dulbecco's MEM/Ham's F-12 (1:1) (Biochrom AG, Berlin, Germany) was supplemented with 10% (v/v) FCS, 100 U/ml penicillin, and 100 U/ml streptomycin.

LB medium for bacterial culture:

10 g tryptone, 5 g yeast extract, 10 g NaCl, 15 g agar (for plates), pH 7.0.

SOC medium for bacterial transformation:

5 g tryptone, 1.25 g yeast extract, 0.15 g NaCl, 0.125 g KCl, 1 M glucose, 1 M $MgCl_2$, 1 M $MgSO_4$.

2.3 Buffers and solutions

1 x NaHBS (+ Ca^{2+}):
145 mM NaCl, 5.4 mM KCl, 1 mM MgCl$_2$, 25 mM glucose, 20 mM HEPES, 1.8 mM CaCl$_2$, pH 7.4.

1 x PBS:
137 mM NaCl, 2.6 mM KCl, 8.1 mM Na$_2$HPO$_4$, 1.4 mM KH$_2$PO$_4$, pH 7.4.

4% PFA solution:
4% (v/v) PFA (paraformaldehyde), 120 mM Na$_2$HPO$_4$, 4% (w/v) saccharose, pH 7.4.

5 x KCM solution:
500 mM KCl, 150 mM CaCl$_2$, 250 mM MgCl$_2$.

Embedding medium:
100 mg Dabco (1,4-Diazabicyclo[2.2.2]octane) was dissolved in 100 µl PBS (pH 8.9) using vortexer and thermomixer. 2.45 ml glycerol and 2.45 ml Vectashield were added subsequently. The solution was incubated under constant shaking at 4 °C in darkness. For storage, the reaction tube was wrapped in aluminum foil and kept at 4 °C.

FSBB (fetal serum blocking buffer):
17% (v/v) FCS, 20 mM Na$_2$HPO$_4$, 450 mM NaCl, 0.3% (v/v) Triton X-100.

High salt buffer:
500 mM NaCl, 20 mM Na$_2$HPO$_4$.

Low salt buffer:
150 mM NaCl, 10 mM Na$_2$HPO$_4$.

Solutions for DNA mini preparation:
Solution 1: 50 mM glucose, 25 mM Tris/HCl pH 8.0, 10 mM EDTA pH 8.0, 100 µg/ml RNAse.
Solution 2: 0.2 M NaOH, 1% (w/v) SDS.
Solution 3: 3 M CH$_3$CO$_2$K, 11.5% (v/v) CH$_3$COOH.

Tris-EDTA (TE):
10 mM Tris/HCl pH 8.0, 0.2 mM EDTA.

2.4 Methods

2.4.1 KCM-transformation of *Escherichia coli* bacteria

For transformation, 1 - 10 µl DNA were mixed with 20 µl 5 x KCM solution and sterile bidest H$_2$O was added to a final volume of 100 µl. 100 µl of KCM competent DH5α cells were thawed on ice and then incubated with the DNA/KCM solution for 30 min on ice. Afterwards, the cells were kept at room temperature (RT) for additional 10 min before 800 µl of the pre-warmed (37 °C) SOC medium were added. The cells were gently mixed (200 rpm) in a cell incubator for 1 h at 37 °C. After the incubation, the cells were plated on agarose dishes containing the selection antibiotic. The dishes were incubated overnight at 37 °C. Positive clones were selected and sub-cultured.

2.4.2 DNA extraction (mini preparation)

Transfected DH5α clones were picked and incubated in 5 ml liquid LB medium supplemented with the selection antibiotic. The cells were incubated overnight at 37 °C and mixed gently with 200 rpm. The next day, 1.5 ml of the cell suspension were transferred to a reaction tube and centrifuged briefly (30 s). The cell pellet was resuspended in 100 µl of solution 1. Cell lysis was induced by adding 200 µl of solution 2. The sample was mixed very carefully and incubated at RT for 5 min. 150 µl of solution 3 were added to the now clear and viscous cell suspension. Next, the suspension was kept on ice for 15 min with occasional gentle mixing. After this incubation step, the suspension was centrifuged at maximum speed (13.000 rpm) for 15 min at RT. The clear supernatant was transferred to a fresh reaction tube, mixed with 300 µl isopropanol in order to precipitate the DNA, and incubated for 5 min at RT. The suspension was then centrifuged at maximum speed for 10 min at RT. The supernatant was discarded and the remaining DNA-containing pellet was washed with 500 µl of 70% ethanol to remove excess salt. The sample was then centrifuged at maximum speed for 10 min at RT and the supernatant was discarded. The pellet was dried at RT or using a heating block (preheated to 40 °C). Finally, the DNA pellet was solubilized in 50 µl bidest H$_2$O or TE buffer and stored at -20 °C.

2.4.3 Site-directed mutagenesis

For site-directed mutagenesis, the QuickChange Site-Directed Mutagenesis Kit (Agilent Technologies Inc., Santa Clara, CA, USA) was used. The mutagenesis primers were designed according to the manual. A Pfu polymerase was used instead of the Pfu Turbo polymerase suggested by the manufacturer. The PCR cycler program was designed as follows: initial denaturation at 98 °C for 30 s, second denaturation at 95 °C for 30 s, primer annealing at 55 °C for one min, polymer extension at 70 °C for 12 min. The steps 2 to 4 were repeated 16 times. After mutagenesis PCR, 1 µl of the DpnI restriction enzyme was added to the PCR product in order to digest methylated template plasmid DNA. Competent DH5α *E.coli* cells were then transformed as described above with the pEGFP-N1 expression vector containing the mutated *P2RY11* receptor cDNA insert. The cells were

plated on kanamycin containing agarose plates and incubated at 37 °C. Clones were picked 10 to 12 h later and transferred to liquid LB medium for overnight growth at 37 °C before the plasmid DNA was extracted. The extracted DNA was test-digested with HindIII and BamHI restriction enzymes in order to verify correct fragment sizes in a 1% agarose gel. The positive clones were selected for sequencing.

2.4.4 Cell culture and transfection of human cell lines

Using the pEGFP-N1 expression vector, C-terminal GFP constructs of human P2Y receptors were stably expressed in human 1321N1 astrocytoma cells or in HEK293 cells. The $P2Y_1$-myc/His receptor was expressed in 1321N1 astrocytoma cells using the pcDNA 3.1/myc-His expression vector.

1321N1 astrocytoma cells were transfected using FuGENE 6 Transfection Reagent and HEK293 cells using DOTAP Liposomal Transfection Reagent. Transfected HEK293 cells were selected with 0.5 mg/ml G418 and grown in DMEM/Ham's F12 (1:1) cell culture medium. Transfected 1321N1 astrocytoma cells were selected with 1.0 mg/ml G418 and grown in DMEM cell culture medium. All cultures were maintained in cell culture incubators with humidified atmosphere at 37 °C and 5% CO_2. The expression of the receptors by the cells was confirmed by detection of the GFP fluorescence using a confocal fluorescence microscope and/or the elevation of $[Ca^{2+}]_i$ after stimulation with the physiological standard nucleotide agonists of the respective P2Y receptor.

FUGENE 6 lipofection of 1321N1 astrocytoma cells was performed as follows: The cells were seeded in cell culture dishes (diameter 6 cm) one day prior to the transfection and grown to 50% - 80% confluency. For transfection, FuGENE 6 Transfection Reagent was mixed with DMEM (final volume 200 µl) and DNA in 3:1 (3 µl FUGENE 6 and 1 µg DNA), 3:2 (3 µl FUGENE 6 and 2 µg DNA), and 6:1 (6 µl FUGENE 6 and 1 µg DNA) ratios. Before the addition of DNA, FUGENE 6 was mixed with medium and incubated for 5 min at RT. The addition of DNA to the mixture was followed by a 30 min incubation at RT. Afterwards, the transfection mixtures were added dropwise to the cells followed by 1.8 ml medium. The cells were kept in the incubator for 4 - 5 h. After this, 2 ml of cell culture medium were added and the cells were incubated overnight. The next day, the medium was renewed and G418 was added.

DOTAP lipofection of HEK293 cells was performed as follows: The cells were seeded in cell culture dishes (diameter 6 cm) one day prior to the transfection and grown to 50% - 80% confluency. 5 µg DNA were mixed with 50 µl HEPES (20 mM) and 30 µl DOTAP were mixed with 70 µl HEPES (20 mM). The DNA and DOTAP solutions were then combined and incubated for 30 min at RT before the addition of 3 ml DMEM/Ham's F12 (1:1) cell culture medium. The final transfection solution was added and the cells were incubated at 37 °C. After 6 - 8 h, the transfection solution was replaced by cell medium and the cells were then incubated for additional 10 h. After that, the cell medium was complemented with G418.

Magnet-assisted transfection with MATra-A nanoparticles was used for co-expression of the $P2Y_1$ and $P2Y_{11}$ or $P2Y_{11}A87T$ receptors in 1321N1 astrocytoma cells. The cells were seeded in cell culture dishes (diameter 6 cm) two days prior to the transfection and grown to 50% - 80% confluency. For double transfections, 2.5 µg of each plasmid DNA (5 µg for single transfections) were diluted in

serum-free DMEM cell medium to a final volume of 400 µl. 6.6 µl of the MATra-A solution were added carefully. After 20 min incubation at RT, the transfection mixture was added drop wise to the cells and complemented with 4 ml serum-free DMEM. The cell culture dishes were then placed on magnet plates and kept in the cell incubator for 15 min. After this step, the medium was changed to DMEM containing 10% FCS and the cells were incubated for about 48 h before measurement.

All transfected HEK293 and 1321N1 astrocytoma cell cultures used in the experiments were derived from the same stock wild type cell cultures to guarantee equal conditions for all experiments.

2.4.5 Single-cell Ca^{2+} measurements

1321N1 astrocytoma or HEK293 cells expressing the P2Y-GFP receptor or wildtype control cells were seeded on cover slides (diameter 22 mm) and grown for two days to approximately 80% density. The cover slides used for HEK293 cell growth were coated with poly-L-lysine to ensure cell adhesion during measurement. Prior to measurement, the cells were incubated in NaHBS buffer complemented with 2 µM of the ratiometric Ca^{2+}-sensitive dye Fura 2/AM for 30 min at 37 °C. If necessary, a P2Y receptor antagonist was added to the incubation buffer.

For standard single-cell Ca^{2+} measurements, used for the determination of the EC$_{50}$ values of nucleotides, the cells were superfused (1 ml/min, 37 °C) with NaHBS buffer containing the agonist and/or antagonist in the desired concentration. Only cells with a clear, plasma membrane-localized GFP-signal and with the typical Ca^{2+} response kinetics upon agonist pulse application were included in the data analysis. The amplitudes of the intracellular Ca^{2+} responses were calculated as described below.

For the analysis of Ca^{2+} response desensitization and resensitization, HEK293 cells expressing the P2Y$_{11}$, the P2Y$_{11}$A87T, or the P2Y$_{11}$A87S receptor were incubated with 100 µM ATP for the prolonged period of 30 min (

Figure *19*). This is sufficient to induce receptor internalization in P2Y$_{11}$ receptor-expressing cells (Ecke *et al.*, 2008). To allow receptor resensitization, the cells were superfused with nucleotide-free NaHBS buffer for 60 min. Finally, a brief 1 min application of 100 µM ATP was used to determine the extent of the recovery of the intracellular Ca^{2+} response.

Intracellular Ca^{2+} measurements with 1321N1 astrocytoma cells co-expressing the P2Y$_1$ and P2Y$_{11}$ or P2Y$_{11}$A87T receptors were performed as follows: Cells with P2Y$_{11}$ or P2Y$_{11}$A87T receptor expression, as verified by GFP fluorescence, were selected for analysis and challenged with 1 µM BzATP. After a recovery period of at least 2 min, 1 µM 2-MeS-ADP was added to verify the co-expression of the P2Y$_1$-myc/His receptor. GFP-positive cells responding to the 2-MeS-ADP stimulus were considered as P2Y$_1$/P2Y$_{11}$ or P2Y$_1$/P2Y$_{11}$A87T co-expressing cells.

For the measurement of the nucleotide-induced Ca^{2+} responses, the ratio of the 510 nm emissions of Fura 2 after subsequent excitations at 340 nm and 380 nm (F340 nm / F380 nm) was determined. Free intracellular Ca^{2+} binds to Fura 2 and causes increased 340 nm excitation and decreased 380 nm excitation. The reduction of [Ca^{2+}]$_i$ has the opposite effect. Thus, changes of the F340 nm / F380 nm ratio can be used to determine the amplitudes of the nucleotide-induced intracellular Ca^{2+} responses, as the changes in the excitation spectrum of Fura 2 directly correlate to the intracellular Ca^{2+} concentration.

The experiments were conducted using a TILL Photonics Polychrome IV setup (FEI Munich GmbH, Gräfelfing, Germany) with a Zeiss Axiovert 135 inverted fluorescence microscope (Carl Zeiss AG, Oberkochen, Germany). The concentration-response curves and EC_{50} values were derived from the average response amplitudes using SigmaPlot (Systat Software Inc., San Jose, CA, USA). As previously reported, the GFP-tagged P2Y receptors are suitable for pharmacological and physiological studies and were found to be functionally indistinguishable from P2Y receptors without GFP tag (Tulapurkar *et al.*, 2004; Ecke *et al.*, 2006; Tulapurkar *et al.*, 2006; Zylberg *et al.*, 2007).

2.4.6 cAMP measurements

Cells expressing the $P2Y_{11}$ or $P2Y_{11}A87T$ receptor were grown in cell culture dishes (diameter 6 cm) to circa 70% confluency. The cells were incubated in NaHBS buffer containing 500 µM isobutyl-methyl-xanthine (IBMX; a non-specific inhibitor of cAMP phosphodiesterases) for 30 min at 37 °C. Nucleotide was then added in the desired concentration in order to activate the P2Y receptors and the cells were incubated for 10 min at 37 °C. The cells were lysed using 0.1 M HCl, scraped from the dishes and sonicated briefly. 100 µl of the cell extract were kept for the determination of total protein concentration using a standard Bradford protein assay. The cAMP content of the cells was determined with the direct cyclic AMP enzyme immunoassay kit from ENZO Life Sciences Inc. (Farmingdale, NY, USA). The following steps were conducted according to the manufacturer's manual.

2.4.7 Nucleotide-induced receptor internalization

For the investigation of the nucleotide-induced internalization of the $P2Y_{11}$, $P2Y_{11}A87T$, $P2Y_{11}A87S$, and $P2Y_{11}A87Y$ receptors, the expressing HEK293 cells were grown on a cover slide (diameter 22 mm) to approximately 70% confluency. After incubation with the respective nucleotide for 60 min, the cells were fixed with 4% PFA for 30 min at RT. After this, the cover slides were washed 3 times with PBS, placed upside down on a glass slide with a drop of embedding medium and sealed with nail polish. The localization of GFP fluorescence was detected using a LSM 510 META laser scanning confocal microscope (Carl Zeiss AG, Oberkochen, Germany) using a 488 nm argon/krypton laser and a 505–530 nm band pass filter.

2.4.8 Immunocytochemistry

1321N1 astrocytoma cells transfected with the magnet-assisted transfection method were fixed with 4% PFA (15 min at RT). The cells were kept overnight in 120 mM Na_2HPO_4 solution. The cover slides were then washed once with low salt buffer and twice with high salt buffer for 10 min, respectively. 60 µl FSBB for blocking and permeabilization were added per cover slide and incubated for 20 min. Subsequently, the primary antibody (mouse monoclonal α-Myc, 1:100 in FSBB) was added to the cover slides and kept overnight at 4 °C. The next day, the cover slides were washed 3 x 10 min with high salt buffer. Following these washing steps, the secondary antibody (Alexa555 goat anti–mouse, 1:200 in FSBB) was applied, and the cells were incubated in darkness for 1.5 h at RT. The cover slides were then washed with high salt buffer, followed by 120 mM Na_2HPO_4 solution, and PBS

for 10 min, respectively. The cover slides were placed upside down on a glass slide with a drop of embedding medium and sealed with nail polish. The localization of fluorescence was detected using a LSM 510 META laser scanning confocal microscope. GFP fluorescence was detected with a 488 nm argon/krypton laser in conjunction with a 505–530 nm band pass filter. Alexa555 fluorescence was detected using a 543 nm helium/neon laser and a 560 nm long pass filter.

2.4.9 Statistical analysis

Statistical analysis was performed with IBM SPSS 21 (International Business Machines Corp., Armonk, NY, USA) using the One-Way ANOVA test followed by a Dunnett-T3 post-hoc test. For the cAMP measurements, the mean values given are based on least two samples with the majority of experiments carried out 3 - 12 times. The average cAMP levels induced by corresponding concentrations of nucleotides were compared statistically. Nucleotide concentrations relevant for the calculation of EC_{50} values were used in at least three independent single-cell Ca^{2+} measurements with an average of 10 - 20 cells per experiment. Statistical differences between individual concentration-response curves were calculated by comparing the average amplitudes of the Ca^{2+} responses (Δ F340 nm / F380 nm) to corresponding concentrations of nucleotide. The comparative analysis of Ca^{2+} responses in GFP-negative and GFP-positive HEK293 cells included 2 - 3 independent experiments with 5 - 40 cells per experiment. The average amplitudes of the Ca^{2+} responses to different nucleotides from GFP-negative and GFP-positive cells were compared statistically. The Ca^{2+} measurements with 1321N1 astrocytoma cells co-expressing the $P2Y_1$ and $P2Y_{11}$ or $P2Y_{11}A87T$ receptors were conducted 3 - 9 times with 4 to 13 cells per experiment. The average amplitudes of the Ca^{2+} responses to BzATP of cells co-expressing the $P2Y_{11}A87T$ and the $P2Y_1$ receptor were compared with the corresponding responses of cells co-expressing the wildtype $P2Y_{11}$ and the $P2Y_1$ receptor. In addition, these responses were statistically compared with BzATP-induced responses of 1321N1 cells single-expressing the $P2Y_{11}A87T$ receptor, $P2Y_{11}$ receptor, or $P2Y_1$ receptor.

Fluorescence intensities of GFP tags, which were C-terminally fused to the wildtype and mutant $P2Y_{11}$ receptors expressed in HEK293 cells (n = 59 – 80 cells), were quantified in fixed cell preparations using the histogram function of the LSM510 Meta software of the LSM 510 META laser scanning confocal microscope.

3. Results

3.1 Characterization of the human P2Y$_{11}$ receptor with the Alanine-(87)-Threonine mutation

3.1.1 Nucleotide potencies at the wildtype P2Y$_{11}$ receptor, compared to mutant P2Y$_{11}$A87T, P2Y$_{11}$A87S, or P2Y$_{11}$A87Y receptors expressed in 1321N1 astrocytoma and HEK293 cells

In order to study the P2Y$_{11}$A87T receptor function, the receptor was expressed by us in 1321N1 astrocytoma cells and the pharmacological profile was determined using single-cell Ca^{2+} measurements (Haas *et al.*, 2014). The data were compared to results obtained with the wildtype P2Y$_{11}$ receptor. 1321N1 astocytoma cells lack endogenous P2Y receptor expression and are, therefore, frequently used for the investigation of P2Y receptors. Additionally, we used HEK293 cells for receptor expression. It was shown before (Ecke *et al.*, 2008) that in HEK293 cells the P2Y$_{11}$ receptor shows new pharmacological and functional properties, which are due to the interaction with endogenous P2Y$_{1}$ receptors.

BzATP is a potent agonist for the P2Y$_{11}$ receptor, and specific within the P2Y receptor family. In 1321N1 astrocytoma cells, no differences in the concentration-dependent intracellular Ca^{2+} responses to BzATP were detected between the P2Y$_{11}$ and the P2Y$_{11}$A87T receptor (Figure 4A). With 0.8 +/- 0.1 µM for the P2Y$_{11}$ receptor and 0.9 +/- 0.07 µM for the P2Y$_{11}$A87T receptor, the EC$_{50}$ values were virtually identical (Table 1).

In sharp contrast, the P2Y$_{11}$A87T receptor expressed in HEK293 cells is completely insensitive to BzATP of up to 100 µM (Figure 4B). However, at the wildtype P2Y$_{11}$ receptor expressed in HEK293 cells the EC$_{50}$ value of BzATP of 1.0 +/- 0.05 µM is very similar to that in 1321N1 astrocytoma cells (Table 2).

In order to investigate whether amino acid polarity at position 87 or amino acid size is the cause for altered receptor functionality, the P2Y$_{11}$A87S and P2Y$_{11}$A87Y receptors were generated and expressed in HEK293 cells. BzATP was a potent agonist for both receptors with EC$_{50}$ values of 0.8 +/- 0.06 µM for the P2Y$_{11}$A87S receptor and 1.6 +/- 0.1 µM for the P2Y$_{11}$A87Y receptor (Table 2). The maximal response amplitude to BzATP of the P2Y$_{11}$A87S receptor, however, was 30% higher (P < 0.01) than that of the P2Y$_{11}$A87Y receptor (Figure 4C). The P2Y$_{11}$A87Y receptor showed maximal responses comparable to the wildtype P2Y$_{11}$ receptor.
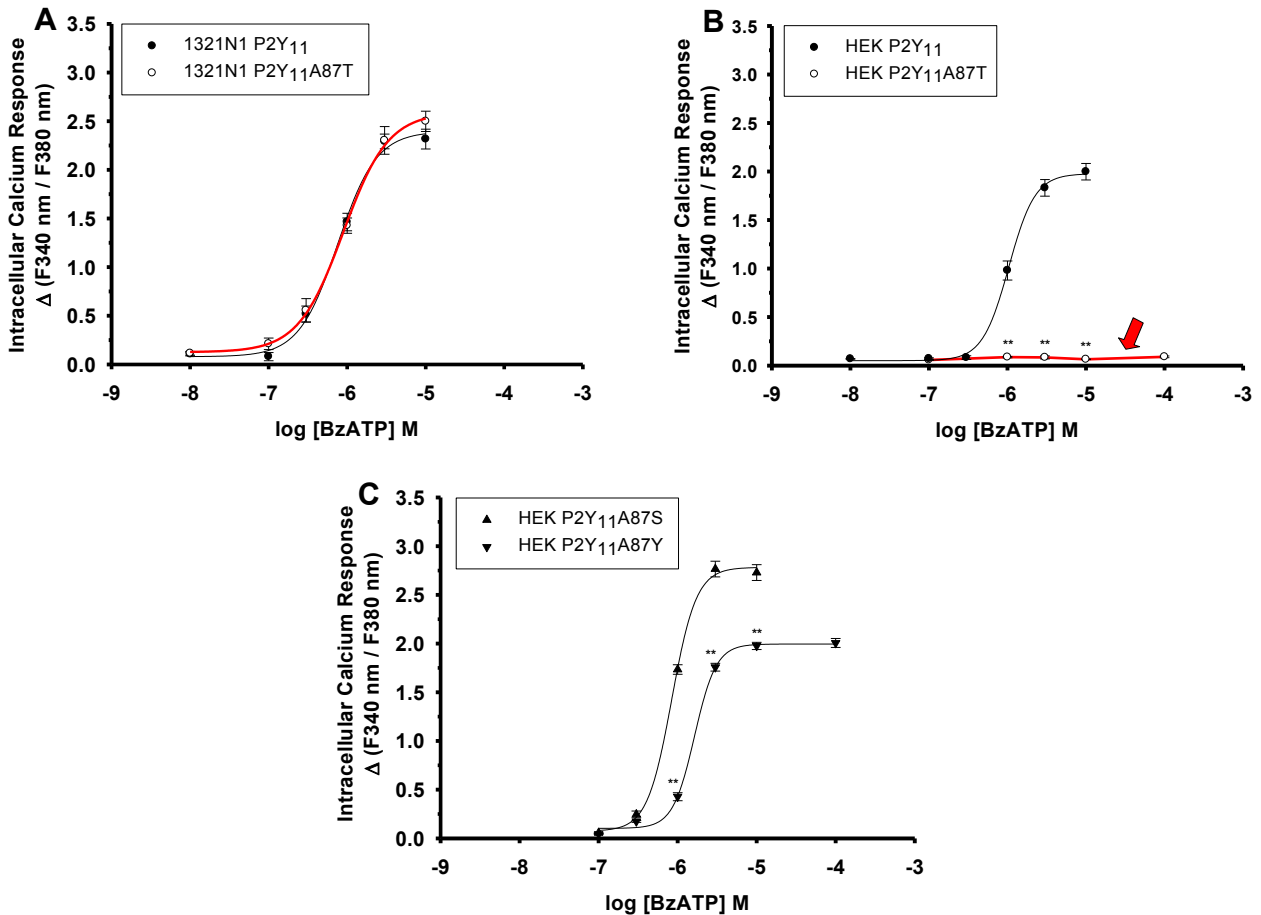
Figure 4: Concentration-response curves for the rise of [Ca²⁺]ᵢ induced by BzATP in 1321N1 astrocytoma cells and HEK293 cells expressing the P2Y₁₁A87T, P2Y₁₁A87S, P2Y₁₁A87Y, or wildtype P2Y₁₁ receptors. Responses were induced in **A:** 1321N1 astrocytoma cells expressing the human P2Y₁₁ or P2Y₁₁A87T receptor, in **B:** HEK293 cells expressing the human P2Y₁₁ or P2Y₁₁A87T receptor, and in **C:** HEK293 cells expressing the human P2Y₁₁A87S or P2Y₁₁A87Y receptor. The cells were pre-incubated with 2 µM Fura-2 AM for 30 min and the change in fluorescence (Δ F340 nm / F380 nm) was detected, as described in methods. Numbers of experiments and analyzed cells are given in methods. ** = significant differences ($P < 0.01$) of Ca^{2+} response amplitudes to the respective concentrations of nucleotides.

The human P2Y₁₁ receptor is activated by 2-MeS-ADP only at high concentrations. This was shown with P2Y₁₁ receptors expressed in 1321N1 astrocytoma cells (Figure 5A), where 2-MeS-ADP has a high EC₅₀ value of 24.2 +/- 0.3 µM (Table 1). The EC₅₀ value for 2-MeS-ADP at the P2Y₁₁A87T receptor expressed in 1321N1 astrocytoma cells was similarly high with 35.6 +/- 0.001 µM. However, 2-MeS-ADP is a very potent agonist at the human P2Y₁ receptor expressed in 1321N1 astrocytoma cells with a very low EC₅₀ value of 0.33 +/- 0.18 nM (Figure 5D).

Due to the endogenous P2Y₁ receptor expression, HEK293 wildtype cells react strongly to 2-MeS-ADP (Figure 5B) with a low EC₅₀ value of 0.04 +/- 0.006 µM (Table 2). Remarkably, in HEK293 cells expressing the P2Y₁₁ receptor the EC₅₀ value of 2-MeS-ADP increased to 0.14 +/- 0.01 µM. Expression of the P2Y₁₁A87T receptor even further increased the EC₅₀ value to 1.2 +/- 0.3 µM ($P < 0.01$). The potency of 2-MeS-ADP at HEK293 cells expressing the P2Y₁₁A87S or P2Y₁₁A87Y receptor (Figure 5C) was on about the same level with the wildtype P2Y₁₁ receptor

(EC$_{50}$ = 0.5 +/- 0.09 µM and 0.1 +/- 0.04 µM, respectively). Again, the P2Y$_{11}$A87S receptor showed an about 40% higher (P < 0.01) maximal response amplitude than the P2Y$_{11}$A87Y receptor. The latter receptor displayed maximal Ca^{2+} responses comparable to that of the P2Y$_{11}$A87T receptor and the wildtype P2Y$_{11}$ receptor.
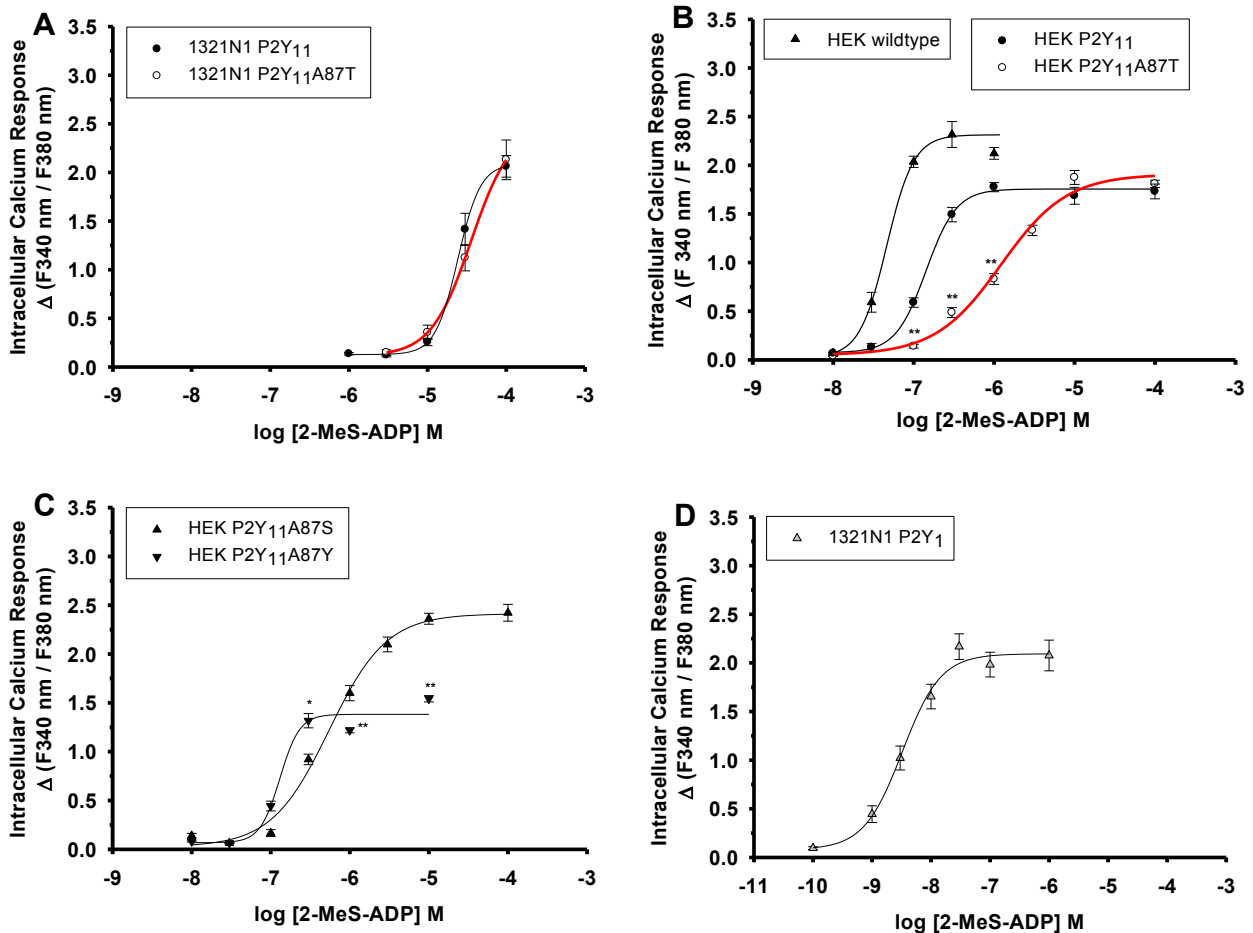
Figure 5: Concentration-response curves for the rise of [Ca^{2+}]$_i$ induced by 2-MeS-ADP in 1321N1 astrocytoma cells and HEK293 cells expressing P2Y$_{11}$A87T, P2Y$_{11}$A87S, P2Y$_{11}$A87Y, or wildtype P2Y$_{11}$ receptors. Responses were induced in **A:** 1321N1 astrocytoma cells expressing the human P2Y$_{11}$ or P2Y$_{11}$A87T receptor, in **B:** HEK293 cells expressing the human P2Y$_{11}$ or P2Y$_{11}$A87T receptor, in **C:** HEK293 cells expressing the human P2Y$_{11}$A87S or P2Y$_{11}$A87Y receptor, and in **D:** 1321N1 astrocytoma cells expressing the human P2Y$_{1}$ receptor. The cells were pre-incubated with 2 µM Fura-2 AM for 30 min and the change in fluorescence (Δ F340 nm / F380 nm) was detected, as described in methods. Numbers of experiments and analyzed cells are given in methods. ** / * = significant differences (P < 0.01; P < 0.05, respectively) of Ca^{2+} response amplitudes to the respective concentrations of nucleotides; B: significant differences of Ca^{2+} response amplitudes to respective concentrations of nucleotides mediated by the P2Y$_{11}$ and the P2Y$_{11}$A87T receptors.

BzATP and 2-MeS-ADP are synthetic nucleotides. Therefore the physiological P2Y receptor ligand ATP was additionally used to investigate the intracellular Ca^{2+} response amplitudes using 1321N1 astrocytoma cells and HEK293 cells (Figure 6). The P2Y$_{11}$ and P2Y$_{11}$A87T receptors expressed in 1321N1 astrocytoma cells (Figure 6A) yield very similar EC$_{50}$ values for ATP with

2.6 +/- 0.4 µM and 2.8 +/- 0.3 µM, respectively (Table 1). For HEK293 cells expressing the $P2Y_{11}$ receptor (Figure 6B), the EC_{50} value of 1.8 +/- 0.08 µM for ATP was identical to the EC_{50} value of 1.8 +/- 0.02 µM at HEK293 wildtype cells (Table 2). In HEK293 cells expressing the $P2Y_{11}A87T$ receptor (Figure 6B), however, the EC_{50} value was significantly ($P < 0.01$) increased to 2.8 +/- 0.2 µM. The $P2Y_{11}A87S$ and $P2Y_{11}A87Y$ receptors expressed in HEK293 cells (Figure 6C) show similarly increased EC_{50} values for ATP (2.9 +/- 0.3 µM and 3.5 +/- 0.5 µM, respectively).
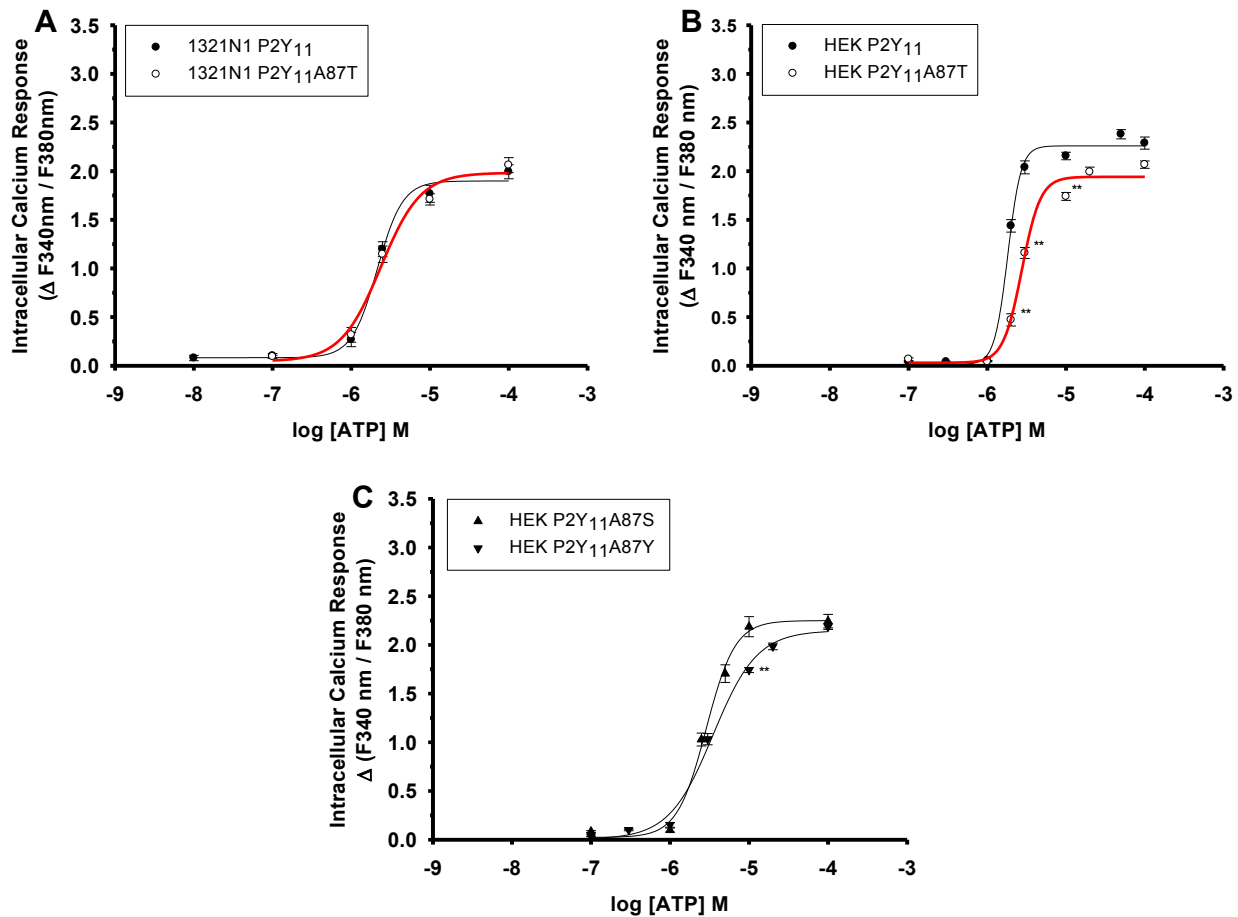
Figure 6: Concentration-response curves for the rise of $[Ca^{2+}]_i$ induced by ATP in 1321N1 astrocytoma cells and HEK293 cells expressing the $P2Y_{11}A87T$, $P2Y_{11}A87S$, $P2Y_{11}A87Y$, or wildtype $P2Y_{11}$ receptors. Responses were induced in **A:** 1321N1 astrocytoma cells expressing the human $P2Y_{11}$ or $P2Y_{11}A87T$ receptor, in **B:** HEK293 cells expressing the human $P2Y_{11}$ or $P2Y_{11}A87T$ receptor, and in **C:** HEK293 cells expressing the human $P2Y_{11}A87S$ or $P2Y_{11}A87Y$ receptor. The cells were pre-incubated with 2 µM Fura-2 AM for 30 min and the change in fluorescence (Δ F340 nm / F380 nm) was detected, as described in methods. Numbers of experiments and analyzed cells are given in methods. ** = significant differences ($P < 0.01$) of Ca^{2+} response amplitudes to the respective concentrations of nucleotides.

Table 1: Potencies (EC$_{50}$ values in µM) of BzATP, 2-MeS-ADP, and ATP at the human wildtype P2Y$_{11}$ and mutated P2Y$_{11}$A87T receptor expressed in 1321N1 astrocytoma cells.

Data were derived from concentration-response curves given in Fig. 4 - 6.

1321N1 astrocytoma cells

Intracellular Ca^{2+} response (EC$_{50}$ (µM) +/- SEM)

Nucleotide	P2Y$_{11}$	P2Y$_{11}$A87T
BzATP (Fig. 4A)	0.8 +/- 0.1	0.9 +/- 0.07
2-MeS-ADP (Fig. 5A)	24.2 +/- 0.3	35.6 +/- 0.001
ATP (Fig. 6A)	2.6 +/- 0.4	2.8 +/- 0.3

Table 2: Potencies (EC$_{50}$ values in µM) of BzATP, 2-MeS-ADP, and ATP at the human wildtype P2Y$_{11}$ receptor and the mutated P2Y$_{11}$A87T, P2Y$_{11}$A87S, and P2Y$_{11}$A87Y receptors expressed in HEK293 cells.

Data were derived from concentration-response curves given in Fig. 4 - 6.

HEK293 cells

Intracellular Ca^{2+} response (EC$_{50}$ (µM) +/- SEM)

Nucleotide	P2Y$_{11}$	P2Y$_{11}$A87T	P2Y$_{11}$A87S	P2Y$_{11}$A87Y	Control: wildtype cells (Fig. 7)
BzATP (Fig. 4)	1.0 +/- 0.05	n.r.	0.8 +/- 0.06	1.6 +/- 0.1	n.r.
2-MeS-ADP (Fig. 5)	0.14 +/- 0.01	1.2 +/- 0.3	0.5 +/- 0.09	0.1 +/- 0.04	0.04 +/- 0.006
ATP (Fig. 6)	1.8 +/- 0.08	2.8 +/- 0.2	2.9 +/- 0.3	3.5 +/- 0.5	1.8 +/- 0.02

Major conclusions

The P2Y$_{11}$ and P2Y$_{11}$A87T receptors show identical Ca^{2+} responses in 1321N1 cells.

In HEK293 cells, the P2Y$_{11}$A87T receptor cannot be activated by BzATP.

Several human P2Y receptors can be activated by adenine or uridine nucleotides. Thus, a technical control experiment was conducted using HEK293 wildtype cells. The intracellular Ca^{2+} responses induced by ATP, BzATP, 2-MeS-ADP, UTP, or UDP were used to evaluate the presence of endogenously expressed P2 receptors. In HEK293 wildtype cells, the $P2Y_1$ receptor specific agonist 2-MeS-ADP induced a strong Ca^{2+} response (Figure 7), thus verifying the presence of endogenous $P2Y_1$ receptors. BzATP is unable to induce Ca^{2+} responses for concentrations of up to 100 μM, demonstrating the absence of endogenous $P2Y_{11}$ receptors. ATP triggers a strong intracellular Ca^{2+} response. However, ATP is an agonist for the $P2Y_1$, $P2Y_2$, and $P2Y_{11}$ receptors as well as for the P2X receptor family of ion channels which could all cause the observed rise of $[Ca^{2+}]_i$. As shown in Figure 8A, the $P2Y_1$ receptor-specific antagonist MRS2179 completely inhibits the Ca^{2+} response to ATP in HEK293 wildtype cells. Therefore, the Ca^{2+} response to ATP is entirely driven by the $P2Y_1$ receptor and there is no contribution of other ATP-activated P2Y receptors. HEK293 wildtype cells show a Ca^{2+} response to UTP (Figure 8A). The $P2Y_2$ receptor can be activated by UTP and ATP. However, $P2Y_2$ receptor activity can be ruled out, since the ATP-induced Ca^{2+} response was inhibited by MRS2179. Therefore, we suggest the presence of the UTP-preferring $P2Y_4$ receptor in these cells. UDP did not induce an intracellular Ca^{2+} response, verifying the absence of $P2Y_6$ receptor activity.

$P2X_1$ and $P2X_7$ receptors can be activated by BzATP with respective EC_{50} values in the nano- and micromolar range (Bianchi *et al.*, 1999; Donnelly-Roberts *et al.*, 2004). As no rise of $[Ca^{2+}]_i$ was detected for BzATP concentrations of up to 100 μM (Figure 7), the expression of these receptors can be ruled out.

In 1321N1 astrocytoma wildtype cells, the presence of the P2Y and P2X receptors, which could theoretically be the cause for a rise of $[Ca^{2+}]_i$, was ruled out, since all tested nucleotides were unable to induce a rise of $[Ca^{2+}]_i$ (Figure 8B).
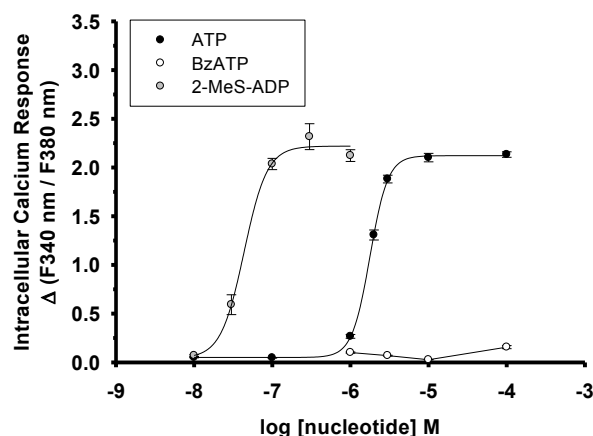
Figure 7: Concentration-response curves for the nucleotide-induced rise of $[Ca^{2+}]_i$ in HEK293 wildtype cells. Responses were induced using ATP, BzATP, or 2-MeS-ADP. The cells were pre-incubated with 2 μM Fura-2 AM for 30 min and the change in fluorescence (Δ F340 nm / F380 nm) was detected, as described in methods. Numbers of experiments and cells are given in methods.
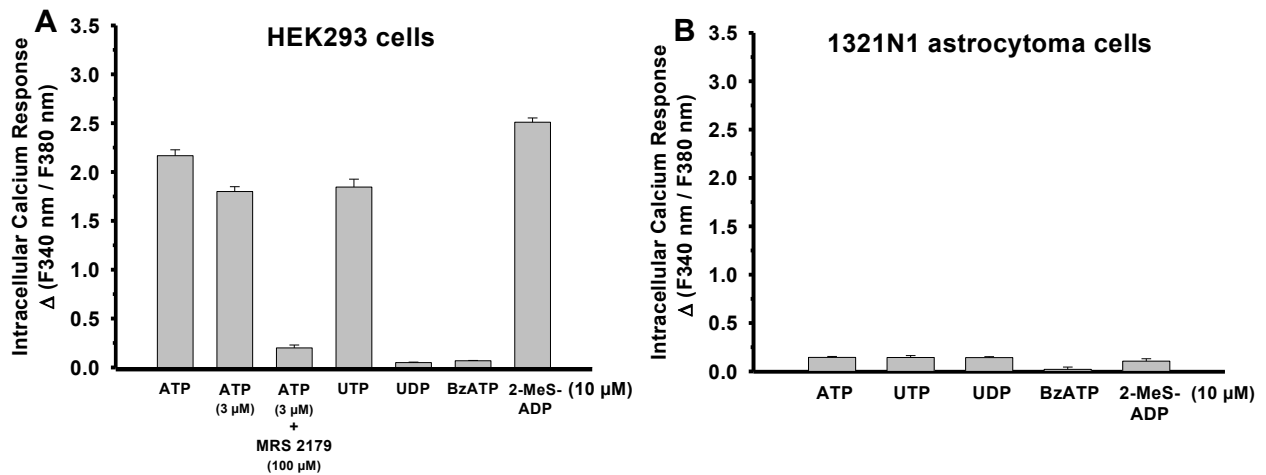
Figure 8: Amplitudes for the rise of $[Ca^{2+}]_i$ in HEK293 wildtype cells and 1321N1 astrocytoma wildtype cells induced by different nucleotides. Responses were induced by ATP without or with the $P2Y_1$ receptor-specific antagonist MRS2179, UTP, UDP, BzATP, and 2-MeS-ADP in **A:** HEK293 wildtype cells and **B:** 1321N1 astrocytoma wildtype cells. The cells were pre-incubated with 2 μM Fura-2 AM for 30 min and the change in fluorescence (Δ F340 nm / F380 nm) was detected, as described in methods. Numbers of experiments and analyzed cells are given in methods.

Using confocal microscopy, the fluorescence intensities of GFP fused to the $P2Y_{11}$, $P2Y_{11}A87T$, $P2Y_{11}A87S$, and $P2Y_{11}A87Y$ receptors in HEK293 cells were quantified in order to verify that the expression levels were equal. There was no statistical difference between fluorescence intensities of the GFP-tagged $P2Y_{11}$, $P2Y_{11}A87T$, and $P2Y_{11}A87S$ receptors (Figure 9). A small albeit significantly reduced fluorescence intensity of the GFP-tagged $P2Y_{11}A87Y$ receptor compared to the $P2Y_{11}$ ($P < 0.05$) receptor was detected.
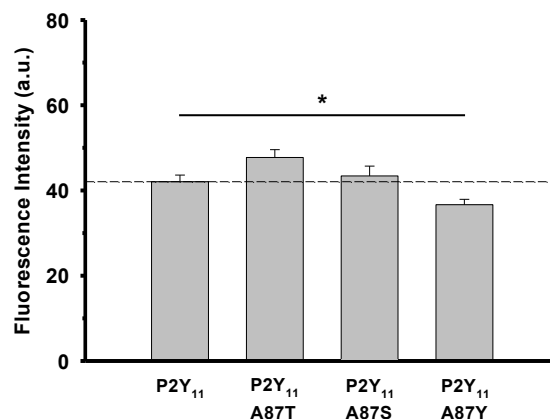
Figure 9: Fluorescence intensities of the $P2Y_{11}$ receptors tagged with GFP expressed in HEK293 cells. Cells were expressing the $P2Y_{11}$-GFP (n = 60), $P2Y_{11}A87T$-GFP (n = 80), $P2Y_{11}A87S$-GFP (n = 59), or $P2Y_{11}A87Y$-GFP (n = 70) receptors (compare Figure 18). GFP fluorescence was detected via confocal microscopy with an excitation wavelength of 488 nm.
* = significant difference ($P < 0.05$) of Ca^{2+} response amplitudes.

3.1.2 Investigation of nucleotide-induced cAMP accumulation in 1321N1 astrocytoma and HEK293 cells expressing the wildtype P2Y$_{11}$ or mutant P2Y$_{11}$A87T receptor

A unique feature of the P2Y$_{11}$ receptor within the P2Y receptor family is the dual coupling to the G$_q$ and G$_s$ signaling pathways. Therefore, the ATP-induced elevation of intracellular cAMP levels in 1321N1 astrocytoma cells and HEK293 cells was compared between wildtype P2Y$_{11}$ receptor and P2Y$_{11}$A87T receptor. In 1321N1 astrocytoma wildtype cells, no cAMP generation was detected for ATP concentrations of up to 50 µM (Figure 10A). ATP equally induced cAMP generation in 1321N1 astrocytoma cells expressing either the P2Y$_{11}$ or the P2Y$_{11}$A87T receptor. In HEK293 wildtype cells, no cAMP synthesis was detected for ATP concentrations of up to 100 µM (Figure 10B). In HEK293 cells expressing the P2Y$_{11}$A87T receptor and treated with 20 µM ATP a significantly (P < 0.05) reduced cAMP generation compared to cells expressing the P2Y$_{11}$ receptor was found.
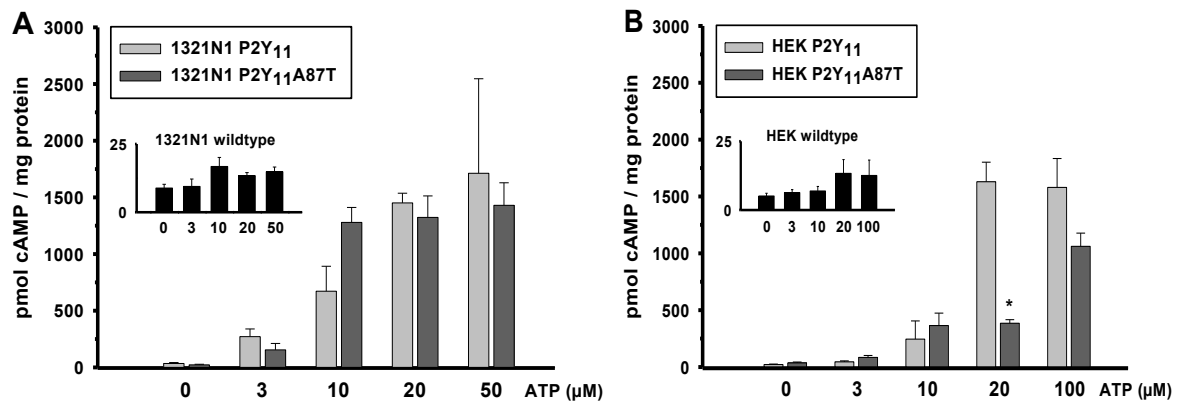
Figure 10: Levels of cAMP accumulation mediated by the P2Y$_{11}$ or P2Y$_{11}$A87T receptor induced by different concentrations of ATP. Data were obtained from **A:** 1321N1 astrocytoma cells and **B:** HEK293 cells. Wildtype cells (inset diagram) are compared to cells expressing the P2Y$_{11}$ or P2Y$_{11}$A87T receptor. The amount of cAMP per mg protein has been determined, as described in methods. * = significant difference (P < 0.05) of respective cAMP responses to 20 µM ATP of HEK293 cells expressing the P2Y$_{11}$ or the P2Y$_{11}$A87T receptor. Numbers of experiments and analyzed cells are given in methods.

3.1.3 Direct comparison of intracellular Ca^{2+} responses of transfected and non-transfected HEK293 cells under identical experimental conditions

GFP fluorescence of labeled P2Y receptors is used in the experiments to identify transfected cells within a cell culture. For the determination of EC$_{50}$ values, nucleotide-induced Ca^{2+} response amplitudes only from GFP-fluorescent cells were included in the analysis, as described before, and non-fluorescent cells were ignored. However, usually about 50% of cells within a cell culture do not show GFP fluorescence. These cells do not express the P2Y receptor of interest. This offers the

opportunity to measure intracellular Ca^{2+} responses of P2Y receptor-expressing cells (GFP-positive) and non-transfected (GFP-negative) wildtype cells under identical experimental conditions (Figure 11).

Ca^{2+} responses were evoked by BzATP, 2-MeS-ADP, or ATP in HEK P2Y$_{11}$ receptor and HEK P2Y$_{11}$A87T receptor cell cultures. Additionally, the response to ATP was analyzed without and with the addition of the P2Y$_1$ receptor antagonist MRS2179 (Table 3). For our analysis, the factor "F" was introduced. "F" is defined as the ratio of the nucleotide-induced Ca^{2+} response amplitude of GFP-positive cells divided by the response amplitude of GFP-negative cells. $F > 1$ shows that the Ca^{2+} response of GFP-positive cells was higher than that of GFP-negative cells, while $F < 1$ indicates a lower response of GFP-positive cells.

Treatment of HEK293 cells expressing the P2Y$_{11}$ receptor with 3 µM BzATP lead to a 9.5-times higher Ca^{2+} response amplitude than in GFP-negative cells at the same time ($P < 0.01$; Figure 12A), meaning that F = 9.5 (Table 3). The addition of 10 µM BzATP lead to a similar result with F = 9.0 ($P < 0.01$). This is consistent with our earlier finding that the Ca^{2+} response to BzATP in HEK293 cells expressing the P2Y$_{11}$ receptor is already near-maximal at a nucleotide concentration of 3 µM (compare Figure 4B). In cultures containing P2Y$_{11}$A87T receptor-expressing cells, 3 µM and 10 µM BzATP lead to a negligible Ca^{2+} response in GFP-positive cells, which was similar to that in GFP-negative cells.

Challenge of cell cultures containing P2Y$_{11}$ receptor-expressing cells with 1 µM or 3 µM 2-MeS-ADP lead to a reduced Ca^{2+} response ($P < 0.01$; Figure 12A) in GFP-positive cells with F = 0.6 and F = 0.8, respectively (Table 3). In cell cultures containing P2Y$_{11}$A87T receptor-expressing cells, the decrease ($P < 0.01$; Figure 12A) was even stronger with F = 0.3 for both concentrations of 2-MeS-ADP.

In agreement with our earlier results (Figure 6B; Figure 7), HEK293 cells expressing the P2Y$_{11}$A87T receptor show a significantly ($P < 0.01$; Figure 12B) decreased Ca^{2+} response to 3 µM ATP, as compared to non-transfected cells (F = 0.6), while HEK293 cells expressing the P2Y$_{11}$ receptor show a slightly but significantly increased ($P < 0.05$; Figure 12B) Ca^{2+} response (F = 1.3). The addition of the antagonist MRS2179 (100 µM) abolished the intracellular Ca^{2+} response to 3 µM ATP of GFP-negative cells. Interestingly, while the P2Y$_1$ receptor antagonist inhibited ATP-induced Ca^{2+} responses in P2Y$_{11}$A87T receptor expressing cells, GFP-positive cells in HEK P2Y$_{11}$ cell cultures were not affected.

10 µM ATP lead to Ca^{2+} response amplitudes, which were comparable to those evoked by 3 µM ATP with F = 1.2 for cultures containing P2Y$_{11}$ receptor-expressing cells and F = 0.6 for cultures containing P2Y$_{11}$A87T receptor expressing cells.

GFP-negative HEK293 cells of all tested cultures showed Ca^{2+} responses to BzATP, 2-MeS-ADP, and ATP, which were similar to the responses of HEK293 wildtype cells measured in a separate culture (Table 3). This confirmed the non-transfected state of the GFP-negative cells. HEK293 cells expressing the P2Y$_{11}$A87T receptor displayed equal or lower Ca^{2+} response amplitudes than the corresponding GFP-negative cells in all measurements. We attribute this characteristics to the interaction of the P2Y$_{11}$A87T receptors with the P2Y$_1$ receptors in these cells.

HEK P2Y$_{11}$A87T receptor cell culture

Comparison of Ca^{2+} responses of GFP+ and GFP- cells
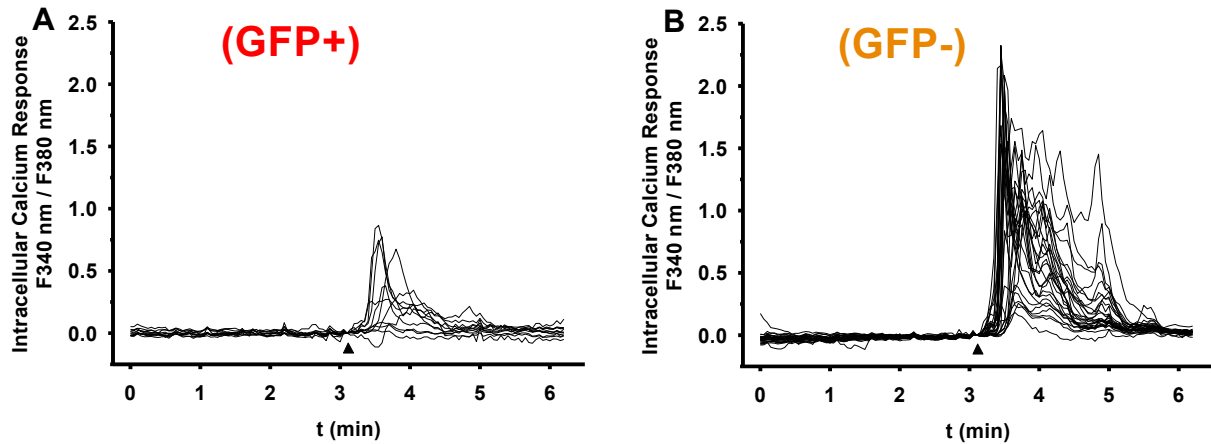
Figure 11: Examples of intracellular Ca^{2+} measurements with a HEK293 cell culture containing P2Y$_{11}$A87T receptor-expressing (GFP+) cells and non-transfected (GFP-) cells. Responses were induced using 2-MeS-ADP (1 µM; black arrowheads). **A:** Traces of the Ca^{2+} response of cells expressing the P2Y$_{11}$A87T receptor (GFP+).
B: Traces of the Ca^{2+} response of non-transfected cells (GFP-).

Fura-2 fluorescence of all cells

GFP-fluorescence of the P2Y$_{11}$A87T receptor-expressing cells
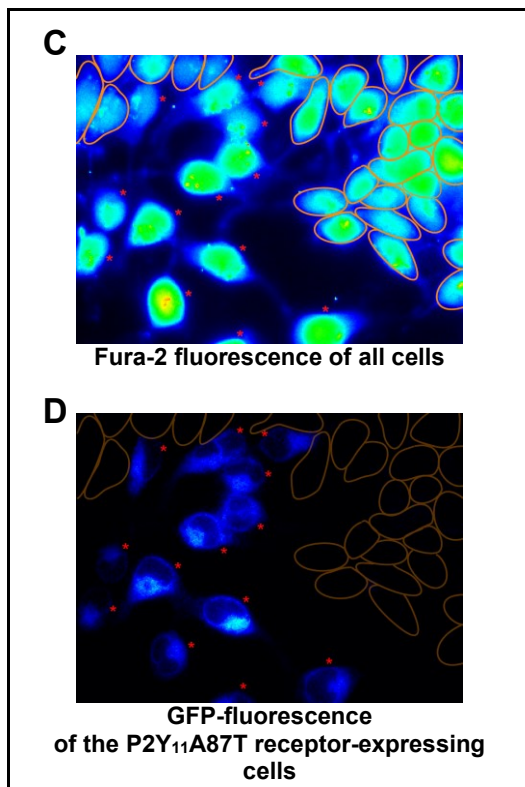
C/D: Fluorescence microscopy with cells used in A and B. **Red asterisks:** GFP+ cells (corresponding to Ca^{2+} responses shown in A). **Orange outlines:** GFP- cells (corresponding to Ca^{2+} responses shown in B) **C:** All HEK293 cells analyzed in this experiment visualized by Fura-2 fluorescence (380 nm excitation). **D:** GFP fluorescence (480 nm excitation) of HEK293 cells expressing the P2Y$_{11}$A87T receptor. For the Ca^{2+} measurements, the cells were pre-incubated with 2 µM Fura-2 AM for 30 min and the change in fluorescence (F340 nm / F380 nm) was detected, as described in methods.

Table 3: Amplitudes of Ca²⁺ responses in HEK293 cell cultures of GFP-positive (GFP+) cells ***expressing the P2Y₁₁ or P2Y₁₁A87T receptor and non-transfected, GFP-negative (GFP-) cells.***
Responses were induced using BzATP, 2-MeS-ADP, ATP, and ATP in combination with the P2Y$_1$ receptor antagonist MRS2179 (compare Figure 12). The cells were pre-incubated with 2 µM Fura-2 AM for 30 min and the change in fluorescence (Δ F340 nm / F380 nm) was detected, as described in methods. If required, MRS2179 was added to the buffer 30 min prior to the measurement and used together with ATP. For data comparison, the factor "F" of the Ca²⁺ response amplitudes of GFP-positive / GFP-negative cells is given. F > 1.0 (green numbers) means that GFP+ cells showed higher response amplitudes than GFP- cells. F ≤ 1.0 (red numbers) means that GFP+ cells showed equal lower response amplitudes than GFP- cells.

Intracellular Ca²⁺ response amplitudes
Δ (F340 nm / F380 nm) +/- SEM

Nucleotide	P2Y₁₁			P2Y₁₁A87T			Control: HEK293 wildtype
	GFP -	GFP +	*F*	GFP -	GFP +	*F*	
BzATP (3 µM)	0.2 +/- 0.02	1.9 +/- 0.07	*9.5*	0.09 +/- 0.02	0.09 +/- 0.02	*1.0*	0.07 +/- 0.01
BzATP (10 µM)	0.2 +/- 0.01	1.8 +/- 0.1	*9.0*	0.2 +/- 0.04	0.07 +/- 0.01	*0.4*	0.07 +/- 0.003
2-MeS-ADP (1 µM)	1.9 +/- 0.06	1.1 +/- 0.1	*0.6*	1.5 +/- 0.1	0.5 +/- 0.08	*0.3*	2.1 +/- 0.06
2-MeS-ADP (3 µM)	3.0 +/- 0.1	2.5 +/- 0.1	*0.8*	2.6 +/- 0.15	0.8 +/- 0.03	*0.3*	2.5 +/- 0.06
ATP (3 µM)	1.6 +/- 0.07	2.0 +/- 0.07	*1.3*	1.9 +/- 0.08	1.2 +/- 0.06	*0.6*	1.8 +/- 0.05
ATP (3 µM) + MRS2179 (100 µM)	0.4 +/- 0.07	1.9 +/- 0.1	*4.8*	0.2 +/- 0.04	0.1 +/- 0.01	*0.5*	0.2 +/- 0.03
ATP (10 µM)	1.8 +/- 0.06	2.2 +/- 0.11	*1.2*	2.5 +/- 0.06	1.6 +/- 0.05	*0.6*	2.2 +/- 0.06
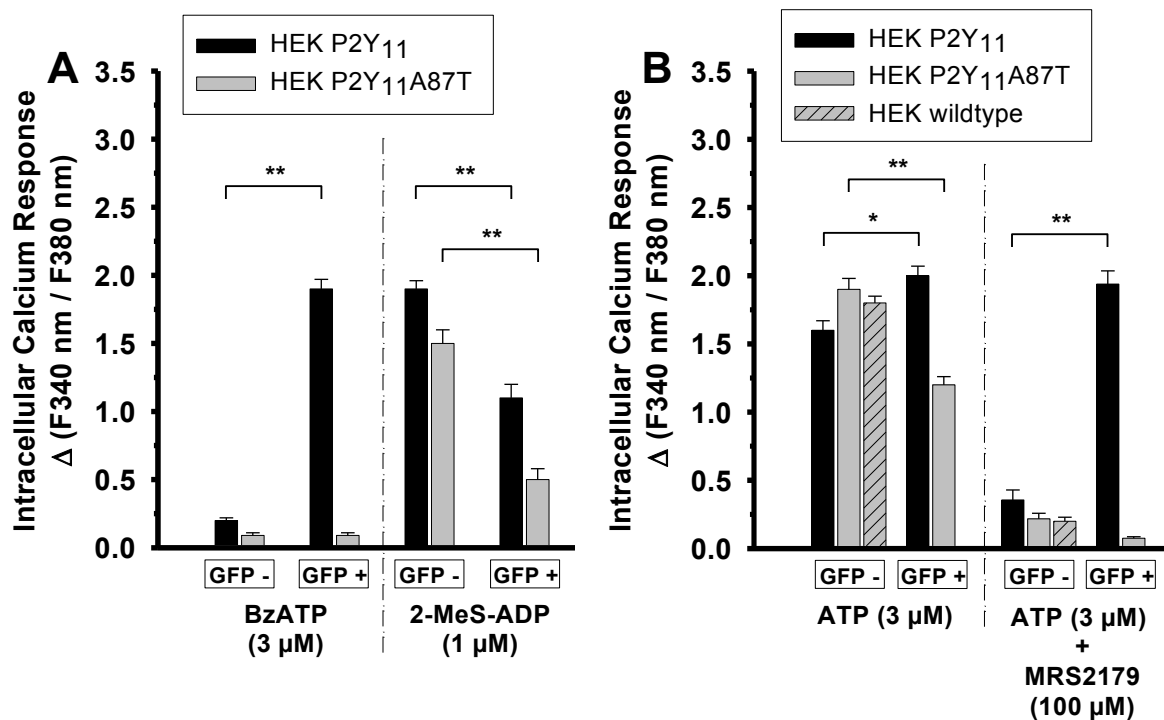
Figure 12: Amplitudes of Ca²⁺ responses of GFP-positive (GFP+) cells expressing the P2Y₁₁ or P2Y₁₁A87T receptor and non-transfected, GFP-negative (GFP-) cells in HEK293 cell cultures. Responses were induced using **A:** BzATP, 2-MeS-ADP, and **B:** ATP without or in combination with the P2Y₁ receptor antagonist MRS2179. The cells were pre-incubated with 2 µM Fura-2 AM for 30 min and the change in fluorescence (Δ F340 nm / F380 nm) was detected, as described in methods. If required, MRS2179 was added to the buffer 30 min prior to the measurement and used together with ATP. **/ * = significant difference ($P < 0.01$; $P < 0.05$, respectively) of Ca²⁺ response amplitudes. Numbers of experiments and analyzed cells are given in methods.

In order to rule out the possibility that it is merely the GFP-tag fused to the P2Y₁₁ or P2Y₁₁A87T receptor, which causes the observed changes in nucleotide-induced intracellular Ca²⁺ responses, the following experiment was conducted. GFP-negative HEK293 cells and cells expressing the G$_q$ coupled protease-activated receptor (PAR) 2 with a C-terminal GFP-tag (Table 4) were challenged with ATP concentrations of 3 µM and 10 µM. Both concentrations of ATP evoked identical Ca²⁺ response amplitudes in GFP-positive and GFP-negative HEK293 cells. Thus, the GFP-tag fused to the P2Y₁₁ or P2Y₁₁A87T receptors did not influence the measurements.

Table 4: Amplitudes of Ca^{2+} responses in HEK293 cell cultures of GFP-positive (GFP+) cells expressing the protease-activated receptor (PAR) 2 and non-transfected, GFP-negative (GFP-) cells. The cells were pre-incubated with 2 µM Fura-2 AM for 30 min and the change in fluorescence (Δ F340 nm / F380 nm) was detected, as described in methods.

<div align="center">

Intracellular Ca^{2+} response amplitudes
Δ (F340 nm / F380 nm) +/- SEM

</div>

Nucleotide	PAR 2		Control: HEK293 wildtype
	GFP -	GFP +	
ATP (3 µM)	1.5 (+/- 0.05)	1.4 (+/- 0.04)	1.8 +/- 0.05
ATP (10 µM)	2.0 (+/- 0.08)	2.0 (+/- 0.06)	2.2 +/- 0.06

3.1.4 Co-expression of the $P2Y_{11}$ or $P2Y_{11}A87T$ receptor with the $P2Y_1$ receptor in 1321N1 astrocytoma cells

Differences in the Ca^{2+} responses mediated by the $P2Y_{11}A87T$ and $P2Y_{11}$ receptor were found only in HEK293 cells, but not in 1321N1 astrocytoma cells. HEK293 cells endogenously express the $P2Y_1$ receptor, but 1321N1 astrocytoma cells lack any endogenous P2Y receptor expression. In order to investigate whether the presence of the $P2Y_1$ receptor is necessary for reduced Ca^{2+} responses mediated by $P2Y_{11}A87T$ receptor, the $P2Y_{11}A87T$ or $P2Y_{11}$ receptors were co-expressed with the $P2Y_1$ receptor in 1321N1 astrocytoma cells (Figure 13). The results were compared to 1321N1 astrocytoma wildtype cells and cells expressing the $P2Y_{11}$ or $P2Y_{11}A87T$ receptor alone.

The intracellular Ca^{2+} concentration of the 1321N1 astrocytoma cells was monitored during treatment with 1 µM of the $P2Y_{11}$ receptor agonist BzATP and, after a recovery period of at least 2 min, a subsequent treatment with 1 µM of the potent $P2Y_1$ receptor agonist 2-MeS-ADP. 1321N1 astrocytoma cells expressing the $P2Y_{11}$ or $P2Y_{11}A87T$ receptor showed clear GFP fluorescence. A response to 2-MeS-ADP verified functional $P2Y_1$ receptor expression. Fluorescence traces showing the Ca^{2+} mobilization in representative experiments with 1321N1 astrocytoma cells co-expressing the $P2Y_1$ with $P2Y_{11}$ or $P2Y_{11}A87T$ receptors and cells expressing the $P2Y_{11}A87T$ receptor alone are presented in Figure 14.

Single-transfected 1321N1 astrocytoma cells expressing only the $P2Y_1$ receptor showed a negligible Ca^{2+} response to BzATP, but a strong response to 2-MeS-ADP (Figure 13). Single-transfected cells expressing the $P2Y_{11}$ or $P2Y_{11}A87T$ receptor showed a strong Ca^{2+} response to BzATP (no statistically significant difference) and no Ca^{2+} response to 2-MeS-ADP. Cells co-expressing the $P2Y_{11}$ with the $P2Y_1$ receptor showed a Ca^{2+} response amplitude to the BzATP stimulus, similar to that of the single-transfected $P2Y_{11}$ or $P2Y_{11}A87T$ receptor-expressing cells.

Only in 1321N1 astrocytoma cells co-expressing the $P2Y_{11}A87T$ with the $P2Y_1$ receptor, there was a significantly reduced Ca^{2+} response to BzATP, compared to cells co-expressing the $P2Y_{11}$ with $P2Y_1$ receptor ($P < 0.01$; Figure 13). Also, the respective responses to BzATP of the cells co-

expressing the $P2Y_{11}A87T$ and $P2Y_1$ receptor was significantly lower than that of cells expressing the $P2Y_{11}A87T$ receptor ($P < 0.01$) or the $P2Y_{11}$ receptor ($P < 0.01$) alone. The Ca^{2+} responses to 2-MeS-ADP of all single- or double-transfected cells with $P2Y_1$ receptor expression were similar.
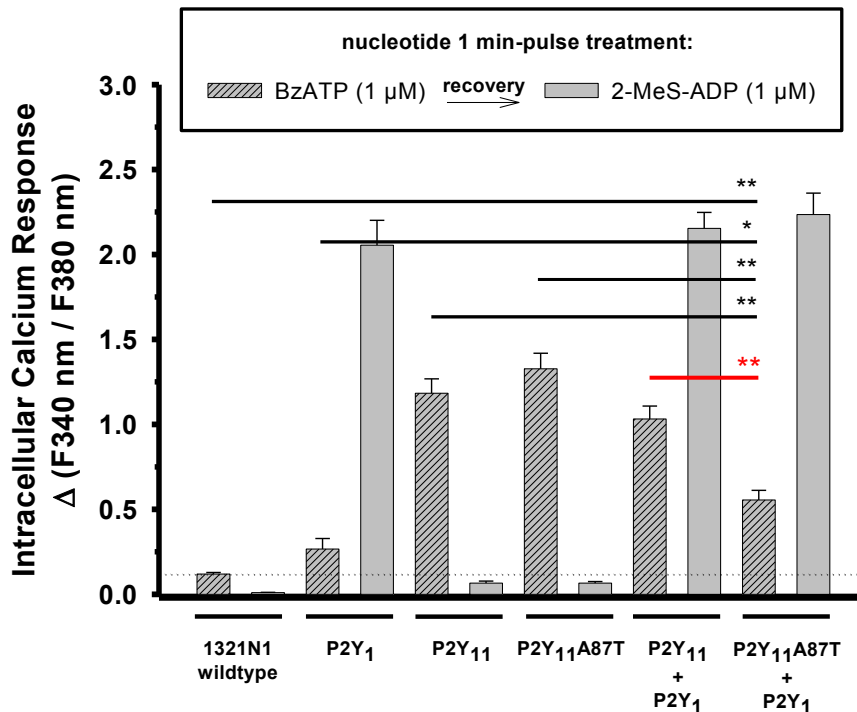
Figure 13: Amplitudes of the rise of $[Ca^{2+}]_i$ in 1321N1 astrocytoma cells co-expressing the $P2Y_1$ and $P2Y_{11}$ or $P2Y_{11}A87T$ receptors, respectively. Response amplitudes were compared with cells expressing the $P2Y_1$, $P2Y_{11}$, or $P2Y_{11}A87T$ receptors alone. Cells were treated sequentially with a 1 min-pulse of BzATP (1 µM) followed by a 1 min-pulse of 2-MeS-ADP (1 µM) after an intermittent recovery period of at least 2 min. This stimulus pattern is given above the bar diagram. The cells were pre-incubated with 2 µM Fura-2 AM for 30 min and the change in fluorescence (Δ F340 nm / F380 nm) was detected, as described in methods. **/ * = significant differences ($P < 0.01$ and $P < 0.05$, respectively) of Ca^{2+} response amplitudes. Dashed line represents background response of 1321N1 wildtype cells to the BzATP treatment. Numbers of experiments and analyzed cells are given in methods.

Major conclusions

Only $P2Y_{11}A87T$ and $P2Y_1$ receptor co-expressing cells show reduced Ca^{2+} response to BzATP.

$P2Y_{11}$ and $P2Y_1$ receptor co-expressing cells and $P2Y_{11}$ and $P2Y_{11}A87T$ receptor single-expressing cells show comparable Ca^{2+} response to BzATP.
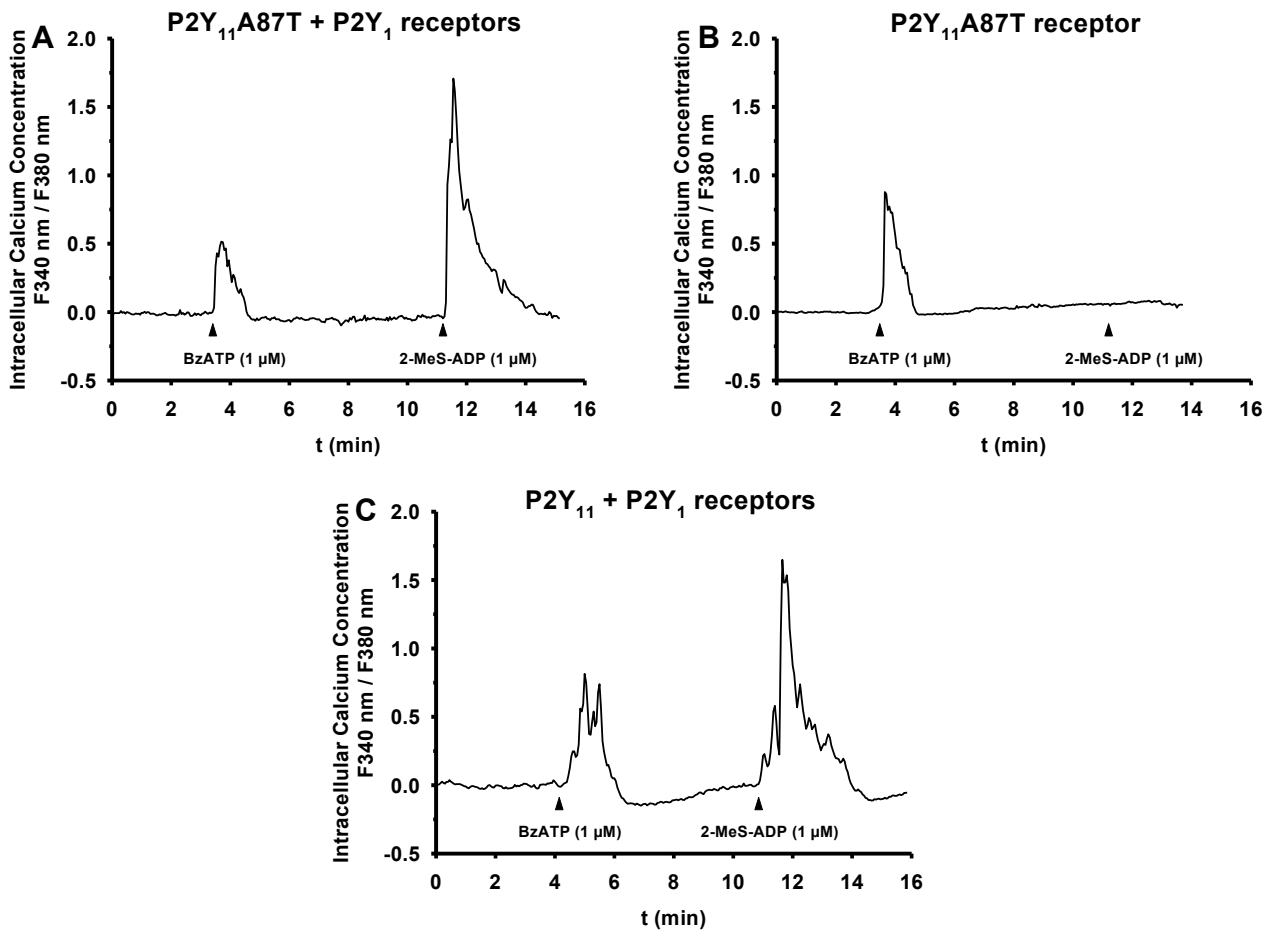
Figure 14: Representative traces for intracellular Ca^{2+} mobilization in single- and double-transfected 1321N1 astrocytoma cells. Responses were induced in cells expressing **A:** the P2Y$_1$ and P2Y$_{11}$A87T receptors, **B:** the P2Y$_{11}$A87T receptor alone, and **C:** the P2Y$_1$ and P2Y$_{11}$ receptors. Cells were treated sequentially with a 1 min-pulse of BzATP (1 µM) followed by a 1 min-pulse of 2-MeS-ADP (1 µM) after an intermittent recovery period of circa 3 min (A/B) or 2 min (C). The cells were pre-incubated with 2 µM Fura-2 AM for 30 min and the change in fluorescence (Δ F340 nm / F380 nm) was detected, as described in methods.

As can be seen in Figure 15, the P2Y$_1$-myc/His, P2Y$_{11}$-GFP, and P2Y$_{11}$A87T-GFP proteins were found to be localized at the plasma membrane in the 1321N1 astrocytoma cells. There was no statistical difference in receptor expression levels according to the GFP and Alexa555 fluorescence levels Figure 16.

The rise of the intracellular Ca^{2+} level mediated by the P2Y$_1$-myc/His receptor expressed in 1321N1 astrocytoma cells was similar to the response mediated by the P2Y$_1$-GFP receptor for concentrations of 2-MeS-ADP of 0.001 µM, 0.01 µM, and 1.0 µM (Figure 17). Only at a concentration of 2-MeS-ADP of 0.001 µM, the P2Y$_1$-myc/His receptor showed a higher response amplitude ($P < 0.05$). Furthermore, the P2Y$_1$-myc/His receptor has been shown before to undergo nucleotide-induced endocytosis in 1321N1 astrocytoma cells, like the P2Y$_1$-GFP receptor (Ecke *et al.*, 2008a). This demonstrates identical functioning of P2Y$_1$ receptors with both tags. This is in line with an earlier study (Tulapurkar *et al.*, 2005) in which the rat P2Y$_2$-GFP and P2Y$_2$-myc/His receptor were compared regarding the nucleotide-induced intracellular Ca^{2+} elevation and were found to respond very similarly.
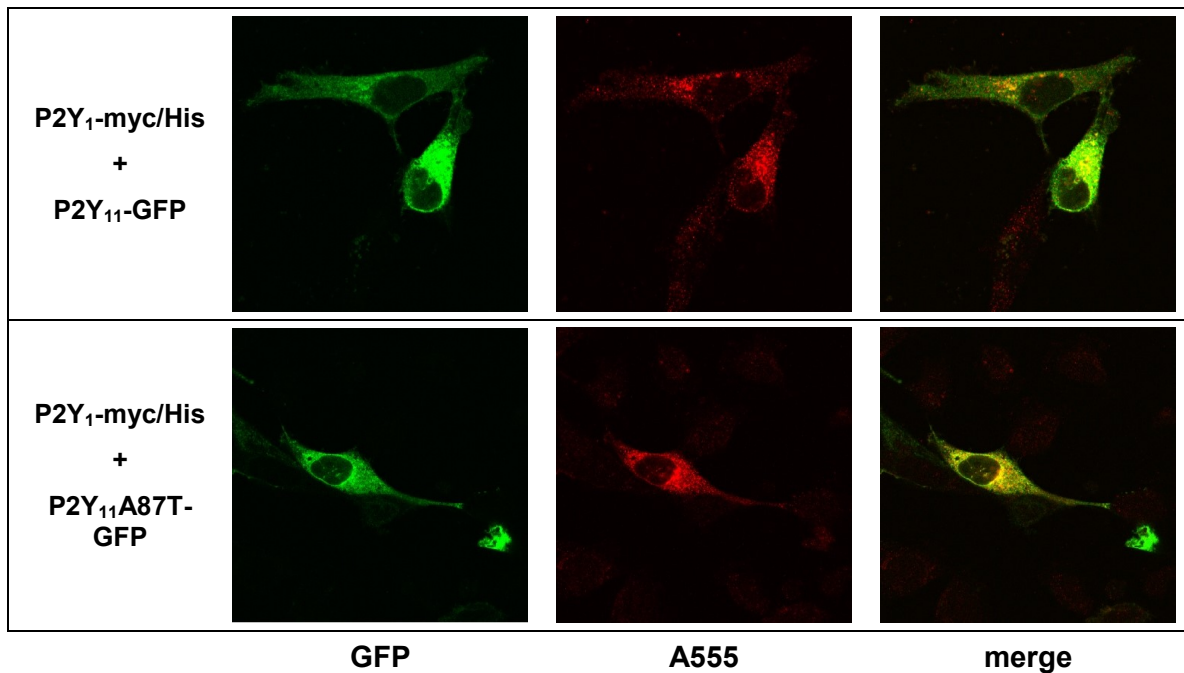
Figure 15: Co-expression of the P2Y$_1$-myc/His and P2Y$_{11}$-GFP or P2Y$_{11}$A87T-GFP receptors in 1321N1 astrocytoma cells. Cells were fixed with para-formaldehyde and GFP-fluorescence (green) was visualized with 488 nm excitation. The P2Y$_1$-myc/His receptors (red) were detected via α-mycA555 antibody binding and excitation at 543 nm. Immunocytochemistry was performed, as described in methods.
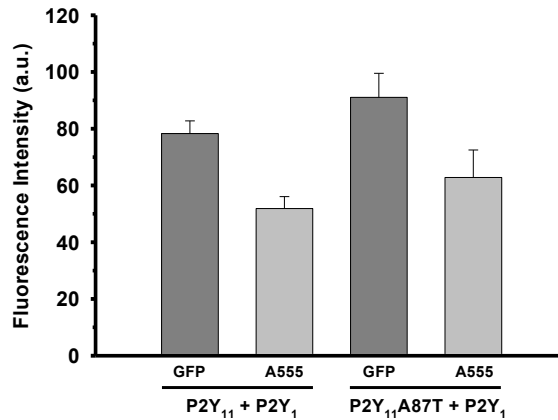
***Figure 16: Fluorescence intensities of GFP and Alexa555 in 1321N1 astrocytoma cells
co-expressing the P2Y$_1$-myc/His and P2Y$_{11}$-GFP (n = 75) or P2Y$_{11}$A87T-GFP receptors (n = 46).***
GFP-fluorescence was visualized with 488 nm excitation. Alexa555 was detected via α-mycA555
antibody binding and excitation at 543 nm (compare Figure 15). Immunocytochemistry was performed,
as described in methods.
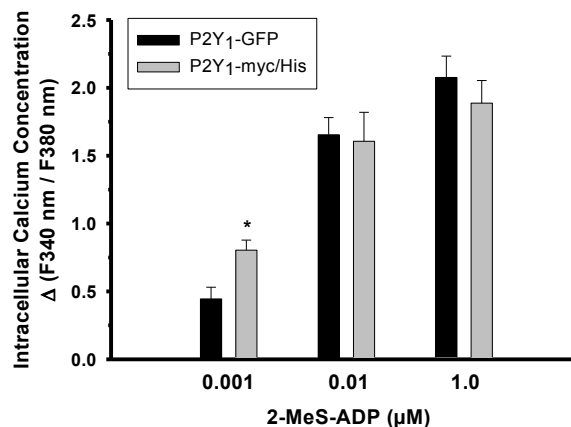
***Figure 17: Amplitudes of the rise of [Ca^{2+}]$_i$ in 1321N1 astrocytoma cells expressing the human
P2Y$_1$-GFP or P2Y$_1$-myc/His receptors.*** Responses were induced using different concentrations of
2-MeS-ADP. The cells were pre-incubated with 2 µM Fura-2 AM for 30 min and the change in
fluorescence (Δ F340 nm / F380 nm) was detected, as described in methods. Numbers of experiments
and analyzed cells are given in methods. * = significant difference (P < 0.05) of the Ca^{2+} responses to
0.001 µM 2-MeS-ADP.

3.1.5 Long-term treatment of HEK293 cells with nucleotides: receptor internalization of P2Y$_{11}$A87T, P2Y$_{11}$A87S, and P2Y$_{11}$A87Y receptors and long-term Ca^{2+} response sensitization

Wildtype P2Y$_{11}$ receptors expressed in HEK293 cells undergo nucleotide-induced
internalization (Ecke *et al.*, 2008). Therefore, the nucleotide-induced change of the localization of the
GFP-labeled P2Y$_{11}$, P2Y$_{11}$A87T, P2Y$_{11}$A87S, and P2Y$_{11}$A87Y receptors in HEK293 cells was
analyzed using confocal microscopy (Figure 18). 100 µM ATP or 100 µM BzATP were applied for
60 min. Untreated control cells showed plasma membrane localization of GFP fluorescence. In the

P2Y$_{11}$ receptor-expressing cells, ATP and BzATP caused a strong receptor internalization, as indicated by the accumulation of spots of GFP fluorescence in the cytosol. However, no nucleotide-induced internalization was detected in cells expressing the P2Y$_{11}$A87T or P2Y$_{11}$A87Y receptor. In cells expressing the P2Y$_{11}$A87S receptor, treatment with ATP lead to a slight receptor internalization and with BzATP to a clear internalization of GFP-labeled receptors.
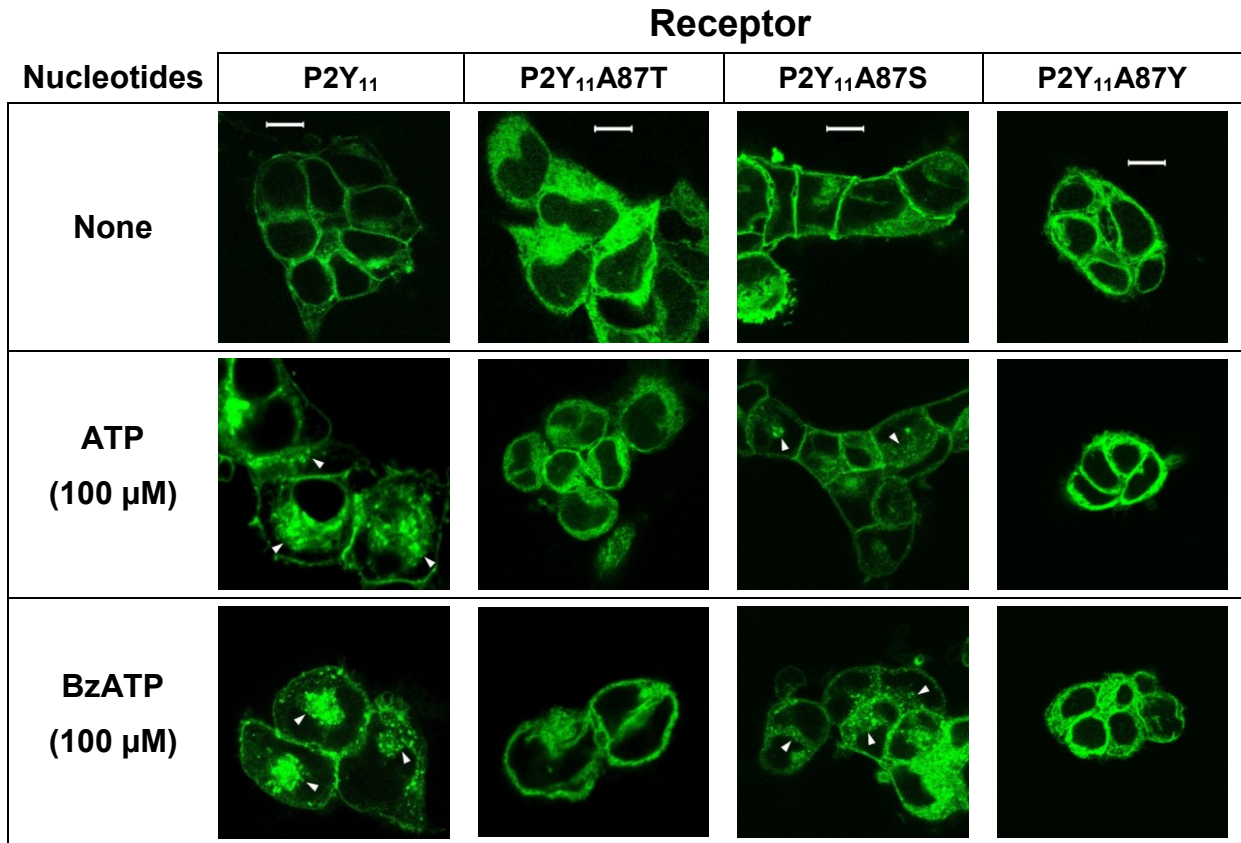
Figure 18: Nucleotide-induced internalization of wildtype P2Y$_{11}$ and mutated P2Y$_{11}$ receptors in HEK293 cells. Localization of GFP fluorescence of the P2Y$_{11}$, P2Y$_{11}$A87T, P2Y$_{11}$A87S, and P2Y$_{11}$A87Y receptors expressed as GFP fusion proteins in HEK293 cells. Representative pictures were taken after treatment with ATP or BzATP for 60 min, or without nucleotide treatment and fixation of the cells with para-formaldehyde. Scale bar represents 10 µm. White arrowheads indicate GFP fluorescence of internalized P2Y$_{11}$ or P2Y$_{11}$A87S receptors.

The lack of receptor internalization after extended treatment with a high concentration of ATP indicates that the prominent detrimental effect of the A87T mutation of the P2Y$_{11}$ receptor is most likely connected to the long-term regulation of intracellular Ca^{2+} signaling. Thus, it was investigated whether the lack of receptor internalization in HEK293 cells expressing the P2Y$_{11}$A87T receptor would result in an overall higher responsiveness of cells after a prolonged treatment with ATP. For this, cells were incubated with 100 µM ATP for 30 min, which is sufficient to induce receptor internalization in P2Y$_{11}$ receptor-expressing cells, and the change of intracellular Ca^{2+} concentration was monitored (Figure 19). After 30 min, ATP was replaced with nucleotide-free buffer and the cells were superfused for 60 min to allow for cell recovery. Finally, a short 1 min treatment with ATP (100 µM) was used to determine the extent of cell responsiveness after 90 min. This gives the long-term sensitivity of cells

co-expressing the $P2Y_1$ with $P2Y_{11}$, $P2Y_{11}A87T$, or $P2Y_{11}A87S$ receptors. In Figure 20A, the first bar represents the initial Ca^{2+} response amplitude to ATP (100 µM). The second bar indicates the remaining level of Ca^{2+}_i after 30 min incubation with ATP (100 µM), and the third bar shows the Ca^{2+} response to the second short treatment with ATP (100 µM). Compared with HEK293 cells expressing the wildtype $P2Y_{11}$ receptor, cells expressing the mutated $P2Y_{11}$ receptors showed stronger desensitization of the Ca^{2+} response after 30 min, which was coupled with stronger resensitization after 90 min.
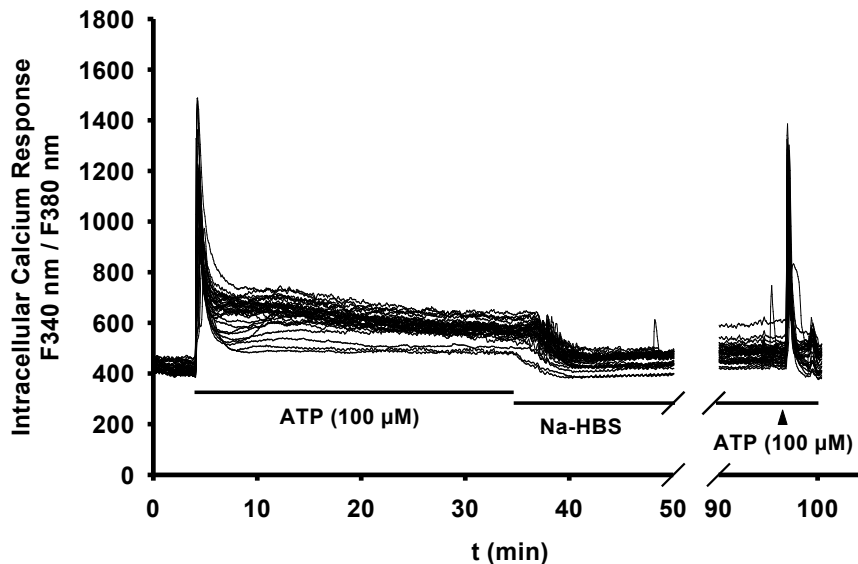
Figure 19: Traces of ATP-induced long-term intracellular Ca^{2+} mobilization in HEK293 cells expressing the $P2Y_{11}A87T$ receptor. Non-normalized, exemplary data from cells of a single experiment are shown. Cells were incubated with ATP for 30 min followed by a 60 min superfusion with nucleotide-free NaHBS buffer for recovery. Finally, a short 1 min ATP stimulus was applied. The cells were pre-incubated with 2 µM Fura-2 AM for 30 min and the change in fluorescence (F340 nm / F380 nm) was detected, as described in methods.

For HEK293 cells expressing the $P2Y_{11}$ receptor, we detected a significantly reduced (P < 0.01) Ca^{2+} level after 30 min continuous ATP-treatment down to 25% of the initial response. After the following 30 min superfusion with nucleotide-free buffer (at a total of 90 min), the intracellular Ca^{2+} response increased only 1.4-fold to 34% of the response at 0 min (P < 0.01). In HEK293 cells expressing the $P2Y_{11}A87T$ receptor, 30 min treatment with ATP reduced the $[Ca^{2+}]_i$ to 15% of the response at 0 min (P < 0.01). The extent of the response desensitization therefore was significantly higher (P < 0.01) than in cells expressing the $P2Y_{11}$ receptor. At 90 min, the Ca^{2+} response was restored with a factor of 3.4 (P < 0.01) as compared to the Ca^{2+} level at 30 min. It thus reached 51% of the response at 0 min. Recovery of the Ca^{2+} response of HEK293 cells expressing the $P2Y_{11}A87T$ receptor therefore was higher than that of $P2Y_{11}$ receptor-expressing cells. The Ca^{2+} response after 30 min continuous ATP-treatment in HEK293 cells expressing the $P2Y_{11}A87S$ receptor was reduced to 12% of the initial response at 0 min (P < 0.01). The response at 90 min was increased significantly (P < 0.01) to 4.8-fold of the response at 30 min, reaching 57% of the initial response at 0 min. Thus, desensitization and recovery of the intracellular Ca^{2+} response of HEK293 cells expressing the

P2Y$_{11}$A87S receptor was comparable to what had been observed for P2Y$_{11}$A87T receptor expressing cells.

A technical control experiment using HEK293 wildtype cells was conducted in order to rule out that stress due to the extended single-cell Ca^{2+} measurements could have caused non-physiological Ca^{2+} levels in the cells (Figure 20B). Cells superfused with NaHBS buffer for 90 min prior to a 1 min treatment with 100 µM ATP showed the same Ca^{2+} response amplitude like cells that were not pretreated. This confirms that the observed changes of intracellular Ca^{2+} responses of the HEK293 cells were not falsified by the experimental conditions.
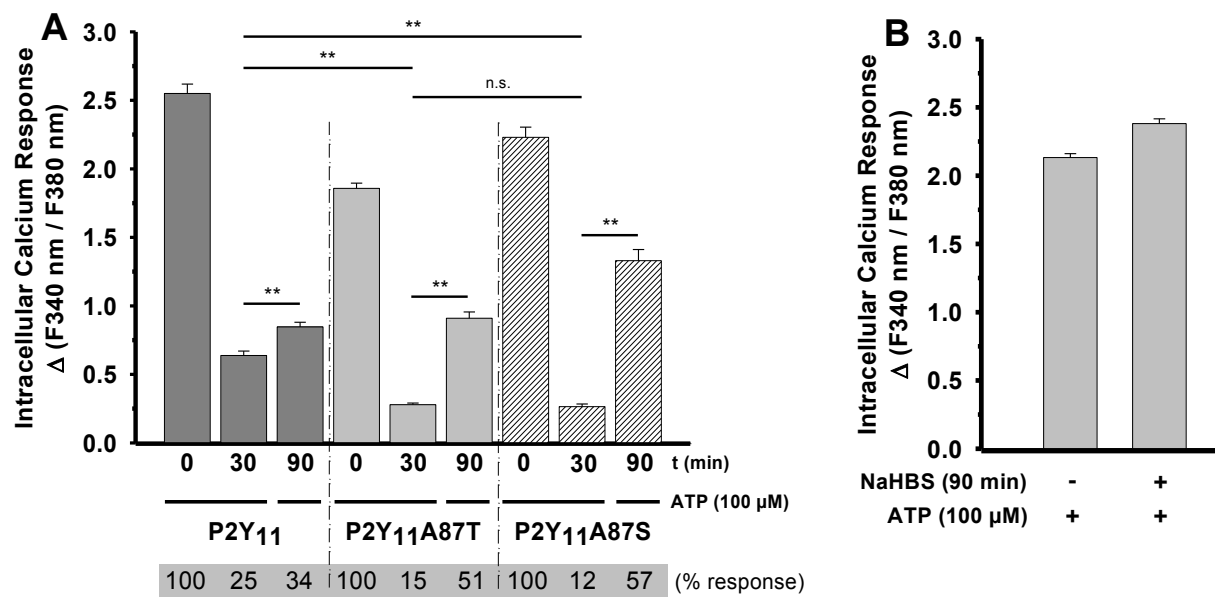
Figure 20: Nucleotide-induced long-term desensitization of Ca^{2+} responses in HEK293 cells expressing the wildtype P2Y$_{11}$, P2Y$_{11}$A87T, or P2Y$_{11}$A87S receptor. A: Amplitudes of the rise of [Ca^{2+}]$_i$ in HEK293 cells expressing the P2Y$_{11}$, P2Y$_{11}$A87T, or P2Y$_{11}$A87S receptors. Cells were incubated with ATP for 30 min followed by a 60 min superfusion with nucleotide-free Na-HBS buffer for recovery. Finally, a short 1 min ATP stimulus was applied. **B:** Amplitudes of the rise of [Ca^{2+}]$_i$ in HEK293 wildtype cells induced by ATP with and without preceding 90 min superfusion with nucleotide-free Na-HBS buffer. The cells were pre-incubated with 2 µM Fura-2 AM for 30 min and the change in fluorescence (Δ F340 nm / F380 nm) was detected, as described in methods. ** = significant differences (P < 0.01) of Ca^{2+} response amplitudes. n.s. = no significant differences of Ca^{2+} response amplitudes. Numbers of experiments and analyzed cells are given in methods.

3.2 Potency of 2-propylthio-substituted derivatives of ATP on 1321N1 astrocytoma cells expressing the human P2Y$_1$, P2Y$_2$, or P2Y$_{11}$ receptors

3.2.1 Investigation of nucleotide potencies at the human P2Y$_{11}$ receptor expressed in 1321N1 astrocytoma cells

For the investigation of the potencies of the novel ATP analogs (Figure 21), single-cell Ca^{2+} measurements were conducted on the human P2Y$_{11}$ receptor expressed in 1321N1 astrocytoma cells. Following the structural features of one of the most potent agonists of the P2Y$_{11}$ receptor, 2-propylthio-ATP-β,γ-dichloromethylene (AR-C67085), a series of 2-propylthio-substituted derivatives of ATP was generated. The novel analogs contained a 2-propylthio modification in combination with a β,γ-CCl$_2$ group and/or a Pα substitution of a non-bridging oxygen. The introduction of the Pα-BH$_3$ or Pα-S substitutions created a new chiral center at this position. As described in Haas *et al.*, 2013, the R*p* configuration was assigned to the A-isomers of borano-substituted nucleotides and to the B-isomers of thio-substituted nucleotides. The S*p* configuration therefore was assigned to the B-isomers of the borano- and to the A-isomers of the thio-substituted analogs. The resulting isomers were investigated separately.
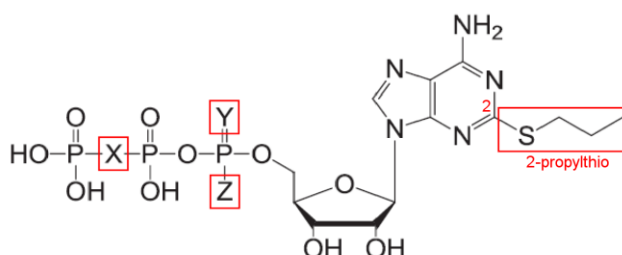
nucleotide	substitutions		
2-propylthio-ATP-αS (A/B)	Y = S	Z = O	X = O
2-propylthio-ATP-αB (A/B)	Y = O	Z = BH$_3$	X = O
2-propylthio-ATP-αS-β,γ-CCl$_2$ (A/B)	Y = S	Z = O	X = CCl$_2$
2-propylthio-ATP-αB-β,γ-CCl$_2$ (A/B)	Y = O	Z = BH$_3$	X = CCl$_2$
2-propylthio-ATP	Y = O	Z = O	X = O

Figure 21: Structure of 2-propylthio-substituted nucleotide derivatives of ATP used for the investigation of potency and selectivity at the P2Y$_{11}$ receptor (modified from Haas *et al.*, 2013).

The well-known diastereoselectivity of the human P2Y$_{11}$ receptor (Ecke *et al.*, 2008b) could not be observed for the isomers of 2-propylthio-ATP-αS, since the concentration-response curves were not significantly different (Figure 22A). The EC$_{50}$ values at the P2Y$_{11}$ receptor were very similar with 0.22 +/- 0.04 µM for the A-isomer and 0.19 +/- 0.06 µM for the B-isomer of the analog (Table 5). Nevertheless, both nucleotides showed a more than 10-times higher potency at the P2Y$_{11}$ receptor

than the physiological standard agonist ATP (EC_{50} = 2.6 +/- 0.6 µM). The isomers of ATP-αS were previously shown to activate the $P2Y_{11}$ receptor with very different potencies (Ecke *et al.*, 2006). Therefore, the 2-propylthio-substitution of the 2-propylthio-ATP-αS analogs is responsible for abolishing the stereospecificity in the activation of the $P2Y_{11}$ receptor.

The structurally similar 2-propylthio-ATP-αB, carrying an α-borano substitution instead of the α-thio group, however, displays a clear and significant $P2Y_{11}$ receptor preference for the B-isomer over the A-isomer (Figure 22B). The EC_{50} value for the B-isomer was at 0.03 +/- 0.01 µM while the EC_{50} value for the A-isomer was at 0.40 +/- 0.05 µM (Table 5). This makes the B-isomer about 13-fold more potent than the A-isomer. Both isomers yielded lower EC_{50} values than ATP. However, while the A-isomer was only about 7-fold more potent, the B-isomer was 87-times more effective than ATP in evoking intracellular Ca^{2+} responses. Also, the diastereoselectivity at the $P2Y_{11}$ receptor of the tested nucleotides was greatest for the isomers of 2-propylthio-ATP-αB.

Like AR-C67085, 2-propylthio-ATP-αS-β,γ-CCl_2 possesses a dichloromethylene group between the β- and γ-phosphate but otherwise resembles the analogs used in Figure 22A. The isomers of the α-thio substituted nucleotide show no prominent diastereoselectivity at the $P2Y_{11}$ receptor (Figure 22C) as the EC_{50} value for the A-isomer was at 0.6 +/- 0.03 µM and for the B-isomer at similar 0.85 +/- 0.2 µM (Table 5). Thus, the B-isomer was about 3-fold more potent and the A-isomer about 4-fold more potent than ATP.

2-propylthio-ATP-αB-β,γ-CCl_2 corresponds to the nucleotides used in Figure 22C but features an α-borano group instead of the α-thio group. Again, the α-BH_3 substitution restores significant stereoselectivity at the $P2Y_{11}$ receptor of the 2-propylthio-ATP derivative compared to the α-thio substituted compound (Figure 22D). The EC_{50} value for the B-isomer was at 0.03 +/- 0.01 µM and for the A-isomer at 0.1 +/- 0.05 µM (Table 5). Thus, the B-isomer was only circa 3-fold more potent than the A-isomer and diastereoselectivity was less pronounced than for 2-propylthio-ATP-αB. Since the B-isomers of 2-propylthio-ATP-αB and 2-propylthio-ATP-αB-β,γ-CCl_2 share the same EC_{50} value of 0.03 µM, the latter also is around 87-fold more potent than ATP.

The potency of 2-propylthio-ATP was shown to be virtually identical to that of ATP. The EC_{50} values of 2.5 +/- 0.5 µM for 2-propylthio-ATP and 2.6 +/- 0.6 µM for ATP were very similar (Table 5). Differences in the concentration-response curves were non-significant (Figure 22E). Therefore, the propylthio-substitution at position 2 of the adenine alone cannot account for an increased potency of the aforementioned nucleotides as compared to that of ATP.

The rank order of potencies for the tested novel adenine nucleotides was found to be: 2-propylthio-ATP-αB(B) = 2-propylthio-ATP-αB-β,γ-CCl_2(B) >> 2-propylthio-ATP-αB-β,γ-CCl_2(A) = 2-propylthio-ATP-αS(B) = 2-propylthio-ATP-αS(A) > 2-propylthio-ATP-αB(A) > 2-propylthio-ATP-αS-β,γ-CCl_2(A) > 2-propylthio-ATP-αS-β,γ-CCl_2(B) >> 2-propylthio-ATP = <u>ATP</u>.
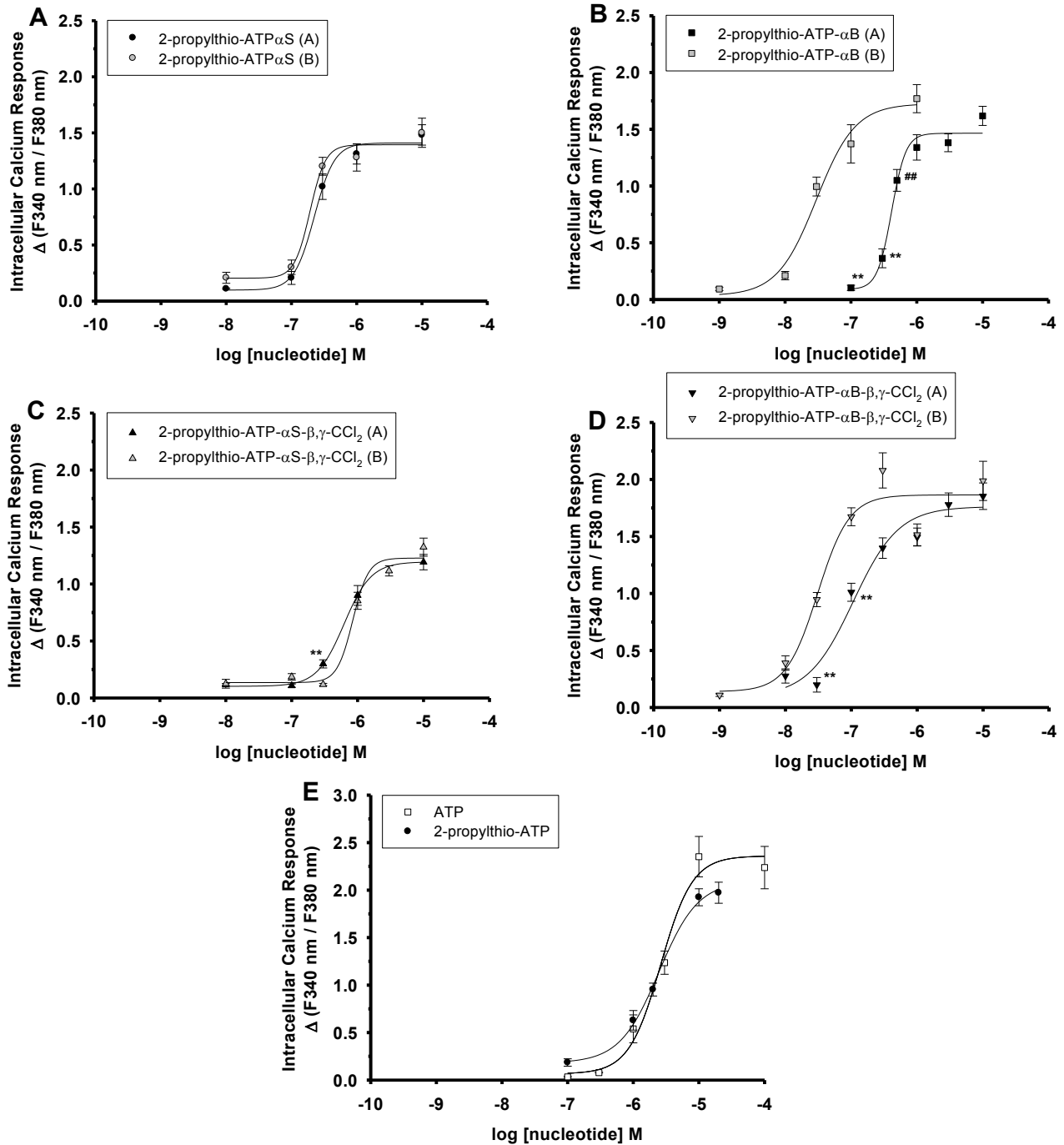
Figure 22: Concentration-response curves for the rise of [Ca²⁺]ᵢ induced by 2-propylthio-substituted analogs of ATP in 1321N1 astrocytoma cells expressing the human P2Y₁₁ receptor. Responses were induced by **A:** 2-propylthio-ATP-αS (A/B), **B:** 2-propylthio-ATP-αB (A/B), **C:** 2-propylthio-ATP-αS-β,γ-CCl₂ (A/B), **D:** 2-propylthio-ATP-αB-β,γ-CCl₂ (A/B), **E:** ATP, and 2-propylthio-ATP. The cells were pre-incubated with 2 μM Fura-2 AM for 30 min and the change in fluorescence (Δ F340 nm / F380 nm) was detected, as described in methods. Numbers of experiments and analyzed cells are given in methods. B: ** = significant differences (P < 0.01) of Ca²⁺ response amplitudes to 0.1 μM of the A-isomer and 0.1 μM and 0.03 μM of the B-isomer of the nucleotide; ## = significant difference (P < 0.01) of Ca²⁺ response amplitudes to 0.5 μM of the A-isomer and 0.1 μM of the B-isomer of the nucleotide. C/D: ** = significant differences (P < 0.01) of Ca²⁺ response amplitudes to the respective concentrations of nucleotides.

Table 5: Potencies (EC$_{50}$ values in μM) of ATP and novel 2-propylthio-substituted analogs of ATP at the human P2Y$_{11}$ receptor expressed in 1321N1 astrocytoma cells. Data were derived from concentration-response curves given in Figure 22.

Nucleotide	Intracellular Ca^{2+} response EC$_{50}$ (μM) +/- SEM
2-propylthio-ATP-αS (A-isomer, Sp)	0.22 +/- 0.04 (Fig. 22A)
2-propylthio-ATP-αS (B-isomer, Rp)	0.19 +/- 0.06 (Fig. 22A)
2-propylthio-ATP-αB (A-isomer, Rp)	0.40 +/- 0.05 (Fig. 22B)
2-propylthio-ATP-αB (B-isomer, Sp)	0.03 +/- 0.01 (Fig. 22B)
2-propylthio-ATP-αS-β,γ-CCl$_2$ (A-isomer, Sp)	0.6 +/- 0.03 (Fig. 22C)
2-propylthio-ATP-αS-β,γ-CCl$_2$ (B-isomer, Rp)	0.85 +/- 0.2 (Fig. 22C)
2-propylthio-ATP-αB-β,γ-CCl$_2$ (A-isomer, Rp)	0.1 +/- 0.05 (Fig. 22D)
2-propylthio-ATP-αB-β,γ-CCl$_2$ (B-isomer, Sp)	0.03 +/- 0.01 (Fig. 22D)
2-propylthio-ATP	2.5 +/- 0.5 (Fig. 22E)
ATP	2.6 +/- 0.6 (Fig. 22E)

Major conclusion

Sp-2-propylthio-ATP-αB and Sp-2-propylthio-ATP-αB-β,γ-CCl$_2$ are the most potent of the tested P2Y$_{11}$ receptor agonists.

3.2.2 Investigation of nucleotide specificity for the P2Y$_{11}$ over the P2Y$_1$ and P2Y$_2$ receptors expressed in 1321N1 astrocytoma cells

Adenine nucleotides can trigger intracellular Ca^{2+} responses not only due to agonistic activity at the P2Y$_{11}$ receptor, but also by activating the P2Y$_1$ or P2Y$_2$ receptors. To verify nucleotide specificity for the P2Y$_{11}$ receptor, the novel 2-propylthio-ATP derivatives therefore were tested on 1321N1 astrocytoma cells expressing P2Y$_1$ or P2Y$_2$ receptors (Figure 23). Response amplitudes to 10 μM of the tested nucleotides at the P2Y$_{11}$ receptor are given in Figure 23A for comparison.

At the P2Y$_1$ receptor, only the B-isomer of 2-propylthio-ATP-αS-β,γ-CCl$_2$ and the A-isomer of 2-propylthio-ATP-αB-β,γ-CCl$_2$ (10 μM each) did not trigger a rise of [Ca^{2+}]$_i$ (Figure 23B). The nucleotides, which showed the highest potency at the P2Y$_{11}$ receptor were the B-isomers of 2-propylthio-ATP-αB-β,γ-CCl$_2$ and 2-propylthio-ATP-αB (EC$_{50}$ values = 0.03 μM). At the P2Y$_1$ receptor

the latter analog triggered a response of about 44% of that of ATP. Since the response to 2-propylthio-ATP-αB-β,γ-CCl$_2$(B) was only about 22% of that of ATP, this nucleotide shows better specificity for the P2Y$_{11}$ receptor over the P2Y$_1$ receptor. For 2-propylthio-ATP, an EC$_{50}$ value of 0.04 +/- 0.01 μM was obtained at the P2Y$_1$ receptor (Figure 24). For the other nucleotide derivates, a clear plateau of the intracellular Ca^{2+} response could not be reached for concentrations of up to 10 μM.
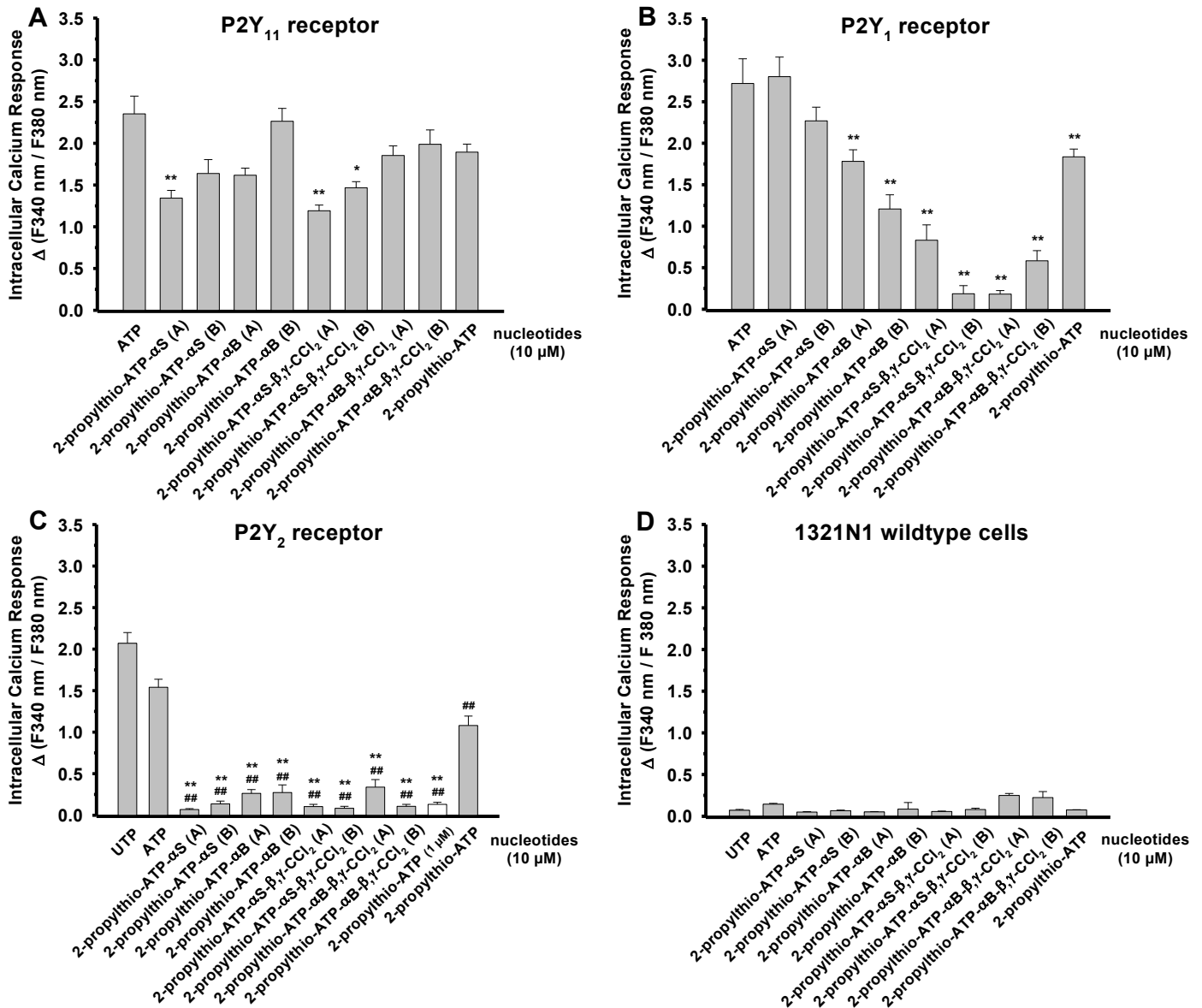
Figure 23: Amplitudes of the rise of [Ca^{2+}]$_i$ induced by the novel 2-propylthio-substituted analogs of ATP in 1321N1 astrocytoma cells expressing the P2Y$_{11}$, P2Y$_1$, or P2Y$_2$ receptor. Ca^{2+} responses were induced using ATP, UTP, 2-propylthio-ATP-αS (A/B), 2-propylthio-ATP-αB (A/B), 2-propylthio-ATP-αS-β,γ-CCl$_2$ (A/B), 2-propylthio-ATP-αB-β,γ-CCl$_2$ (A/B), and 2-propylthio-ATP in cells expressing the **A:** P2Y$_{11}$ receptor, **B:** P2Y$_1$ receptor, **C:** P2Y$_2$ receptor, or **D:** 1321N1 astrocytoma wildtype cells. The cells were pre-incubated with 2 μM Fura-2 AM for 30 min and the change in fluorescence (Δ F340 nm / F380 nm) was detected, as described in methods. Numbers of experiments and analyzed cells are given in methods. **/ * = significant differences (P < 0.01; P < 0.05, respectively) of Ca^{2+} response amplitudes to ATP and the tested nucleotide derivatives. ## = significant differences (P < 0.01) of Ca^{2+} response amplitudes to UTP and the tested nucleotide derivatives.

At the P2Y$_2$ receptor, only a concentration of 10 µM of 2-propylthio-ATP evoked a notable response (Figure 23C). A plateau of the intracellular Ca^{2+} response could, however, not be reached. The response to the other nucleotide derivatives did not exceed baseline or was minimal.

None of the tested nucleotides, including the physiological nucleotides UTP and ATP, evoked an intracellular Ca^{2+} response in 1321N1 astrocytoma wildtype cells for a concentration of 10 µM (Figure 23D).
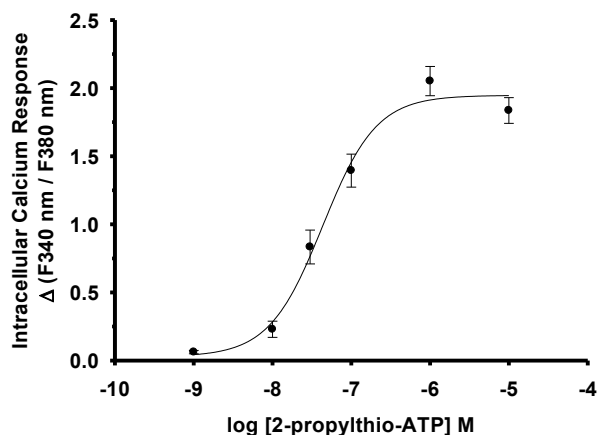
Figure 24: Concentration-response curve for the rise of [Ca^{2+}]$_i$ in 1321N1 astrocytoma cells expressing the human P2Y$_1$ receptor induced by 2-propylthio-ATP. The cells were pre-incubated with 2 µM Fura-2 AM for 30 min and the change in fluorescence (Δ F340 nm / F380 nm) was detected, as described in methods. Numbers of experiments and analyzed cells are given in methods.

3.2.3 Investigation of cAMP accumulation induced by the 2-propylthio-ATPαB analogs in 1321N1 astrocytoma cells expressing the human P2Y$_{11}$ receptor

The P2Y$_{11}$ receptor is dually coupled to the G$_q$ and G$_s$ signaling pathways. Therefore, the nucleotides with the lowest EC$_{50}$ value for the induction of the G$_q$ pathway were tested whether they activate the adenylyl cyclase in 1321N1 astrocytoma cells expressing the human P2Y$_{11}$ receptor (Figure 25). The B-isomers of 2-propylthio-ATP-αB and 2-propylthio-ATP-αB-β,γ-CCl$_2$ were tested at concentrations of 0.01 to 10 µM and achieved a comparable accumulation of intracellular cAMP. The half-maximal concentrations were approximately 0.1 µM. This corresponds to the EC$_{50}$ values of both nucleotides of 0.03 µM for the rise of [Ca^{2+}]$_i$ at the P2Y$_{11}$ receptor.

In order to analyze, whether the specificity of the P2Y$_{11}$ receptor for the B-isomers of the nucleotide derivatives can be detected for the induction of the G$_s$ pathway as well, we additionally tested the A-isomer of 2-propylthio-ATP-αB. For a concentration of up to 10 µM, only a weak accumulation of cAMP was detected. This confirms the diastereospecificity of the receptor for both signaling pathways.

P2Y$_{11}$ receptors labeled with GFP were used for measurements. In order to verify that the GFP tag had no influence on the experimental results, ATP was used on 1321N1 astrocytoma cells expressing either the P2Y$_{11}$-myc/His or the P2Y$_{11}$-GFP receptor (Figure 26). There were no differences in the concentration-dependent elevation of [cAMP].
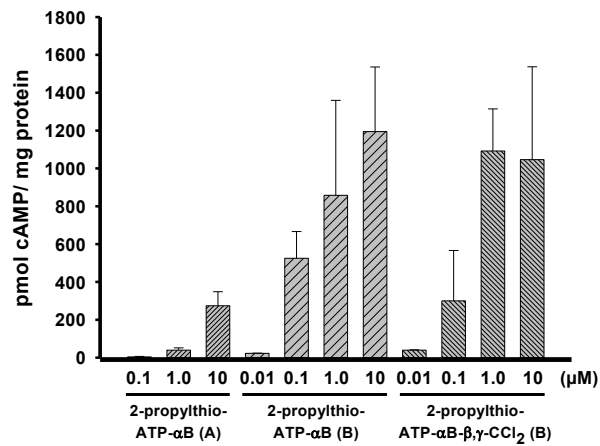
Figure 25: Levels of cAMP accumulation mediated by the P2Y$_{11}$-GFP receptor induced by different concentrations of 2-propylthio-ATP-αB (A-isomer and B-isomer) and 2-propylthio-ATP-αB-β,γ-CCl$_2$(B). Data were obtained from 1321N1 astrocytoma cells expressing the P2Y$_{11}$-GFP receptor. The amount of cAMP per mg protein has been determined, as described in methods. Numbers of experiments and analyzed cells are given in methods.
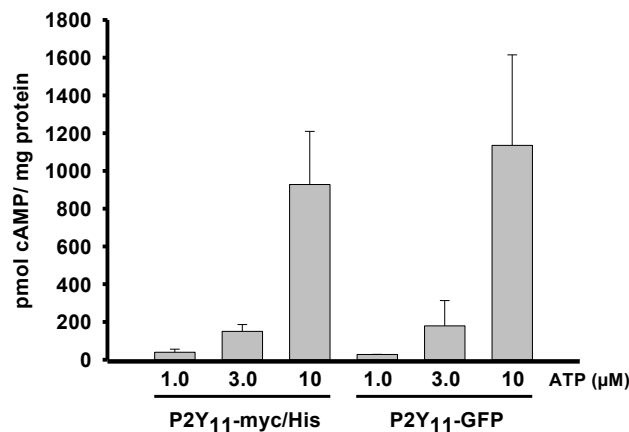
Figure 26: Levels of P2Y$_{11}$-myc/His or P2Y$_{11}$-GFP receptor-mediated cAMP accumulation induced by different concentrations of ATP. Data were obtained from 1321N1 astrocytoma cells. The amount of cAMP per mg protein has been determined, as described in methods. Numbers of experiments and analyzed cells are given in methods.

3.3 Potency of 5-OMe-substituted derivatives of UDP on 1321N1 astrocytoma cells expressing the human P2Y$_2$, P2Y$_4$, and P2Y$_6$ receptors

3.3.1 Investigation of nucleotide potencies at the human P2Y$_6$ receptor expressed in 1321N1 astrocytoma cells

1321N1 astrocytoma cells were used for the expression of the human P2Y$_6$ receptor. A series of novel 5-OMe-substiuted derivatives of UDP was investigated for nucleotide potency at this receptor using single-cell Ca^{2+} measurements (Figure 27). In addition to the OMe-substitution at position 5 of the uracil ring, two of the novel nucleotide compounds included a BH$_3$-group at the α-phosphate substituting a non-bridging oxygen (5-OMe-UDP-αB and (5-OMe-U)-P$_3$αB-(5-OMe-U)). This substitution results in the introduction of a new chiral center at the α-phosphate. The Rp configuration was assigned to the A-isomers and the Sp configuration to the B-isomers, as described in Ginsburg-Shmuel *et al.*, 2012. The resulting isomers were investigated separately.
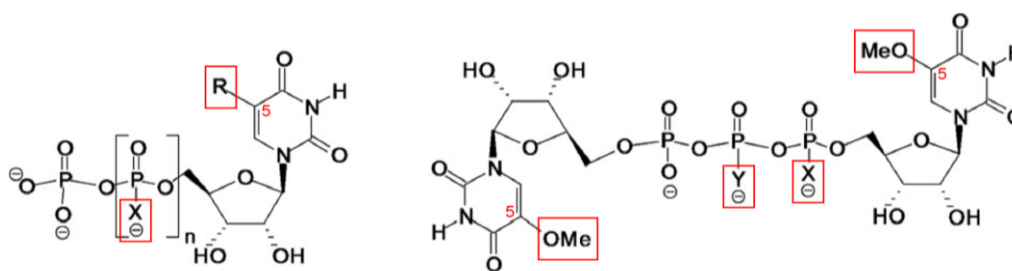
nucleotide	substitutions			
5-OMe-UDP	X = O		n = 1	R = OMe
5-OMe-UDP-αB (A/B)	X = BH$_3$		n = 1	R = OMe
(5-OMe-U)-P$_3$αB-(5-OMe-U) (A/B)	X = BH$_3$	Y = O		
(5-OMe-U)-P$_3$βB-(5-OMe-U)	X = O	Y = BH$_3$		
(5-OMe-U)-P$_3$-(5-OMe-U)	X = O	Y = O		

Figure 27: Structure of 5-OMe-substituted nucleotide and di-nucleotide derivates of UDP used for the investigation of potency and selectivity at the P2Y$_6$ receptor (modified from Ginsburg-Shmuel *et al.*, 2012).

All nucleotide analogs displayed the ability to activate the P2Y$_6$ receptor. There is a striking preference for the A-isomer of 5-OMe-UDP-αB over the B-isomer (Figure 28A). The EC$_{50}$ value of the A-isomer was determined to be 0.008 +/- 0.003 µM, while for the B-isomer it was 4.9 +/- 0.62 µM (Table 6). The potency of the A-isomer therefore was more than 600-times higher. A plateau of the concentration-response curve of the A-isomer was reached at a nucleotide concentration of 0.1 µM.

For the B-isomer, no intracellular Ca^{2+} response was detected for concentrations below 3 µM, while the plateau was reached at 10 µM.

A similar but less pronounced selectivity of the $P2Y_6$ receptor for the A-isomer was found for the di-nucleotide (5-OMe-U)-$P_3\alpha B$-(5-OMe-U) (Figure 28B). The EC_{50} value for the A-isomer was 0.14 +/- 0.01 and 2.0 +/- 0.45 µM for the B-isomer. Thus, the A-isomer was about 14-fold more potent than the B-isomer. The Ca^{2+} response amplitudes induced by 0.1 to 10 µM of the B-isomer were significantly lower (P < 0.01) than the respective responses to the A-isomer.
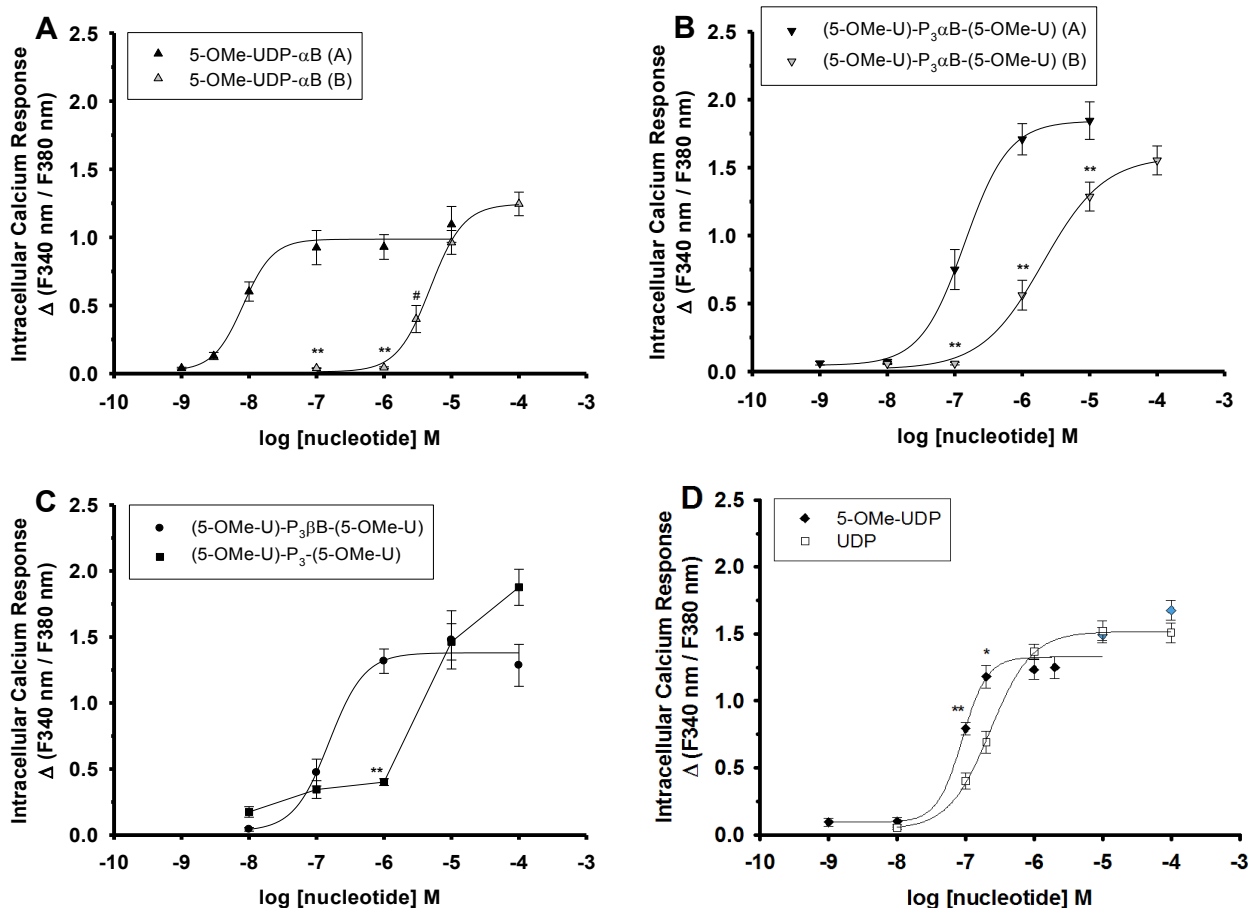
Figure 28: Concentration-response curves for the rise of [Ca²⁺]ᵢ induced by 5-OMe-substituted analogs of UDP in 1321N1 astrocytoma cells expressing the human P2Y₆ receptor. Responses were induced by **A:** 5-OMe-UDP-αB (A/B), **B:** (5-OMe-U)-P₃αB-(5-OMe-U) (A/B), **C:** (5-OMe-U)-P₃βB-(5-OMe-U), and (5-OMe-U)-P₃-(5-OMe-U), **D:** 5-OMe-UDP, and UDP. Blue diamond symbols in D indicate a potential second increase of the Ca^{2+} response for concentrations of 5-OMe-UDP higher than 10 µM. The cells were pre-incubated with 2 µM Fura-2 AM for 30 min and the change in fluorescence (Δ F340 nm / F380 nm) was detected, as described in methods. Numbers of experiments and analyzed cells are given in methods. ** / * = significant differences (P < 0.01; P < 0.05, respectively) of Ca^{2+} response amplitudes to the respective concentrations of nucleotides. # = significant differences (P < 0.05) between Ca^{2+} response amplitudes to 3 µM 5-OMe-UDP-αB(B) and 1 µM and 10 µM of 5-OMe-UDP-αB(A).

The di-nucleotide derivative (5-OMe-U)-$P_3\beta B$-(5-OMe-U) carries a borano-substitution at the middle phosphate, which does not introduce a chiral center at this position. The EC_{50} value of this analog was at 0.2 +/- 0.04 µM (Figure 28C). For (5-OMe-U)-P_3-(5-OMe-U), which lacks a borano-

substitution, a clear plateau for the rise of $[Ca^{2+}]_i$ could not be reached for nucleotide concentrations up to 100 µM. Therefore, the EC_{50} value can be estimated to be > 10 µM. A nucleotide concentration of 1 µM (5-OMe-U)-P_3-(5-OMe-U) yielded a significantly lower (P < 0.01) Ca^{2+} response amplitude than (5-OMe-U)-$P_3\beta B$-(5-OMe-U).

The direct comparison of the potencies of 5-OMe-UDP and the physiological standard agonist UDP (Figure 28D) revealed a slightly lower EC_{50} value for the 5-OMe-substituted nucleotide (EC_{50} = 0.09 +/- 0.02 µM and 0.23 +/- 0.009 µM, respectively). Therefore, 5-OMe-UDP was about 2.6-fold more potent than UDP. A significantly higher Ca^{2+} response for 5-OMe-UDP was detected at a nucleotide concentration of 0.1 µM (P < 0.01) and 0.2 µM (P < 0.05).

Figure 28D shows that the plateau of the Ca^{2+} response can be reached with a concentration of 5-OMe-UDP of around 1 µM. However, for 10 µM and 100 µM of 5-OMe-UDP (blue symbols in Figure 28D), the amplitude of the intracellular Ca^{2+} response seems to be further increased. The amplitudes for these concentrations of 5-OMe-UDP were in the range of the maximal amplitudes observed for the parent compound UDP, but they indicate a possible second increase of the intracellular Ca^{2+} response at the $P2Y_6$ receptor. As the nature of this remains unknown, the EC_{50} value of 5-OMe-UDP was deduced from the first phase of the Ca^{2+} response (from 0.001 µM to 10 µM 5-OMe-UDP).

The rank order of potencies for the tested novel uridine nucleotides was found to be: 5-OMe-UDP-αB(A) >> 5-OMe-UDP > (5-OMe-U)-$P_3\alpha B$-(5-OMe-U)(A) > (5-OMe-U)-$P_3\beta B$-(5-OMe-U) = UDP > (5-OMe-U)-$P_3\alpha B$-(5-OMe-U)(B) > 5-OMe-UDP-αB(B) > (5-OMe-U)-P_3-(5-OMe-U). The most potent nucleotide, 5-OMe-UDP-αB(A), was about 29-times more potent than UDP.

Table 6: Potencies (EC$_{50}$ values in µM) of UDP and novel 5-OMe-substituted derivatives of UDP at the human P2Y$_6$ receptor expressed in 1321N1 astrocytoma cells. Data were derived from concentration-response curves given in Figure 28.

Nucleotide	Intracellular Ca^{2+} response EC$_{50}$ (µM) +/- SEM
5-OMe-UDP-αB (A-isomer, R*p*)	0.008 +/- 0.003 (Fig. 28A)
5-OMe-UDP-αB (B-isomer, S*p*)	4.9 +/- 0.62 (Fig. 28A)
(5-OMe-U)-P$_3$αB-(5-OMe-U) (A-isomer, R*p*)	0.14 +/- 0.01 (Fig. 28B)
(5-OMe-U)-P$_3$αB-(5-OMe-U) (B-isomer, S*p*)	2.0 +/- 0.45 (Fig. 28B)
(5-OMe-U)-P$_3$βB-(5-OMe-U)	0.2 +/- 0.04 (Fig. 28C)
(5-OMe-U)-P$_3$-(5-OMe-U)	> 10 (Fig. 28C)
5-OMe-UDP	0.09 +/- 0.02 (Fig. 28D)
UDP	0.23 +/- 0.009 (Fig. 28D)

Major conclusion

R*p*-5-OMe-UDP-αB is the most potent P2Y$_6$ receptor agonist known to date.

3.3.2 Investigation of nucleotide specificity for the P2Y$_6$ over the P2Y$_2$ and P2Y$_4$ receptors expressed in 1321N1 astrocytoma cells

Besides the human P2Y$_6$ receptor, the P2Y$_2$ and P2Y$_4$ receptors can be activated by uridine-nucleotides. To prove that the Ca^{2+} responses observed in the concentration-response-experiments in Figure 28 indeed were caused by the activation of the P2Y$_6$ receptor, 10 µM of the insurmountable P2Y$_6$ receptor antagonist MRS2578 have been added to the 1321N1 astrocytoma cells expressing the P2Y$_6$ receptor (Figure 29A). The antagonist was added to the cells 30 min prior to the Ca^{2+} measurements and was co-applied with 10 µM of 5-OMe-UDP-αB(A). MRS2578 was able to significantly reduce the intracellular Ca^{2+} response to the 5-OMe-UDP-αB(A) by circa 78% (P < 0.01).

Figure 29B shows representative traces of intracellular Ca^{2+} responses elicited by 10 µM 5-OMe-UDP-αB(A) without or with the addition of 10 µM of MRS2578. These results demonstrate that the observed intracellular Ca^{2+} responses are indeed mediated by the P2Y$_6$ receptor expressed in the 1321N1 astrocytoma cells.
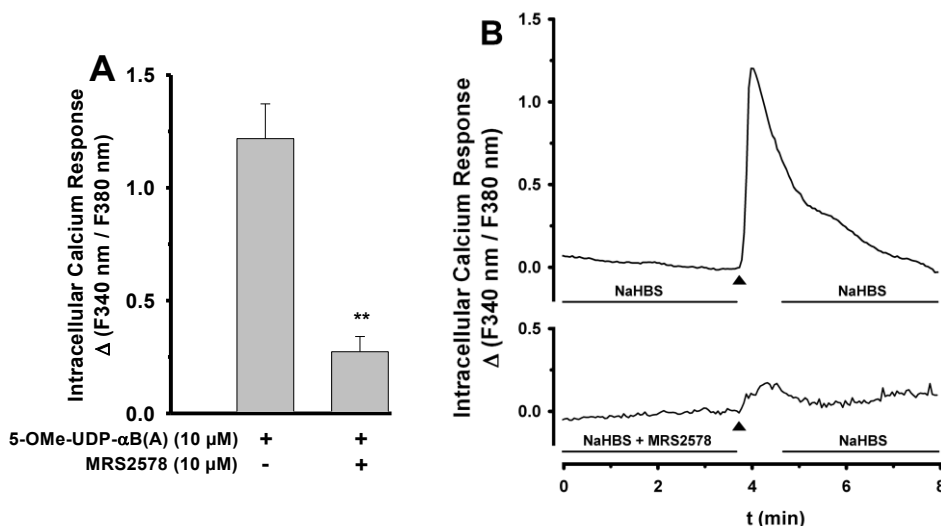
Figure 29: Nucleotide-induced rise of [Ca²⁺]ᵢ in 1321N1 astrocytoma cells expressing the human P2Y₆ receptor testing 5-OMe-UDP-αB(A) and the P2Y₆ receptor antagonist MRS2578. **A:** Amplitudes of the Ca^{2+} response after treatment with 10 µM 5-OMe-UDP-αB (A-isomer) compared with the respective response amplitude after pre-incubation with the P2Y₆ receptor specific antagonist MRS2578. **B:** Representative traces of single-cell Ca^{2+} measurements with 10 µM 5-OMe-UDP-αB (A-isomer) without or with the addition of 10 µM of the P2Y₁ receptor antagonist MRS2578. Graphs represent mean values from 3 to 5 cells from one experiment. Arrow heads mark the respective start of the 1 min applications of R*p*-5-OMe-UDP-αB without or with MRS2578. Cells were pre-incubated with 2 µM Fura-2/AM for 30 min and the change in fluorescence (Δ F340 nm / F380 nm) was detected, as described in methods. ** = Statistically significant ($P < 0.01$) decrease of [Ca²⁺]ᵢ induced by the nucleotide agonist after co-treatment with MRS2578 compared to treatment with nucleotide agonist alone.

Although the P2Y₂ and P2Y₄ receptors prefer uridine-triphosphates over uridine-diphosphates, the novel UDP derivates were tested on 1321N1 astrocytoma cells expressing the P2Y₂ and P2Y₄ receptors as well as on wildtype cells (Figure 30). In cells expressing the P2Y₂ receptor, the physiological agonist UTP evoked a strong intracellular Ca^{2+} response (Figure 30A). However, none of the novel 5-OMe-substituted derivatives of UPD caused a substantial response at a nucleotide concentration of 100 µM (50 µM in the case of 5-OMe-UDP). In cells expressing the P2Y₄ receptor, UTP treatment yielded strong Ca^{2+} responses (Figure 30B). Responses to all novel nucleotide derivatives were significantly lower ($P < 0.01$). Only 5-OMe-UDP at concentrations of 10 µM and 50 µM caused a notable response. In 1321N1 astrocytoma wildtype cells, all the tested nucleotides were inactive (Figure 30C).
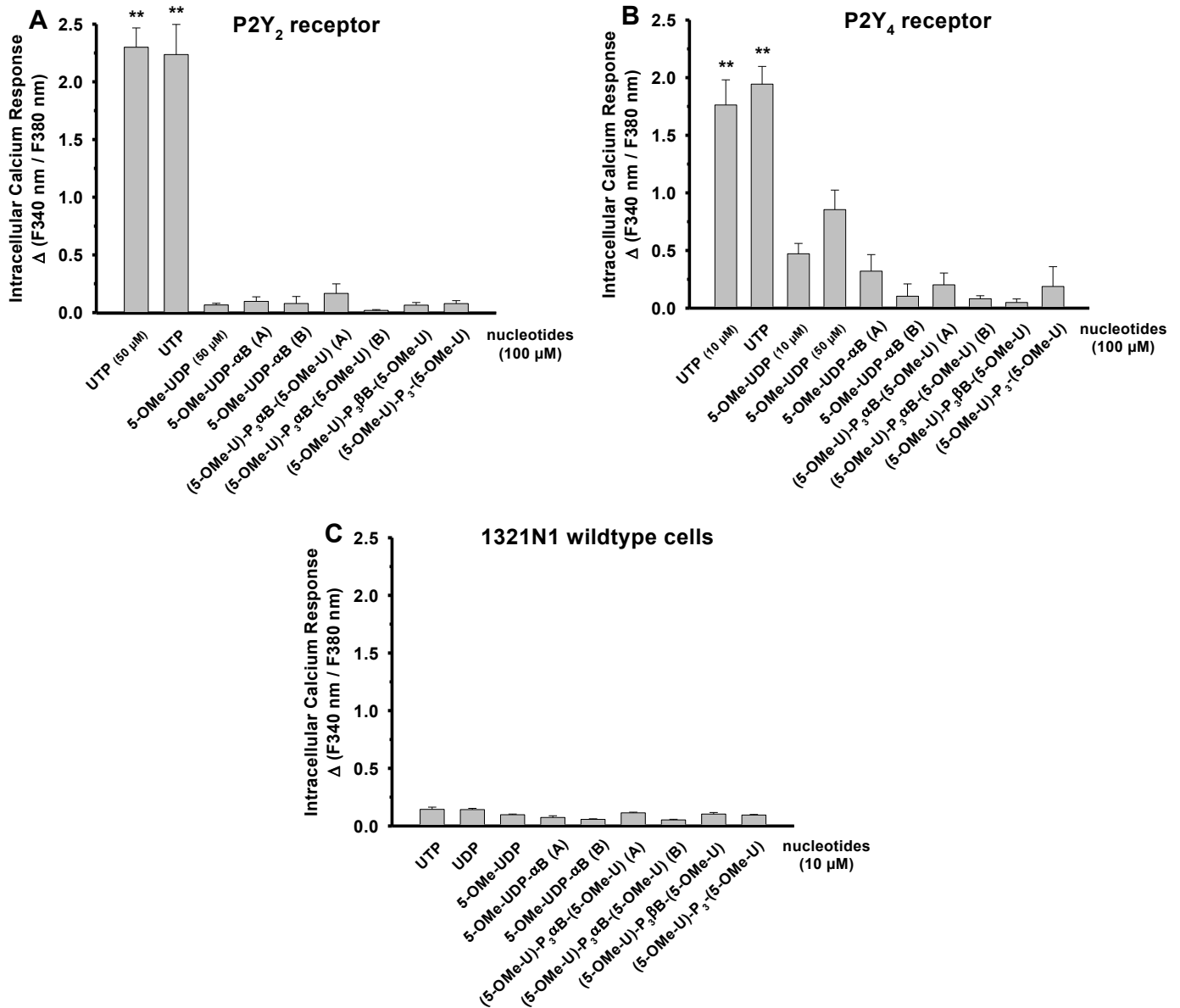
Figure 30: Amplitudes of the rise of [Ca²⁺]ᵢ in 1321N1 astrocytoma cells induced by novel 5-OMe-substituted analogs of UDP. Responses were induced in cells expressing the human **A:** P2Y₂ receptor, **B:** P2Y₄ receptor, or in **C:** 1321N1 astrocytoma wildtype cells using UTP, UDP, 5-OMe-UDP-αB (A-isomer and B-isomer), (5-OMe-U)-P₃αB-(5-OMe-U) (A-isomer and B-isomer), (5-OMe-U)-P₃βB-(5-OMe-U), (5-OMe-U)-P₃-(5-OMe-U), or 5-OMe-UDP. The cells were pre-incubated with 2 µM Fura-2 AM for 30 min and the change in fluorescence (Δ F340 nm / F380 nm) was detected, as described in methods. Numbers of experiments and analyzed cells are given in methods.

** = significant difference (P < 0.01) of Ca²⁺ response amplitudes between UTP and the tested nucleotide derivatives.

4. Discussion

4.1 Characterization of the Alanine-(87)-Threonine mutation of the human $P2Y_{11}$ receptor

The investigation of naturally occurring genetic polymorphisms leads to new insights about the functional roles of mutated amino acids in receptor activity. The identification and careful analysis of resulting aberrant receptor functions can answer the question of how specific receptor mutations affect cellular processes, and how that may contribute to the development of disorders. A SNP of the human $P2Y_{11}$ receptor, which causes a switch from the non-polar amino acid alanine to the polar threonine at position 87 (A87T), was statistically connected to an increased risk for AMI and elevated levels of C-reactive protein (Amisten *et al.*, 2007). In our work, the first pharmacological and functional characterization of the $P2Y_{11}$A87T receptor was undertaken. For this, the receptor was expressed in the human HEK293 and 1321N1 astrocytoma cell lines. A comparative overview of nucleotide-induced cellular responses mediated by the non-mutated and the mutated $P2Y_{11}$ receptors is given in Table 7 and Table 8 for 1321N1 astrocytoma cells and HEK293 cells, respectively.

The A87T mutation of the $P2Y_{11}$ receptor impairs Ca^{2+} signaling, but this impairment is found only in cells co-expressing the $P2Y_1$ receptor.

In 1321N1 astrocytoma cells, the $P2Y_{11}$ receptor-specific agonist BzATP induced identical intracellular Ca^{2+} responses irrespective of whether the wildtype $P2Y_{11}$ receptor or the mutated $P2Y_{11}$A87T receptor was expressed (Figure 4A). 1321N1 astrocytoma cells provide a P2Y receptor-null background (Figure 8B). Thus, isolated responses of the P2Y receptors expressed in these cells are detected. In line with the finding of Ecke *et al.* (2008), BzATP was a potent agonist at the wildtype $P2Y_{11}$ receptor expressed in HEK293 cells (Figure 4B). Importantly, the Ca^{2+} response to BzATP of HEK293 cells was completely absent when the mutant $P2Y_{11}$A87T receptor was expressed (Figure 4B). In these HEK293 cells, endogenous $P2Y_1$ receptors are present. This was verified here by evoking a Ca^{2+} response using the $P2Y_1$ receptor-specific agonist 2-MeS-ADP (Figure 8A). Also, the ATP-induced response was inhibited by the $P2Y_1$ receptor-specific antagonist MRS2179 (Figure 8A), a 2'-deoxy-adenosine derivative featuring phosphate groups at the 3' and the 5' position and an N^6-methyl substituent at the nucleobase. Based on multiple lines of evidence using GST-pulldown, FRET, immunocytochemistry, and siRNA experiments, as well as pharmacological analysis, the work by Ecke *et al.*, (2008) verified that the $P2Y_{11}$ receptor and the $P2Y_1$ receptor form hetero-oligomers with a unique functionality. This can be seen either in HEK293 cells or in 1321N1 astrocytoma cells, which express both receptors. This receptor interaction is very likely to take place as well between the $P2Y_{11}$A87T and $P2Y_1$ receptors in HEK293 cells. In line with this notion, we found the complete loss of the BzATP-induced Ca^{2+} response in $P2Y_{11}$A87T receptor-expressing HEK293 cells, but not in 1321N1 astrocytoma cells, which do not allow the formation of the receptor oligomers. It is thus important to note that the A87T mutation *per se* is not sufficient to alter the $P2Y_{11}$ receptor functionality.

At the $P2Y_{11}$ and $P2Y_{11}A87T$ receptors expressed in 1321N1 astrocytoma cells, 2-MeS-ADP is only a weak agonist (Figure 5A). In HEK293 cells expressing the $P2Y_{11}A87T$ receptor, the potency of this agonist is significantly lower than it is in cells expressing the wildtype $P2Y_{11}$ receptor (Figure 5B). Interestingly, the expression of the non-mutated $P2Y_{11}$ wildtype receptor already leads to a decrease of the 2-MeS-ADP potency when compared with HEK293 wildtype cells. This very likely reflects the fact that in HEK293 wildtype cells, the response to 2-MeS-ADP is solely carried by the endogenous $P2Y_1$ receptor. In the $P2Y_{11}$ receptor-expressing HEK293 cells, a response of the functionally distinct $P2Y_1/P2Y_{11}$ hetero-oligomer is observed. The additional reduction of potency of 2-MeS-ADP in HEK293 cells expressing the $P2Y_{11}A87T$ receptor indicates that the A87T mutation has indeed a detrimental effect on the $P2Y_1/P2Y_{11}$ oligomer signaling function.

This latter notion is further solidified by the comparative analysis of ATP potencies in 1321N1 astrocytoma cells and HEK293 cells. There was, again, no difference in nucleotide potency between either 1321N1 astrocytoma cells expressing the $P2Y_{11}$ receptor or cells expressing the $P2Y_{11}A87T$ receptor (Figure 6A). Using HEK293 cells, a small but significant reduction of the EC_{50} value of ATP at the $P2Y_{11}A87T$ receptor was found when compared with the $P2Y_{11}$ receptor (Figure 6B). It is important to consider that, in contrast to the synthetic nucleotides BzATP and 2-MeS-ADP, ATP is a physiological agonist for both the $P2Y_1$ and $P2Y_{11}$ receptors with important functions throughout the human organism. Although the reduction of ATP potency at $P2Y_{11}A87T$ receptor-expressing HEK293 cells was only 1.6-fold (Table 2), the severity of the pathological consequences of the receptor mutation might be due to the long-term build-up of small cellular aberrations.

Table 7: Nucleotide-induced cellular responses mediated by the $P2Y_{11}A87T$, wildtype $P2Y_{11}$, and $P2Y_1$ receptor in 1321N1 astrocytoma cells in absence of endogenous P2Y receptor expression. ([1] = Major *et al.*, 2004b; [2] = Abbracchio *et al.*, 2006; [3] = Ecke *et al.*, 2008)

1321N1 astrocytoma cells
P2Y receptor expression (transfection)

Response	$P2Y_{11}$	$P2Y_{11}A87T$	$P2Y_1$
Intracellular Ca^{2+} signaling	*Strong* response to ATP *Strong* response to BzATP *Weak* response to 2-MeS-ADP	*Strong* response to ATP *Strong* response to BzATP *Weak* response to 2-MeS-ADP **> Identical to the wildtype $P2Y_{11}$ receptor**	*Strong* response to ATP[1] *No* response to BzATP *Strong* response to 2-MeS-ADP
Intracellular cAMP signaling	*Strong* response to ATP	*Strong* response to ATP **> Identical to the wildtype $P2Y_{11}$ receptor**	*(No coupling to G_s or G_i signaling[2])*
Nucleotide-induced receptor internalization	*No* effect [3]	Not determined	*Strong* effect [3]

Table 8: Nucleotide-induced cellular responses mediated by the P2Y₁₁A87T, P2Y₁₁A87S, P2Y₁₁A87Y, and wildtype P2Y₁₁ receptor in HEK293 cells in presence of endogenous P2Y₁ receptors.

HEK293 cells
P2Y receptor expression (transfection)

Response	P2Y₁₁	P2Y₁₁A87T	P2Y₁₁A87S	P2Y₁₁A87Y
		in comparison with the wildtype P2Y₁₁ receptor		
Intracellular Ca²⁺ signaling	*Strong* response to ATP / *Strong* response to BzATP / *Strong* response to 2-MeS-ADP	*Reduced* response to ATP / *No* response to BzATP / *Reduced* response to 2-MeS-ADP	*Reduced* response to ATP / *Similar* response to BzATP / *Similar* response to 2-MeS-ADP	
Intracellular cAMP signaling	*Strong* response to ATP	*Reduced* response to ATP	Not determined	Not determined
Nucleotide-induced receptor internalization	*Strong* ATP-induced receptor internalization / *Strong* BzATP-induced receptor internalization	*No* effect	*Weak* ATP-induced receptor internalization / *Strong* BzATP-induced receptor internalization	*No* effect
Long-term intracellular Ca²⁺ signaling	*Strong* desensitization after 60 min challenge with ATP / *Weak* recovery of the response after a following 90 min incubation in the absence of ATP	*Stronger* desensitization after 60 min challenge with ATP / *Strong* recovery of the response after a following 90 min incubation in the absence of ATP		Not determined

Due to the change from a non-polar alanine to a polar threonine residue at position 87 of the P2Y₁₁ receptor, amino acid polarity was suggested by Amisten and coworkers in 2007 to be the cause for altered receptor function. To test this hypothesis, additional P2Y₁₁ receptor mutants were generated by us using site-directed mutagenesis. In the case of the P2Y₁₁A87S receptor, the alanine-87 was replaced with a small polar serine residue. The P2Y₁₁A87Y receptor featured a bulky polar threonine residue at the respective position within the protein. It was found that the A87S and A87Y mutations of the P2Y₁₁ receptor rescue the potency of BzATP and 2-MeS-ADP in HEK293 cells (Table 2). Since the P2Y₁₁A87S and P2Y₁₁A87Y receptors show restored nucleotide-induced Ca²⁺ responses, amino acid polarity can be ruled out to be the reason for the observed alterations of P2Y₁₁A87T receptor functionality. It is noteworthy that the maximal Ca²⁺ amplitudes to BzATP and 2-MeS-ADP of the P2Y₁₁A87S receptor were higher than those of the other P2Y₁₁ mutant receptors and the wildtype P2Y₁₁ receptor (Figure 4C and Figure 5C). Analyzing the fluorescence intensities of

the C-terminal GFP tags of the $P2Y_{11}$ receptors used in this study, the expression level of the $P2Y_{11}A87S$ receptor in HEK293 cells was found to be comparable to that of the other receptors (Figure 9). Only for the $P2Y_{11}A87Y$ receptor, the expression level was slightly reduced, but Ca^{2+} responses mediated by this receptor were comparable to those of $P2Y_{11}$ receptor-expressing cells. Thus, different expression levels cannot be the cause of the differences in potencies or maximal response amplitudes observed for the different nucleotides. Also, there were no significant differences of maximal Ca^{2+} responses to ATP induced by any of the $P2Y_{11}$ receptors (Figure 6). Therefore, the relatively higher maximal responses to BzATP and 2-MeS-ADP of the $P2Y_{11}A87S$ receptor have little physiological relevance.

Other endogenous G_q-coupled P2Y receptors with preference for uridine and/or adenine nucleotides could contribute to the nucleotide-induced intracellular Ca^{2+} responses described above. We found that besides the $P2Y_1$ receptor, the $P2Y_4$ receptor is likely to be the only other G_q-coupled P2Y receptor that is functionally expressed in the HEK293 cells. The cells show a rise of $[Ca^{2+}]_i$ after treatment with ATP and UTP (Figure 8). Both nucleotides can activate the $P2Y_2$ receptor and UTP is the physiological standard agonist for the $P2Y_4$ receptor. However, the response to ATP was completely inhibited by the $P2Y_1$ receptor-specific antagonist MRS2179. Therefore, we conclude that there was no ATP-induced $P2Y_2$ receptor activation and the $P2Y_2$ receptor can thus also be ruled out to be the source for the UTP-induced Ca^{2+} response.

Our data show that the expression of the $P2Y_{11}A87T$ receptor in HEK293 cells can lead to reduced nucleotide-induced intracellular Ca^{2+} responses when compared with cells expressing the $P2Y_{11}$ receptor or wildtype cells. However, those comparisons are based on separate experiments using cells from different cultures (Table 2). In order to verify our findings under identical experimental conditions, we investigated transfected (GFP-positive) and non-transfected (GFP-negative) cells of the same cell culture simultaneously (Figure 11). Responses of GFP-positive cells expressing the $P2Y_{11}A87T$ receptor under all conditions were always equal to or lower than the responses of the respective GFP-negative cells, as can easily be deduced from the F-values shown in Table 3. This is in line with the hypothesis that the A87T mutation is detrimental for the $P2Y_1/P2Y_{11}$ receptor oligomer function and confirms the data from the concentration-response experiments. Responses of GFP-negative cells were comparable to those of the wildtype HEK293 cells of a separate control culture, thus confirming the wildtype nature of GFP-negative cells.

In line with the concentration-response data (Figure 4), the $P2Y_{11}A87T$ receptor in GFP-positive cells showed no response to BzATP, which is similar for the GFP-negative cells (Table 3). On the other hand, the $P2Y_{11}$ receptor in GFP-positive cells mediated a strong response to BzATP.

Similar to the concentration-response data (Figure 5), GFP-positive cells with $P2Y_{11}$ or $P2Y_{11}A87T$ receptor-expression showed a significantly lower response amplitude induced by 2-MeS-ADP than GFP-negative cells (Figure 12A). We attribute this to the $P2Y_1/P2Y_{11}$ receptor interaction in the GFP-positive cells.

Treatment of HEK $P2Y_{11}$ receptor cultures with the physiological standard agonist ATP showed a slight but significant increase of the response amplitude in comparison with the GFP-negative cells (Figure 12B). The same treatment applied to HEK $P2Y_{11}A87T$ receptor cultures gave a significantly reduced response amplitude for GFP-positive cells, when compared with GFP-negative

cells. A critical experiment was the use of the $P2Y_1$ receptor-specific antagonist MRS2179 (Figure 12B). The antagonist was able to completely inhibit the response to ATP in GFP-negative cells in all cultures including the wildtype HEK293 cells of a separate control culture. This result confirms that these ATP-induced intracellular Ca^{2+} response are based on the $P2Y_1$ receptor activity. Interestingly, while GFP-positive cells expressing the $P2Y_{11}$ receptor were unaffected by the antagonist, the response to ATP of $P2Y_{11}A87T$ receptor expressing cells was inhibited by the antagonist. This confirms a functional difference of the $P2Y_{11}$ and $P2Y_{11}A87T$ receptors, when they are expressed in HEK293 cells.

The GFP-tag of the receptors was not the reason for the observed alterations of the Ca^{2+} response amplitudes, since HEK293 cells expressing the PAR2-GFP receptor (a GPCR, which cannot be activated by extracellular nucleotides) and GFP-negative cells within the same culture showed identical ATP-induced Ca^{2+} responses (Table 4).

The deleterious effect of the A87T mutation of the $P2Y_{11}$ receptor in cells which co-express the $P2Y_1$ receptor is confirmed in double-transfected 1321N1 astrocytoma cells.

The most striking result of the single-cell Ca^{2+} measurements discussed above was the complete absence of BzATP-induced intracellular Ca^{2+} response of HEK293 cells expressing the $P2Y_{11}A87T$ receptor. This observation was not made with 1321N1 astrocytoma cells expressing this receptor (Figure 4). As we attribute this substantial reduction of nucleotide potency in HEK293 cells to an impaired functionality of the $P2Y_{11}A87T$ receptor interaction with the endogenous $P2Y_1$ receptor, it was critical to validate this hypothesis in the P2Y receptor-null background of 1321N1 astrocytoma cells. Therefore, the $P2Y_1$ receptor was co-expressed in 1321N1 astrocytoma cells with either the wildtype $P2Y_{11}$ receptor or the mutant $P2Y_{11}A87T$ receptor. The expression of the $P2Y_{11}$ receptor was verified via detection of the GFP fluorescence, and the respective cells were challenged with 1 μM of the $P2Y_{11}$ receptor-specific agonist BzATP (Figure 13). The functional co-expression of the $P2Y_1$ receptor was verified with 1 μM 2-MeS-ADP given after at least 2 min recovery time following the detection of the BzATP-induced response (Figure 14). This concentration of 2-MeS-ADP is high enough to yield a strong $P2Y_1$ receptor-mediated Ca^{2+} response but too low to activate the $P2Y_{11}$ or $P2Y_{11}A87T$ receptors (Figure 5A, D). Accordingly, in control experiments with 1321N1 cells expressing only the $P2Y_{11}$ or the $P2Y_{11}A87T$ receptor there was no response to the 2-MeS-ADP stimulus and a strong response to BzATP. In 1321N1 cells solely expressing the $P2Y_1$ receptor, a negligible response to BzATP was detected, and a strong response to 2-MeS-ADP could be observed. Importantly, 1321N1 cells co-expressing the $P2Y_{11}A87T$ receptor and the $P2Y_1$ receptor showed a significantly reduced ($P < 0.01$) Ca^{2+} response amplitude to BzATP, when compared with cells co-expressing the $P2Y_{11}$ and the $P2Y_1$ receptor.

Furthermore, the BzATP-induced response amplitude of 1321N1 cells co-expressing the $P2Y_{11}$ and the $P2Y_1$ receptor was identical to the respective response of single-transfected cells expressing the $P2Y_{11}$ or $P2Y_{11}A87T$ receptors without the $P2Y_1$ receptor. Hence, these results are in line with our findings derived from HEK293 cells. Therefore, the A87T mutation of the $P2Y_{11}$ receptor has significant consequences for cells co-expressing the $P2Y_1$ receptor. The functional interaction of $P2Y_1$ and $P2Y_{11}$ receptors has been demonstrated by Ecke *et al.* in 2008 to take place in HEK293 cells as well as in 1321N1 cells. Therefore, we have good reason to assume that the SNP causing the

A87T mutation has a deleterious effect on the function of the receptor oligomer in all human cells co-expressing the respective receptors. The reduction of the response to BzATP of 1321N1 cells co-expressing the $P2Y_1$ and $P2Y_{11}A87T$ receptors was not as severe as in HEK293 cells, however. This might be due to different cell type-specific characteristics. Along the same line, the response to the test concentration of 1 µM of 2-MeS-ADP was identical in all 1321N1 astrocytoma cells with $P2Y_1$ receptor expression, while in HEK293 cells expressing the $P2Y_{11}$ receptors a reduced Ca^{2+} response was found.

The A87T mutation of the $P2Y_{11}$ receptor is detrimental to cAMP signaling in HEK293 cells.

The human $P2Y_{11}$ receptor is coupled not only to G_q-mediated intracellular Ca^{2+} signaling, but also to G_s-mediated activation of adenylyl cyclase. Since a deleterious effect of the A87T mutation on $P2Y_{11}$ receptor functions might also affect this signaling pathway, the ATP-induced accumulation of intracellular cAMP was investigated in 1321N1 astrocytoma cells and HEK293 cells (Figure 10). In accordance with the data from the Ca^{2+} measurements, a significant reduction in intracellular cAMP generation could be found only in HEK293 cells expressing the $P2Y_{11}A87T$ receptor, but not in 1321N1 astrocytoma cells. Thus for G_q and G_s signaling, an altered $P2Y_{11}$ receptor function was detected only in those cells, which co-express the $P2Y_1$ receptor. This further underlines our hypothesis that the A87T mutation primarily affects the interaction of the $P2Y_{11}$ and $P2Y_1$ receptors in respective cells.

Nucleotide-induced receptor internalization is not found in HEK293 cells expressing the $P2Y_{11}A87T$ receptor.

The formation of $P2Y_1/P2Y_{11}$ receptor-oligomers in HEK293 cells and 1321N1 astrocytoma cells has also been demonstrated by Ecke *et al.* in 2008 in experiments studying the nucleotide-induced internalization of the $P2Y_{11}$ receptor. The $P2Y_{11}$ receptor is unable to undergo internalization, when expressed in the P2Y receptor-null background of 1321N1 astrocytoma cells. However, the $P2Y_{11}$ receptor acquires this ability, when the $P2Y_1$ receptor is additionally expressed. This effect was found in transfected 1321N1 astrocytoma cells, or in HEK293 cells. Our data from Ca^{2+} and cAMP measurements discussed above support the hypothesis that the A87T mutation of the $P2Y_{11}$ receptor interferes with $P2Y_1/P2Y_{11}$ receptor-oligomer functions.

Thus, we compared the nucleotide-induced internalization of the wildtype $P2Y_{11}$ receptor with that of the $P2Y_{11}$ receptor mutants generated by us. The receptors were expressed in HEK293 cells and incubated for 60 min with 100 µM of the physiological standard agonist ATP or 100 µM of the $P2Y_{11}$ receptor-specific agonist BzATP (Figure 18). The $P2Y_{11}A87T$ receptor showed no sign of internalization under these conditions. The wildtype $P2Y_{11}$ receptor, on the other hand, was strongly internalized as seen by the prominent accumulation of intracellular GFP fluorescence. Similar to the $P2Y_{11}A87T$ receptor, the $P2Y_{11}A87Y$ receptor was not internalized. The $P2Y_{11}A87S$ mutant receptor, however, showed slight ATP-induced internalization and a strong BzATP-induced internalization.

The mutant $P2Y_{11}$ receptors which do not display internalization upon nucleotide treatment are functional receptors since they are capable of inducing intracellular Ca^{2+} or cAMP signaling. It has been proposed that the binding of different ligands to GPCRs may evoke physiologically active receptor conformations with different signaling specificity (Fergusson *et al.*, 2001; Kenakin *et al.,* 2007; Galandrin *et al.,* 2007; Hoffmann *et al.*, 2008a). These ligand-dependent conformations may

selectively trigger some downstream signaling pathways of the receptor, while other possible signaling pathways remain inactive. Following this concept, agonist-selective signaling of P2Y receptors via G proteins or β-arrestins may differentially activate Ca^{2+} signaling, cAMP signaling, β-arrestin-mediated ERK phosphorylation, receptor internalization, or possibly other signaling pathways. This concept was confirmed by Hoffmann and coworkers (2008b) who found that the recruitment of either β-arrestin 1 or β-arrestin 2 to the $P2Y_2$ receptor depends on the type of nucleotide, which is used for activating the receptor. ATP treatment would result in stronger β-arrestin 2 than β-arrestin 1 translocation, while UTP induction triggered equal β-arrestin 1 and 2 recruitment. The µ-opioid receptor provides another example of agonist-dependent signaling. Morphine is not able to trigger µ-opioid receptor phosphorylation and internalization, while etorphine can cause these processes (Zhang $et\ al.$, 1998). Only after a non-physiological over-expression of GRK2, morphine-induced phosphorylation of the µ-opioid receptor and subsequent internalization has been detected.

The results of our study demonstrate that the A87T mutation of the $P2Y_{11}$ receptor affects G protein signaling and receptor internalization alike. The severity of the impairment of the $P2Y_{11}$ receptor functions, however, is not equal for all nucleotides and signaling pathways.

The A87T mutation of the $P2Y_{11}$ receptor enhances desensitization, but improves resensitization of the intracellular Ca^{2+} response in comparison with the non-mutated $P2Y_{11}$ receptor.

The $P2Y_{11}A87T$ receptor completely lacks nucleotide-induced internalization in HEK293 cells over a time-span of 60 min. This indicates that the patho-physiological relevance of the mutation could depend more on the alteration of the long-term rather than short-term activity of the receptor. Eventually, this could lead to a higher cell responsiveness to prolonged exposures to natural activating nucleotides, like ATP.

Therefore, long-term Ca^{2+} measurements with HEK293 cells expressing the $P2Y_{11}$, $P2Y_{11}A87T$, or $P2Y_{11}A87S$ receptors were conducted (Figure 20A). The cells were challenged with a sustained 30 min exposure to ATP (100 µM) to allow receptor activation, subsequent response desensitization and, if possible, receptor internalization. After a following 60 min recovery period in nucleotide-free buffer, the retained cell responsiveness was determined by application of a 1 min pulse of ATP (100 µM; Figure 19). After the 30 min-treatment with ATP, cells expressing the $P2Y_{11}$ receptor showed a Ca^{2+} response level of 25% of the response at the start of the measurement (t = 0 min; Figure 20A). The cells expressing the $P2Y_{11}A87T$ or $P2Y_{11}A87S$ receptor showed a significantly lower Ca^{2+} response level of 15% and 12% of the response at 0 min, respectively. At first glance, one would expect the opposite result, as 30 min of nucleotide treatment triggers the internalization of the wildtype $P2Y_{11}$ receptor, while the $P2Y_{11}A87T$ receptor would remain at the plasma membrane and the $P2Y_{11}A87S$ receptor shows light internalization only (Figure 18). Therefore, the entirety of the $P2Y_{11}A87T$ receptors and the majority of the $P2Y_{11}A87S$ receptors would still be accessible to extracellular nucleotides and a higher resulting Ca^{2+} level was to be expected. However, it is known that GPCR desensitization due to phosphorylation via GRKs or second messenger kinases precedes receptor internalization (Ferguson $et\ al.$, 2001). Therefore, it is possible that $P2Y_{11}A87T$ and $P2Y_{11}A87S$ receptor desensitization via phosphorylation takes place despite the lack of receptor

internalization. The latter could be a consequence of a dysfunctional β-arrestin recruitment or binding and would not affect desensitizing receptor kinase activity.

After the final ATP-treatment at 90 min, hence at the end of the 60 min recovery period following the 30 min desensitization phase, the cells expressing the $P2Y_{11}$ receptor showed a poorly improved Ca^{2+} response (34% of the response at 0 min; Figure 20A). The cells expressing the mutated receptors showed a Ca^{2+} response of 51% ($P2Y_{11}A87T$ receptor) and 57% ($P2Y_{11}A87S$ receptor) of the respective responses at 0 min. This means that the HEK293 cells expressing mutated $P2Y_{11}$ receptors showed a much greater Ca^{2+} response recovery than cell expressing the non-mutated receptor (Figure 20A). This could be a consequence of the malfunctioning receptor internalization, as the receptors are still in place at the plasma membrane. On the other hand, dephosphorylation and resensitization of GPCRs were reported to depend on the internalization into endosomes and subsequent recycling to the plasma membrane (Ferguson *et al.*, 2001). Therefore, the mechanistic details of the desensitization process of the $P2Y_{11}A87T$ and $P2Y_{11}A87S$ receptor-induced responses remain to be elucidated. It is possible that the observed desensitization of the intracellular Ca^{2+} responses is not caused at the receptor level, but it could take place at some other point of the downstream signaling pathway. This possibility has to be considered, since Ecke *et al.* (2008) found that the $P2Y_{11}$ receptor is not capable of nucleotide-induced internalization in 1321N1 astrocytoma cells. Thus, $P2Y_{11}$ receptor desensitization in a physiological context without $P2Y_1$ receptor co-expression would have to rely on a mechanism, which does not involve $P2Y_{11}$ receptor internalization into endosomes.

General conclusions: Genetic polymorphisms of the $P2Y_{11}$ receptor might contribute to neurodegenerative diseases and immune disorders via altered long-term cell activity.

Our experimental data show that the effect of the A87T mutation on downstream signaling depends on the co-expression of the $P2Y_1$ receptor and, most likely, the formation of the $P2Y_1/P2Y_{11}$ receptor hetero-oligomers. Thus, future investigations of the A87T polymorphism of the human $P2Y_{11}$ receptor should consider possible $P2Y_1$ receptor interactions.

The $P2Y_{11}A87T$ receptor can activate ATP-induced Ca^{2+} and cAMP signaling in HEK293 cells, but a significant reduction of the potency of ATP was found. This possibly impairs long-term cellular functions. The mutated receptor fails to internalize in consequence of the ATP stimulus in $P2Y_1$ receptor-expressing HEK293 cells. This is expected to have a major impact on the regulation of $P2Y_{11}$ receptor-induced intracellular responses.

We found an apparently faster resensitization of the Ca^{2+} response in cells expressing the $P2Y_1$ plus the $P2Y_{11}A87T$ receptor in long-term experiments, which could be due to the lack of receptor internalization. We suggest that this might ultimately result in increased patho-physiological cell activity over an extended period of time. As the SNP leading to the A87T mutation has been linked to an increased risk for AMI (Amisten *et al.*, 2008), the SNP possibly contributes to the patho-physiological activity of immune cells in atherosclerosis, which is the main cause for AMI. Several immune cells known for their role in atherosclerosis, such as dendritic cells, macrophages, and mast cells co-express the $P2Y_1$ and $P2Y_{11}$ receptors. Near the necrotic cores of atherosclerotic sites, these cells are exposed to high concentrations of extracellular nucleotides, including ATP, due to a long-lasting chronic inflammation (Tabas, 2010).

Another SNP in the 3' UTR of the *P2RY11* gene was connected to narcolepsy with cataplexy, an auto-immune disease resulting in the loss of hypocretin-producing neurons (Kornum *et al.*, 2011). This SNP was reported result in impaired $P2Y_{11}$ receptor-mediated protection against ATP-induced cell death. Furthermore, reduced expression levels of the $P2Y_{11}$ receptor in CD8+ T-lymphocytes and natural killer cells were found, which could have a long-term effect on the nucleotide-induced activity of these cells.

Therefore, genetic polymorphisms of the $P2Y_{11}$ receptor might primarily affect long-term cell activity and could by this way contribute to the pathogenesis of neurodegenerative diseases and immune disorders in general. Thus, the modulation of the $P2Y_{11}$ receptor activity is a promising goal for future therapeutic approaches.

4.2 Novel nucleotide derivatives as agonists for the human $P2Y_{11}$ receptor or the $P2Y_6$ receptor

4.2.1 Evaluation of 2-propylthio-substituted derivatives of ATP as $P2Y_{11}$ receptor agonists

The nucleotide analog AR-C67085 (2-propylthio-ATP-β,γ-CCl$_2$) has been found to be one of the most potent agonists at the human $P2Y_{11}$ receptor (Communi *et al.*, 1999). In this study by Communi and coworkers, the potency for the $P2Y_{11}$ receptor-mediated elevation of IP$_3$ in 1321N1 astrocytoma cells has been reported to be 7-fold higher than that of the physiological standard agonist ATP, 1.2-fold higher than that of the $P2Y_{11}$ receptor-specific BzATP, and 1.5-fold higher than that of ATP-γS. In our study, we aimed to develop a $P2Y_{11}$ receptor agonist with increased potency and enhanced selectivity. Therefore we used analogs based on the structure of AR-C67085. 2-propylthio and β,γ-dichloromethylene substituents, which both can be found in AR-C67085, were introduced into ATP in different combinations with Pα-borano or Pα-thio substitutions (Figure 21). With the Pα substitutions, we specifically aimed to increase agonist selectivity for the $P2Y_{11}$ receptor over its closest homolog, the $P2Y_1$ receptor. These receptors display opposite diastereoselectivity for Pα-substituted nucleotides as has been described before in our laboratory (Major *et al.*, 2004b; Ecke *et al.*, 2006). It has been suggested by Major *et al.* (2004b) that the isomeric preference of the $P2Y_1$ receptor for certain isomers of Pα-substituted nucleotides has its origin in the lost interaction between a Pα-oxygen and a Mg^{2+} ion, which is coordinated within the binding pocket of the receptor. We assume a similar mechanistic reason for the diastereoselectivity of the $P2Y_{11}$ receptor. Ecke *et al.* (2006) reported that the preferred isomers of Pα-substituted nucleotides show improved potencies at the $P2Y_1$ and $P2Y_{11}$ receptors. We therefore expected increased agonist potency by using Pα-substituted derivatives of AR-C67085.

Here, we analyzed the nucleotide-induced intracellular Ca^{2+} responses in 1321N1 astrocytoma cells mediated by the adenine nucleotide-accepting $P2Y_1$, $P2Y_2$, and $P2Y_{11}$ receptors. We also studied cAMP responses induced by the $P2Y_{11}$ receptor. This lead to important conclusions regarding structure-activity relationships of the novel nucleotides.

The P2Y₁₁ receptor prefers Sp(B)-isomers of the Pα-borano substituted analogs over the respective Rp(A)-isomers.

The S*p*(B)-isomers of 2-propylthio-ATP-αB and 2-propylthio-ATP-αB-β,γ-CCl₂ show higher potency at the P2Y₁₁ receptor than the respective R*p*(A)-isomers (Table 5). The B-isomer of the former was about 13-fold more potent than its A-isomer, while the B-isomer of the latter was about 3-fold more potent. This is in accordance with the previous results of Ecke *et al.* (2006). There, the S*p*-isomer of ATP-αB was about 7-fold more potent at the P2Y₁₁ receptor than the respective R*p*-isomer, which was equipotent to ATP. The preferred isomer of the Pα-thio substituted derivative, R*p*-ATP-αS, was found in this study to be about 6-fold more potent than the respective S*p*-isomer. Interestingly, in our study the P2Y₁₁ receptor showed no significant preference for either isomer of 2-propylthio-ATP-αS and 2-propylthio-ATP-αS-β,γ-CCl₂ (Figure 22A/C). Thus, only the addition of a Pα-borano group lead to diastereoselectivity at the P2Y₁₁ receptor and also yielded the most potent analogs. Nevertheless, all Pα-modifications lead to a substantial increase of potency compared with ATP.

A	B
2-propylthio-ATP-αB	**2-propylthio-ATP-αB-β,γ-CCl₂**
EC₅₀ (P2Y₁₁ receptor) = 0.03 µM (B-isomer)	**EC₅₀ (P2Y₁₁ receptor) = 0.03 µM (B-isomer)**
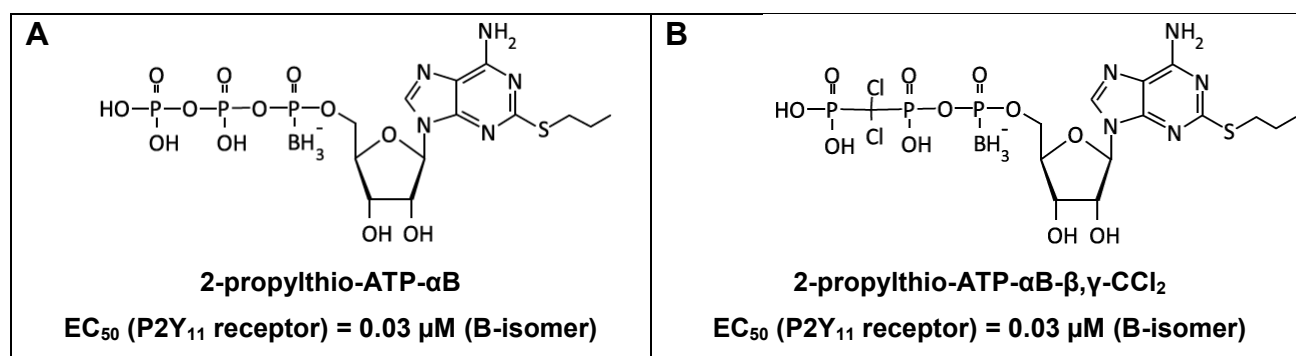
Figure 31: Structure of the most potent of the 2-proplythio-substituted derivatives of ATP tested at the human P2Y₁₁ receptor expressed in 1321N1 astrocytoma cells.
A: 2-propylthio-ATP-αB, **B:** 2-propylthio-ATP-αB-β,γ-CCl₂.

Combined modifications at the C2 position and at the α-phosphate of ATP can result in strongly enhanced agonist activity at the P2Y₁₁ receptor.

Computational modeling of the P2Y₁₁ receptor by Zylberg *et al.* (2007) revealed the existence of a confined hydrophobic pocket near the C2 position of an ATP molecule coordinated inside the receptor binding pocket. This has prompted the hypothesis that modifications at the C2 position of ATP might enhance nucleotide potency at the P2Y₁₁ receptor due to improved nucleotide binding. However, nucleotides with C2 substitutions like 2-MeS-ATP and 2-Cl-ATP have been found by Ecke *et al.* in 2006 to be only weak agonists of the P2Y₁₁ receptor. Importantly, the addition of Pα-borano or Pα-thio groups to these analogs significantly increased the nucleotide potency. The combination of C2 and Pα substitutions in 2-MeS-ATP-αB lead to one of the most potent P2Y₁₁ receptor agonist in the study of Ecke and coworkers (EC₅₀ value for the B-isomer = 0.26 µM; EC₅₀ value for ATP = 2.83 µM).

Similar to the C2-substituted ATP derivatives in these earlier studies, 2-propylthio-ATP showed no enhanced potency in the present study, when compared with ATP (EC₅₀ = 2.5 µM and 2.6 µM, respectively; Table 5). However, the combination of the Pα-borano substitution with the 2-propylthio group remarkably reduced the EC₅₀ value. 2-propylthio-ATP-αB (Figure 31) turned out to

69

be one of the most potent $P2Y_{11}$ receptor agonist in the present study with an EC_{50} value for the B-isomer of 0.03 µM. This novel $P2Y_{11}$ receptor agonist was 87-times more potent than the physiological standard agonist ATP. As the B-isomers of neither ATP-αB (EC_{50} = 0.34 µM; Ecke *et al.*, 2006) nor 2-propylthio-ATP (EC_{50} = 2.5 µM) are as potent as the B-isomer of 2-propylthio-ATP-αB, the combination of the C2 and the Pα modifications in the latter nucleotide are the reason for substantial increase of potency.

The dichloromethylene modification between β- and γ-phosphates does not affect nucleotide potency of ATP derivatives at the $P2Y_{11}$ receptor.

The introduction of a β,γ-dichloromethylene group to 2-propylthio-ATP-αB has lead only to a minor enhancement of potency of the A-isomer of 2-propylthio-ATP-αB-β,γ-CCl_2 (Figure 31), in comparison to the A-isomer of 2-propylthio-ATP-αB (Table 5). The potency of the B-isomer was actually identical, with an EC_{50} value of 0.03 µM. Thus, the addition of the β,γ-CCl_2 group was not beneficial regarding nucleotide potency. Moreover, in 2-propylthio-ATP-αS-β,γ-CCl_2 the β,γ-CCl_2 group was detrimental to the potency of both isomers when compared with 2-propylthio-ATP-αS.

Substitutions of the bridging oxygen in the phosphate chain can be used to increase resistance against cleavage by e-NTPDases (Eliahu *et al.*, 2010). Nevertheless, AR-C67085, which carries a CCl_2 substituent between the β- and γ-phosphates, was reported to have a short half-life in human of about 2 min (Humphries *et al.*, 1995). This, however, was likely due to cleavage between the α- and β-phosphates, as the diphosphate nucleotide metabolite of AR-C67085 has not been detected. Pα-borano substitutions have been reported to increase nucleotide stability against hydrolysis by NPP1 and NPP3 before (Nahum *et al.*, 2006; Ginsburg *et al.*, 2012). Hence, the combined modifications in 2-propylthio-ATP-αB-β,γ-CCl_2 are expected to provide enhanced resistance against hydrolysis compared to 2-propylthio-ATP-αB. Thus, despite the fact that the B-isomers of both analogs showed identical EC_{50} values, 2-propylthio-ATP-αB-β,γ-CCl_2 is possibly the more promising nucleotide scaffold for future drug development.

The dichloromethylene modification between β- and γ-phosphates improves $P2Y_{11}$ receptor specificity.

It is an important criterion for drug candidates to specifically activate or inactivate only one of the receptors within the P2Y receptor family. The $P2Y_1$, $P2Y_2$, and $P2Y_{11}$ receptors are all coupled to the same G_q signaling pathway and can all be activated by adenosine nucleotides. At the $P2Y_1$ receptor, both isomers of 2-propylthio-ATP-αS, the A-isomer of 2-propylthio-ATP-αB, and 2-propylthio-ATP induced strong intracellular Ca^{2+} responses to nucleotide concentrations of 10 µM (Figure 23B). However, only for 2-propylthio-ATP a complete concentration-response-curve could be established (Figure 24), and the EC_{50} value was calculated to be 0.04 µM. In the group of nucleotides without a dichloromethylene substitution, the B-isomer of 2-propylthio-ATP-αB displayed the lowest intracellular Ca^{2+} response. However, the β,γ-CCl_2-substituted nucleotides generally induced lower Ca^{2+} responses to nucleotide concentrations of 10 µM than the nucleotides without a β,γ-CCl_2-group. The R*p*-isomers of 2-propylthio-ATP-αS-β,γ-CCl_2 (= B-isomer) and 2-propylthio-ATP-αB-β,γ-CCl_2 (= A-isomer) induced the lowest responses in 1321N1 astrocytoma cells expressing the $P2Y_1$ receptor. As these nucleotides were potent agonists of the $P2Y_{11}$ receptor, the dichloromethylene group between the β- and γ-phosphate increased the specificity of the novel nucleotide analogs for the $P2Y_{11}$ over the $P2Y_1$

receptor. Thus, the benefit of the dichloromethylene group here is primarily lies within increased $P2Y_{11}$ receptor specificity, rather than an enhanced potency.

As described in the introduction (chapter 1.2), the human $P2Y_2$ receptor equally accepts UTP and ATP. Of the tested compounds, none but 2-propylthio-ATP was able to induce a notable intracellular Ca^{2+} response at this receptor for a nucleotide concentration of 10 µM (Figure 23C). However, 2-propylthio-ATP is only a weak agonist of the $P2Y_2$ receptor since a concentration of 1 µM did not result in a detectable Ca^{2+} response.

AR-C67085 is an antagonist at the $P2Y_{12}$ (Ingall *et al.*, 1999) and $P2Y_{13}$ receptors (Marteau *et al.*, 2003). Both receptors are coupled to G_i signaling and therefore mediate the nucleotide-induced inhibition of intracellular cAMP signaling. The novel nucleotide derivatives tested here are based on the structure of AR-C67085. Therefore, an antagonistic activity at the $P2Y_{12}$ and $P2Y_{13}$ receptors should be addressed in future studies.

The novel 2-propylthio-ATP derivatives reveal that the diastereospecificity of the human $P2Y_{11}$ receptor affects the induction of cAMP responses.

The activation of the $P2Y_{11}$ receptor triggers the elevation of the intracellular cAMP concentration via G_s signaling and subsequent activation of AC. The B-isomers of 2-propylthio-ATP-αB and 2-propylthio-ATP-αB-β,γ-CCl$_2$ were the most potent analogs for the induction of $[Ca^{2+}]_i$ elevation in $P2Y_{11}$ receptor-expressing 1321N1 astrocytoma cells. These analogs triggered cAMP accumulation in a concentration-dependent manner (Figure 25). The EC_{50} value for the induction of cAMP signaling by both nucleotides can be estimated to be around 0.1 µM. This is in line with their equal potency for the induction of Ca^{2+} signaling (EC_{50} = 0.03 µM each). Also in accordance with the data from the intracellular Ca^{2+} measurements is our finding that 2-propylthio-ATP-αB(B) and 2-propylthio-ATP-αB-β,γ-CCl$_2$(B) were more potent than ATP to trigger cAMP increase (Figure 26). The difference in potency for the induction of Ca^{2+} signaling between the two isomers of 2-propylthio-ATP-αB was 13-fold. We found a similar difference between these isomers in the ability to cause intracellular cAMP accumulation, since the A-isomer of 2-propylthio-ATP-αB induced only a weak response at 10 µM. This demonstrates a diastereoselective activation of both the G_q and G_s signaling pathways via the human $P2Y_{11}$ receptor.

4.2.2 Evaluation of 5-methoxy-substituted derivatives of UDP as $P2Y_6$ receptor agonists

5-OMe and Pα substitutions in UDP highly increase the nucleotide potency at the $P2Y_6$ receptor.

Substitutions at position 5 of the nucleobase of uridine nucleotides are well tolerated by the $P2Y_6$ receptor since 5-Br-UTP (Communi *et al.*, 1996), 5-Br-UDP, and 5-I-UDP (Nicholas *et al.*, 1996; Besada *et al.*, 2006) show agonist activity at this receptor. Here, we investigated the potency of 5-OMe-substituted derivatives of UDP at the uridine nucleotide-preferring $P2Y_2$, $P2Y_4$, and $P2Y_6$ receptors expressed in 1321N1 astrocytoma cells to induce intracellular Ca^{2+} responses (Figure 27). Additionally, substitutions of non-bridging oxygen at the phosphate chain, introducing a new chiral center, of several mono- and di-nucleotide analogs were analyzed. As discussed above, Pα-

substituents of non-bridging oxygen have been reported to increase the potency of agonists at the P2Y$_1$ and P2Y$_{11}$ receptors (Major *et al.*, 2004b; Ecke *et al.*, 2006) before.

The C5-substition in 5-OMe-UDP makes the compound about 2.6-fold more potent at the P2Y$_6$ receptor than the physiological standard agonist UDP (Table 6). The additional introduction of a Pα-borano substitution, resulting in 5-OMe-UDP-αB (Figure 32), further increased the nucleotide potency by a factor of 11 for the R*p*(A)-isomer. Thus, 5-OMe-UDP-αB(A) was about 29-fold more potent than UDP, which makes it the most potent P2Y$_6$ receptor agonist known to date. Furthermore, the S*p*(B)-isomer showed a more than 600-times lower potency than the corresponding A-isomer. As a consequence, the B-isomer was 21-fold less potent than UDP. These findings demonstrate a previously unknown diastereoselectivity of the human P2Y$_6$ receptor and emphasize the potential to enhance agonist potency by exploiting the receptor diastereoselectivity. However, in contrast to the highly potent 5-OMe-UDP-αB, 5-OMe-UTP-αB was a poor agonist of the P2Y$_6$ receptor (Ginsburg-Shmuel *et al.*, 2012). Hence, the 5-OMe and Pα substitutions could not overcome the P2Y$_6$ receptor preference for uridine 5'-diphosphates over the respective triphosphates.

5-OMe-UDP-αB

EC$_{50}$ (P2Y$_6$ receptor) = 0.008 µM (A-isomer)
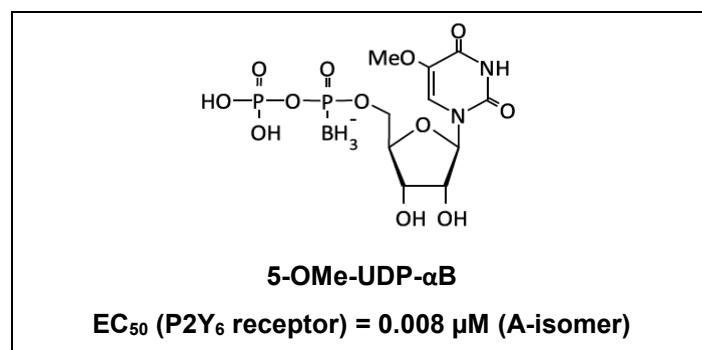
Figure 32: Structure of 5-OMe-UDP-αB, the most potent of the 5-OMe-substituted derivatives of UDP tested at the human P2Y$_6$ receptor expressed in 1321N1 astrocytoma cells.

Despite the fact that Up$_3$U (uridine 5'-triphosphate 5''-uridine) was reported to be a potent agonist of the P2Y$_6$ receptor (EC$_{50}$ for the rise of [Ca^{2+}]$_i$ = 0.92 µM; Shaver *et al.*, 2005), the 5-OMe-substituted Up$_3$U derivative (5-OMe-U)-P$_3$-(5-OMe-U) tested here was only a poor agonist of the P2Y$_6$ receptor (EC$_{50}$ > 10 µM). The combination of this 5-OMe-substituted di-nucleotide scaffold with a boranated α-phosphate, resulting in (5-OMe-U)-P$_3$αB-(5-OMe-U), lead to greatly improved potencies for both isomers (EC$_{50}$ = 0.14 µM and 2.0 µM for the A- and B-isomer, respectively). However, the potency of the A-isomer was still about 18-fold lower than that of the corresponding mono-nucleotide 5-OMe-UDP-αB(A). Apparently, the 5-OMe substitution or potentially the presence of a double 5-OMe substitution was detrimental for the potency of the di-nucleotides. Diastereoselectivity of the P2Y$_6$ receptor for the isomers of (5-OMe-U)-P$_3$αB-(5-OMe-U) was detectable, but was much less pronounced than for the isomers of 5-OMe-UDP-αB. The A-isomer of (5-OMe-U)-P$_3$αB-(5-OMe-U) was only 14-times more potent than the B-isomer.

Our data indicate that the position of the borano substitution in uridine di-nucleotides is of lesser relevance for the potency at the P2Y$_6$ receptor. The relatively low EC$_{50}$ value of 0.2 µM for the non-chiral   (5-OMe-U)-P$_3$βB-(5-OMe-U)   almost   equaled   the   EC$_{50}$ value   of

(5-OMe-U)-P$_3\alpha$B-(5-OMe-U)(A) of 0.14 µM. Importantly, and similar to the observations made with the mono-nucleotides, the borano-substituents at the phosphate chain generally enhanced the potency at the human P2Y$_6$ receptor of all 5-OMe-substituted di-nucleotides.

Boranated phosphates improve P2Y$_6$ receptor selectivity of 5-OMe-UDP analogs.

None of the tested 5-OMe-UDP derivatives showed agonist activity at the human P2Y$_2$ receptor (Figure 30A). At the P2Y$_4$ receptor, 5-OMe-UDP caused a moderate intracellular Ca^{2+} response for a nucleotide concentration of 50 µM, which reached about 50% of the maximal response at the P2Y$_6$ receptor (Figure 30B). The additional substitution of a non-bridging oxygen bound to the α-phosphate by a borano group lead to greatly reduced potency at the P2Y$_4$ receptor of the 5-OMe-UDP derivatives, thus influencing nucleotide specificity in favor of the P2Y$_6$ receptor.

The insurmountable P2Y$_6$ receptor antagonist MRS2578 (10 µM) reduced the intracellular Ca^{2+} response to 5-OMe-UDP-αB(A), which was given at the same concentration, by almost 80% (Figure 29). This result proves that responses to the tested novel nucleotide analogs are indeed driven by the P2Y$_6$ receptor.

4.2.3 Conclusions about structure-activity relationships of the novel P2Y$_{11}$ and P2Y$_6$ receptor agonists

The ability to selectively activate P2Y receptors in a physiological context, i.e. expressed in the multi-receptor environment of a human cell or tissue, is a main goal for the development of novel P2Y receptor agonists. It can help treating P2Y receptor-associated disorders but also facilitate the research of physiological and patho-physiological purinergic processes. For this reason, a large number of differently modified nucleotide analogs was evaluated in the past at the known human P2Y receptors. Here, novel nucleotide derivatives specifically synthesized for P2Y$_{11}$ and P2Y$_6$ receptor activation were successfully investigated, and promising findings about structure-activity relationships were achieved.

The combination of 2-propylthio and PαB substitutions in ATP greatly enhanced nucleotide potency at the P2Y$_{11}$ receptor, β,γ-CCl$_2$ modification was beneficial for receptor selectivity.

Here, we identified some of the most potent P2Y$_{11}$ receptor agonists known. The B-isomers of 2-propylthio-ATP-αB and 2-propylthio-ATP-αB-β,γ-CCl$_2$ have EC$_{50}$ values in the nanomolar range which are about 87-times lower than the EC$_{50}$ value of the physiological standard agonist ATP. AR-C67085, which is structurally related to the novel nucleotides investigated in the present study, was reported to be only 7-fold more potent than ATP for inducing the elevation of IP$_3$ (Communi *et al.*, 1999). 2-propylthio-ATP-αB(B) and 2-propylthio-ATP-αB-β,γ-CCl$_2$(B) have been shown to be suitable for the dual activation of the G$_q$ and G$_s$ signaling pathways linked to the P2Y$_{11}$ receptor. The Pα substitution of 2-propylthio-ATP-derived nucleotides enhanced the nucleotide potency and revealed that the P2Y$_{11}$ receptor has a diastereoselectivity not only for the activation of nucleotide-induced Ca^{2+} signaling but also for cAMP signaling. The β,γ-CCl$_2$ substitution improved the specificity of the nucleotide analogs for the P2Y$_{11}$ receptor over the P2Y$_1$ receptor. This modification is also expected to enhance the hydrolytic stability in concert with the Pα-borano substitutions. This makes the Sp(B)-isomer of 2-propylthio-ATP-αB-β,γ-CCl$_2$ a most interesting candidate for future drug development.

The 5-OMe substitution in UDP in addition to a PαB modification greatly enhanced nucleotide potency at the P2Y₆ receptor.

The 5-OMe substitution at the nucleobase of UDP together with the Pα-borano modification resulted in the most potent P2Y$_6$ receptor agonist known to date: 5-OMe-UDP-αB(A). Also, the experimental results provide the first evidence for a diastereoselectivity of the human P2Y$_6$ receptor.

Nucleotides are notoriously unstable extracellular compounds, as intercellular purinergic signaling often depends on the quick modulation of the respective physiological pathways by hydrolytic enzymes. To be suitable drug candidates, however, nucleotides must provide some chemical and metabolic stability. It was found by Ginsburg-Shmuel *et al.* (2012) that a PαB substitution in UDP was detrimental to the hydrolytic stability under gastric juice conditions, likely due to the vulnerability of the phosphate-borano-bond to acidic hydrolysis. Nevertheless, the half-lifetime of circa 17 h of the A-isomer of 5-OMe-UDP-αB highly recommends this compound as a drug candidate. The resistance against hydrolysis by NPP1 and 3 was significantly enhanced by the PαB substitution of 5-OMe-UDP-αB(A) when compared with UDP and 5-OMe-UDP. This shows that Pα-borano-substituted UDP derivatives are poor substrates for NPP1 and 3. In human blood serum, which contains multiple hydrolyzing enzymes, a 50% hydrolysis of 5-OMe-UDP-αB(A) was found after 17 h. 5-OMe-UDP had a half-lifetime of around 12 h, and UDP of only 2.4 h. Thus, the 5-OMe-group significantly increased the resistance to hydrolysis in human blood serum and the introduction of a Pα-borano group even further enhanced the nucleotide stability.

Furthermore, di-nucleotide derivatives of 5-OMe-UDP might be promising drug candidates, in spite of the comparably low potency at the P2Y$_6$ receptor. We base this suggestion on the fact that the di-nucleotide scaffold has been reported to provide enhanced chemical and metabolic stability (Yerxa *et al.*, 2002; Shaver *et al.*, 2005).

5. Zusammenfassung

Im humanen *P2RY11* Gen spielen SNP (Single-Nucleotide-Polymorphism) eine Rolle bei der langfristigen Entwicklung verschiedener Krankheiten. Ein SNP in der 3' UTR steht zum Beispiel mit Narkolepsie/Kataplexie, reduzierter Expression des $P2Y_{11}$ Nukleotid-Rezeptors in Immunzellen und einer gesteigerten Anfälligkeit für ATP-induzierten Zelltod in Verbindung. Ein weiterer häufiger SNP im kodierenden Bereich dieses Gens führt zur Synthese der Ala-87-Thr (A87T) Variante des $P2Y_{11}$ Rezeptors. Der mutierte Rezeptor enthält ein polares Threonin statt des unpolaren Alanin am Ende der Transmembranregion-2. Diese Mutation steht mit erhöhtem Herzinfarktrisiko und gesteigerter Konzentration von C-reaktivem Protein in Zusammenhang. Die vorliegende Arbeit beschreibt die erste funktionelle Charakterisierung des mutierten $P2Y_{11}A87T$ Rezeptors. Im Vergleich mit dem $P2Y_{11}$ Wildtyp-Rezeptor konnten wir in HEK293 Zellen eine substantielle Reduktion der Nukleotid-induzierten Ca^{2+} und cAMP Antworten feststellen. Kontrollexperimente ergaben, dass diese Unterschiede nicht eine Folge reduzierter Expressionsspiegel des $P2Y_{11}A87T$ Rezeptors sind. Ferner konnten wir in HEK293 Zellen keine Nukleotid-induzierte Internalisierung des $P2Y_{11}A87T$ Rezeptors beobachten. Trotzdem führte die Langzeit-Stimulation mit ATP zu einer, im Vergleich zum $P2Y_{11}$ Wildtyp-Rezeptor, verstärkten Desensitivierung der intrazellulären Ca^{2+}-Antwort. Die anschließende Resensitivierung der Ca^{2+}-Antwort war jedoch deutlich verstärkt. Diese Ergebnisse demonstrieren einen großen Einfluss des $P2Y_{11}A87T$ Rezeptors auf zelluläre Langzeit-Antworten.

Von großer Bedeutung ist unser Befund, dass eine funktionelle Beeinträchtigung des $P2Y_{11}A87T$ Rezeptors nur in den Zellen gemessen werden konnte, die gleichzeitig den $P2Y_1$ Rezeptor exprimierten. Die Oligomerisierung der $P2Y_1$ und $P2Y_{11}$ Rezeptoren wurde bereits in einer früheren Studie experimentell belegt. Wir schlussfolgern daher, dass die A87T Mutation des $P2Y_{11}$ Rezeptors zu einer Beeinträchtigung der Funktionalität des Rezeptor-Oligomers führt. Zukünftige Untersuchungen zur Rolle des humanen $P2Y_{11}A87T$ Rezeptors sollten daher eine Co-Expression des $P2Y_1$ Rezeptors berücksichtigen. Das betrifft weitere Untersuchungen über die Verbindung des $P2Y_{11}A87T$ Rezeptors zu gesteigertem Herzinfarktrisiko, und auch Studien zu Inflammation und Prozessen des Immunsystems mit bekannter $P2Y_{11}$ Rezeptor Beteiligung.

Da die Aktivität von P2Y Rezeptoren bei zahlreichen physiologischen und pathologischen Prozessen wichtig ist, stellt die Regulierung der Rezeptoren ein vielversprechendes Ziel für künftige therapeutische Ansätze dar. Wir konnten neue chirale Agonisten für humane P2Y Rezeptoren identifizieren. Diese Liganden, synthetisiert von Prof. B. Fischer von der Bar-Ilan University in Ramat-Gan (Israel), können als Basis für weitere pharmakologische Entwicklungen dienen. S*p*-2-propylthio-ATP-αB und S*p*-2-propylthio-ATP-αB-β,γ-CCl₂ gehören zu den potentesten bekannten $P2Y_{11}$ Rezeptor-Agonisten und zeigten eine jeweils 87-fach höhere Potenz, als ATP. R*p*-5-OMe-UDP-αB ist der potenteste bislang bekannte $P2Y_6$ Rezeptor-Agonist. Er ist 29-fach potenter als UDP und offenbarte eine bislang unbekannte Diastereoselektivität des $P2Y_6$ Rezeptors. Diese Ergebnisse verdeutlichen, dass die Berücksichtigung der Stereoselektivität von P2Y Rezeptoren für das Design stabiler, selektiver und sehr potenter Agonisten von entscheidender Bedeutung ist.

6. Abstract

Single-nucleotide polymorphisms (SNP) of the human *P2RY11* gene are connected to the long-term development of several disorders. A SNP in the 3' UTR is associated with narcolepsy/cataplexy, reduced expression levels of the $P2Y_{11}$ nucleotide receptor in immune cells, and enhanced susceptibility to ATP-induced cell death. A frequent SNP in the coding region of the gene leads to the Ala-87-Thr (A87T) variant of the $P2Y_{11}$ receptor. The resulting mutant $P2Y_{11}A87T$ receptor contains a polar threonine residue near the end of the transmembrane region-2 instead of a nonpolar alanine. This mutation is associated with increased risk for acute myocardial infarction and elevated levels of C-reactive protein. We here present the first functional characterization of the $P2Y_{11}A87T$ receptor. Nucleotide-induced Ca^{2+} and cAMP responses mediated by the $P2Y_{11}A87T$ receptor in HEK293 cells were substantially reduced, in comparison with the wildtype $P2Y_{11}$ receptor. Control experiments verified that these reductions were not due to reduced expression levels of the mutated $P2Y_{11}A87T$ receptors. We further found that the mutant receptor lacks nucleotide-induced internalization in HEK293 cells. Nevertheless, prolonged treatment with ATP leads to increased desensitization of the Ca^{2+} response, compared with the wildtype $P2Y_{11}$ receptor. This is followed by enhanced resensitization of the Ca^{2+} response. This finding demonstrates an important influence of the $P2Y_{11}A87T$ receptor on long-term cellular responses.

Importantly, we detected functional impairments of the mutant $P2Y_{11}A87T$ receptor only in cells, which co-express the $P2Y_{11}A87T$ receptor together with the $P2Y_1$ receptor. Oligomerization of $P2Y_1$-$P2Y_{11}$ receptors has been shown before by several lines of evidence in a previous study. We thus conclude that the A87T amino acid shift in the $P2Y_{11}$ receptor has a detrimental effect on the functionality of the oligomer. Consequently, future research on the contribution of the A87T mutation of the human $P2Y_{11}$ receptor to cellular dysfunctions and pathological processes should consider $P2Y_1$ receptor co-expression in cells. This includes studies of the contribution of the $P2Y_{11}A87T$ receptor to acute myocardial infarction but also other inflammatory and immune system-related processes with known $P2Y_{11}$ receptor contribution.

Since P2Y receptor activity is connected to many physiological and pathological processes, the modulation of P2Y receptor signaling is a promising goal for future therapeutic approaches. We identified novel chiral agonists of human P2Y receptors. The ligands, synthesized by Prof. B. Fischer from the Bar-Ilan University, Ramat-Gan, Israel, are a basis for further drug development. We identified S*p*-2-propylthio-ATP-αB and S*p*-2-propylthio-ATP-αB-β,γ-CCl₂ as the most potent known agonists of the $P2Y_{11}$ receptor with 87-fold higher potency than ATP. We found that R*p*-5-OMe-UDP-αB is the most potent $P2Y_6$ receptor agonist known so far. It is 29-fold more potent than UDP and revealed a previously unknown diastereoselectivity of the $P2Y_6$ receptor. Thus, exploiting the stereoselectivity of P2Y receptors is vital for the development of stable, selective, and very potent agonists.

7. Abbreviations

#

[Ca^{2+}]$_i$: intracellular calcium concentration

2-Cl-ATP: 2-chloro-adenosine 5'-triphosphate

2-Cl-ATP-αB: 2-chloro-adenosine 5'-triphosphate-α-borano

2-MeS-ADP: 2-methlythio-adenosine 5'-diphosphate

2-MeS-ATP: 2-methylthio-adenosine 5'-triphosphate

2-MeS-ATP-αB: 2-methylthio-adenosine 5'-triphosphate-α-borano

5-Br-UTP: 5-bromo-uridine 5'-triphosphate

5-I-UDP: (5-iodo-uridine 5'-diphosphate)

7TMR: seven-transmembrane receptor

A

ABC: ATP-binding cassette

AC: adenylyl cyclase

ADP: adenosine 5'-diphosphate

AMP: adenosine 5'-monophosphate

AMI: acute myocardial infarction

ATP: adenosine 5'-triphosphate

ATP-αB: adenosine 5'-triphosphate-α-borano

ATP-βS: adenosine 5'-triphosphate-β-thio

ATP-γS: adenosine 5'-triphosphate-γ-thio

Ap$_3$A: adenosine 5'-triphospho 5''-adenosine, diadenosine triphosphate

Ap$_4$A: adenosine 5'-tetraphospho 5''-adenosine, diadenosine tetraphosphate

Ap$_5$A: adenosine 5'-pentaphospho 5''-adenosine, diadenosine pentaphosphate

Ap$_6$A: adenosine 5'-hexaphospho 5''-adenosine, diadenosine hexaphosphate

Ap$_4$U: adenosine 5'-tetraphosphate 5''-uridine

AR-C67085: 2-propylthio-ATP-β,γ-dichloromethylene

B

BzATP: 2'(3')-O-(4-Benzoylbenzoyl)adenosine 5'-triphosphate

C

cAMP: 3'-5'-cyclic adenosine monophosphate

CDP: cytidine 5'-diphosphate

cGMP: 3'-5'-cyclic guanosine monophosphate

CFTR: cystic fibrosis transmembrane conductance regulator

CTP: cytidine 5'-triphosphate

CysLT$_1$R: cysteinyl leukotriene receptor 1

D

Dabco: 1,4-Diazabicyclo[2.2.2]octane

dATP: 2'-deoxyadenosine 5'-triphosphate

DC: dendritic cell

E

E-NTPDase: ecto-nucleoside triphosphate diphosphohydrolase

E-NPP: ecto-nucleotide pyrophosphatase/phosphodiesterase

Ecto-NDPK: ecto-nucleoside diphosphokinase

EL: extracellular loop

Erk: extracellular signal-related protein kinase

F

FAD: flavin adenine dinucleotide

FCS: fetal calf serum

FRET: fluorescence resonance energy transfer

G

GC: guanylyl cyclase

GPCR: G protein-coupled receptor

GRK: G protein-coupled receptor kinase

GST: glutatione S-transferase

GTP: guanosine 5'-triphosphate

H

HNP: human neutrophil peptide

I

IBMX: isobutyl-methyl-xanthine

IL: interleukin

ITP: inosine 5'-triphosphate

IP$_3$: inositol-1,4,5-trisphosphate

M

MAPK: mitogen-activated protein kinase

mBMMC: mouse bone marrow-derived mast cell

MRS2179: N^6-methyl-2'-deoxyadenosine 3',5' diphosphate

MRS2578: 1,4-di-[(3-isothio-cyanato phenyl)-thioureido]butane

MRS2957: N^4-methoxy-cytidine 5'-triphosphate 5''-uridine

N

NAD: nicotinamide adenine dinucleotide

NADP: nicotinamide adenine dinucleotide phosphate

NO: nitric oxide

P

PKA: protein kinase A / cAMP-dependent protein kinase

PKC: protein kinase C

PLC: protein lipase C

P_i: orthophosphate

PP_i: pyrophosphate

R

RT: room temperature

S

siRNA: small interfering ribonucleic acid

SNP: single-nucleotide polymorphism

T

TNF-α: tumor necrosis factor-α

TTP: thymidine 5'-triphosphate

U

Up₃U: uridine 5'-triphospho 5''-uridine, diuridine triphosphate

UTP: uridine 5'-triphosphate

UTP-βS: uridine 5'-triphosphate-β-thio

UDP: uridine 5'-diphosphate

V

VNUT: vesicular nucleotide transporter SLC17A9

8. References

Abbracchio M.P., Burnstock G., Boeynaems J., Barnard E.A., Boyer J.L., Kennedy C., et al. International Union of Pharmacology LVIII: update on the P2Y G protein-coupled nucleotide receptors: from molecular mechanisms and pathophysiology to therapy. Pharmacol Rev. 2006, 58:281-341.

Adamson S.E., Leitinger N. The role of pannexin1 in the induction and resolution of inflammation. FEBS Lett. 2014, 588(8):1416-1422.

Albright R.A., Chang W.C., Robert D., Ornstein D.L., Cao W., Liu L., et al. NPP4 is a procoagulant enzyme on the surface of vascular endothelium. Blood. 2012, 120(22):4432-40.

Amisten S., Melander O., Wihlborg A., Berglund G., Erlinge D. Increased risk of acute myocardial infarction and elevated levels of C-reactive protein in carriers of the Thr-87 variant of the ATP receptor $P2Y_{11}$. Eur Heart J. 2007, 28:13–18.

Berchtold S., Ogilvie A.L., Bogdan C., Mühl-Zürbes P., Ogilvie A., Schuler G., Steinkasserer A. Human monocyte derived dendritic cells express functional P2X and P2Y receptors as well as ecto-nucleotidases. FEBS Lett. 1999, 458(3):424-8.

Berg J.M., Tymoczko J.L., Stryer L. Biochemistry. 5th edition. New York: W H Freeman; 2002.

Besada P., Shin D.H., Costanzi S., Ko H., Mathe C., Gagneron J., et al. Structure-activity relationships of uridine 5'-diphosphate analogues at the human $P2Y_6$ receptor. J Med Chem. 2006, 49:5532-5543.

Bell P.D., Lapointe J.Y., Sabirov R., Hayashi S., Peti-Peterdi J., Manabe K., et al. Macula densa cell signaling involves ATP release through maxi anion channel. Proc Natl Acad Sci U S A. 2003, 100(7):4322-7.

Bianchi B.R., Lynch K.J., Touma E., Niforatos W., Burgard E.C., Alexander K.M., et al. Pharmacological characterization of recombinant human and rat P2X receptor subtypes. Eur J Pharmacol. 1999, 376(1-2):127-138.

Bodin P., Burnstock G. Evidence that release of adenosine triphosphate from endothelial cells during increased shear stress is vesicular. J Cardiovasc Pharmacol. 2001, 38(6):900-8.

Bours M.J., Swennen E.L., Di Virgilio F., Cronstein B.N., Dagnelie P.C. Adenosine 5'-triphosphate and adenosine as endogenous signaling molecules in immunity and inflammation. Pharmacol Ther. 2006, 112(2):358-404.

Burnstock G. Purinergic signalling. Br J Pharmacol. 2006, 147:S172–S181.

Burnstock G. Physiology and pathophysiology of purinergic neurotransmission. Physiol Rev. 2007, 87(2):659-797.

Burnstock G. Purinergic signalling and disorders of the central nervous system. Nat Rev Drug Discov. 2008, 7(7):575-90.

Burrell H.E., Bowler W.B., Gallagher J.A., Sharpe G.R. Human keratinocytes express multiple P2Y-receptors: evidence for functional $P2Y_1$, $P2Y_2$, and $P2Y_4$ receptors. J Invest Dermatol. 2003, 120(3):440-7.

Camargo C.A. Jr., Smithline H.A., Malice M.P., Green S.A., Reiss T.F. A randomized controlled trial of intravenous montelukast in acute asthma. Am J Respir Crit Care Med. 2003, 167(4):528-33.

Carracedo G., Guzman-Aranguez A., Loma P., Pintor J. Diadenosine polyphosphates release by human corneal epithelium. Exp Eye Res. 2013, 113:156-61.

Carroll J.S., Ku C.J., Karunarathne W., Spence D.M. Red blood cell stimulation of platelet nitric oxide production indicated by quantitative monitoring of the communication between cells in the bloodstream. Anal Chem. 2007, 79(14):5133-8.

Carter R.L., Fricks I.P., Barrett M.O., Burianek L.E., Zhou Y., Ko H., et al. Quantification of G_i-mediated inhibition of adenylyl cyclase activity reveals that UDP is a potent agonist of the human $P2Y_{14}$ receptor. Mol Pharmacol. 2009, 76(6):1341-8.

Chambers J.K., Macdonald L.E., Sarau H.M., Ames R.S., Freeman K., Foley J.J., et al. A G protein-coupled receptor for UDP-glucose. J Biol Chem. 2000, 275(15):10767-71.

Communi D., Motte S., Boeynaems J., Pirotton S. Pharmacological characterization of the human $P2Y_4$ receptor. Eur J Pharmacol. 1996, 317(2-3):383-9.

Communi D., Parmentier M., Boeynaems J.M. Cloning, functional expression and tissue distribution of the human $P2Y_6$ receptor. Biochem Biophys Res Commun. 1996, 222(2):303-8.

Communi D., Govaerts C., Parmentier M., Boeynaems J. Cloning of a human purinergic P2Y receptor coupled to phospholipase C and adenylyl cyclase. J Biol Chem. 1997, 272:31969-73.

Communi D., Robaye B., Boeynaems J. Pharmacological characterization of the human $P2Y_{11}$ receptor. Br J Pharmacol. 1999, 128:1199-206.

Communi D., Suarez-Huerta N., Dussossoy D., Savi P., Boeynaems J.M. Cotranscription and intergenic splicing of human *P2Y$_{11}$* and *SSF1* genes. J Biol Chem. 2001, 276(19):16561-6.

Costanzi S., Joshi B.V., Maddileti S., Mamedova L., Gonzalez-Moa M.J., Marquez V.E., et al. Human $P2Y_6$ receptor: molecular modeling leads to the rational design of a novel agonist based on a unique conformational preference. J Med Chem. 2005, 48:8108–8111.

Corriden R., Insel P.A. Basal release of ATP: an autocrine-paracrine mechanism for cell regulation. Sci Signal. 2010, 3(104):re1.

Costanzi S., Mamedova L., Gao Z., Jacobson K.A. Architecture of P2Y nucleotide receptors: Structural comparison based on sequence analysis, mutagenesis, and homology modeling. J Med Chem. 2004, 47(22): 5393–5404.

Cox M.A., Gomes B., Palmer K., et al. The pyrimidinergic $P2Y_6$ receptor mediates a novel release of proinflammatory cytokines and chemokines in monocytic cells stimulated with UDP. Biochem Biophys Res Commun. 2005, 330:467–473.

Di Virgilio F., Boeynaems J.M., Robson S.C. Extracellular nucleotides as negative modulators of immunity. Curr Opin Pharmacol. 2009, 9(4):507-13.

Donnelly-Roberts D.L., Namovic M.T., Faltynek C.R., Jarvis M.F. Mitogen-activated protein kinase and caspase signaling pathways are required for $P2X_7$ receptor ($P2X_7R$)-induced pore formation in human THP-1 cells. J Pharmacol Exp Ther. 2004, 308:1053-1061.

Ecke D., Tulapurkar M.E., Nahum V., Fischer B., Reiser G. Opposite diastereoselective activation of $P2Y_1$ and $P2Y_{11}$ nucleotide receptors by adenosine 5'-O-(alpha-boranotriphosphate) analogues. Br J Pharmacol. 2006, 149(4):416-23.

Ecke D., Hanck T., Tulapurkar M.E., Schäfer R., Kassack M., Stricker R., Reiser G. Hetero-oligomerization of the $P2Y_{11}$ receptor with the $P2Y_1$ receptor controls the internalization and ligand selectivity of the $P2Y_{11}$ receptor. Biochem J. 2008a, 409:107-116.

Ecke D., Fischer B., Reiser G. Diastereoselectivity of the $P2Y_{11}$ nucleotide receptor: mutational analysis. Br J Pharmacol. 2008b, 155(8):1250-5.

Eliahu S., Martin-Gil A., Perez de Lara M.J., Pintor J., Camden J., Weisman G.A., et al. 2-MeS-β,γ-CCl$_2$-ATP is a potent agent for reducing intraocular pressure. J Med Chem. 2010, 53:3305–19.

Elliott M.R., Chekeni F.B., Trampont P.C., Lazarowski E.R., Kadl A., Walk S.F., et al. Nucleotides released by apoptotic cells act as a find-me signal to promote phagocytic clearance. Nature. 2009, 461(7261):282-6.

El-Tayeb A., Qi A., Müller C.E. Synthesis and structure-activity relationships of uracil nucleotide derivatives and analogues as agonists at human $P2Y_2$, $P2Y_4$, and $P2Y_6$ receptors. J Med Chem. 2006, 49(24):7076-87.

Feng C., Mery A.G., Beller E.M., Favot C., Boyce J.A. Adenine nucleotides inhibit cytokine generation by human mast cells through a G_s-coupled receptor. J Immunol. 2004, 173(12):7539-47.

Ferguson S.S. Evolving concepts in G protein-coupled receptor endocytosis: the role in receptor desensitization and signaling. Pharmacol Rev. 2001, 53(1):1-24.

Fredholm B.B., IJzerman A.P., Jacobson K.A., Klotz K.N., Linden J. International Union of Pharmacology. XXV. Nomenclature and classification of adenosine receptors. Pharmacol Rev. 2001, 53(4):527-52.

Fredholm B.B., IJzerman A.P., Jacobson K.A., Linden J., Müller C.E. International Union of Basic and Clinical Pharmacology. LXXXI. Nomenclature and classification of adenosine receptors-an update. Pharmacol Rev. 2011, 63(1):1-34.

Freedman J.E., Loscalzo J., Barnard M.R., Alpert C., Keaney J.F., Michelson A.D. Nitric oxide released from activated platelets inhibits platelet recruitment. J Clin Invest. 1997, 100(2):350-6.

Gatof D., Kilic G., Fitz J.G. Vesicular exocytosis contributes to volume-sensitive ATP release in biliary cells. Am J Physiol Gastrointest Liver Physiol. 2004, 286(4):G538-46.

Galandrin S., Oligny-Longpré G., Bouvier M. The evasive nature of drug efficacy: implications for drug discovery. Trends Pharmacol Sci. 2007, 28(8):423-30.

Gerasimovskaya E.V., Ahmad S., White C.W., Jones P.L., Carpenter T.C., Stenmark K.R. Extracellular ATP is an autocrine/paracrine regulator of hypoxia-induced adventitial fibroblast growth. Signaling through extracellular signal-regulated kinase-1/2 and the Egr-1 transcription factor. J Biol Chem. 2002, 277(47):44638-50.

Giniatullin R., Nistri A. Desensitization properties of P2X3 receptors shaping pain signaling. Front Cell Neurosci. 2013, 7:245.

Ginsburg-Shmuel T., Haas M., Schumann M., Reiser G., Kalid O., Stern N., Fischer B. 5-OMe-UDP is a potent and selective $P2Y_6$-receptor agonist. J Med Chem. 2010, 53(4):1673-85.

Ginsburg-Shmuel T., Haas M., Grbic D., Arguin G., Nadel Y., Gendron F.P., Reiser G., Fischer B. UDP made a highly promising stable, potent, and selective P2Y6-receptor agonist upon introduction of a boranophosphate moiety. Bioorg Med Chem. 2012, 20(18):5483-95.

Goding J.W., Grobben B., Slegers H. Physiological and pathophysiological functions of the ecto-nucleotide pyrophosphatase/phosphodiesterase family. Biochim Biophys Acta. 2003, 1638(1):1-19.

González-Alonso J., Olsen D.B., Saltin B. Erythrocyte and the regulation of human skeletal muscle blood flow and oxygen delivery: role of circulating ATP. Circ Res. 2002, 91(11):1046-55.

González-Alonso J. ATP as a mediator of erythrocyte-dependent regulation of skeletal muscle blood flow and oxygen delivery in humans. J Physiol. 2012, 590(Pt 20):5001-13.

Grbic D.M., Degagné É., Larrivée J.F., Bilodeau M.S., Vinette V., Arguin G., et al. $P2Y_6$ receptor contributes to neutrophil recruitment to inflamed intestinal mucosa by increasing CXC chemokine ligand 8 expression in an AP-1-dependent manner in epithelial cells. Inflamm Bowel Dis. 2012, 18(8):1456-69.

Guzmán-Aranguez A., Crooke A., Peral A., Hoyle C.H., Pintor J. Dinucleoside polyphosphates in the eye: from physiology to therapeutics. Prog Retin Eye Res. 2007, 26(6):674-87.

Haas M., Ben-Moshe I., Fischer B., Reiser G. Sp-2-propylthio-ATP-α-B and Sp-2-propylthio-ATP-α-B,β-γ-dichloromethylene are novel potent and specific agonists of the human P2Y$_{11}$ receptor. Biochem Pharmacol. 2013, 86(5):645-55.

Haas M., Shaaban A., Reiser G. Alanine-(87)-threonine polymorphism impairs signaling and internalization of the human P2Y$_{11}$ receptor, when co-expressed with the P2Y$_1$ receptor. J Neurochem. 2014, 129(4):602-13.

Hisadome K., Koyama T., Kimura C., Droogmans G., Ito Y., Oike M. Volume-regulated anion channels serve as an auto/paracrine nucleotide release pathway in aortic endothelial cells. J Gen Physiol. 2002, 119(6):511-20.

Hoffmann C., Moro S., Nicholas R.A., Harden T.K., Jacobson K.A. The role of amino acids in extracellular loops of the human P2Y$_1$ receptor in surface expression and activation processes. J Biol Chem. 1999, 274(21):14639-47.

Hoffmann C., Zürn A., Bünemann M., Lohse M.J. Conformational changes in G-protein-coupled receptors-the quest for functionally selective conformations is open. Br J Pharmacol. 2008a, 153 Suppl 1:S358-66.

Hoffmann C., Ziegler N., Reiner S., Krasel C., Lohse M.J. Agonist-selective, receptor-specific interaction of human P2Y receptors with β-arrestin-1 and -2. J Biol Chem. 2008b, 283(45):30933-41.

Hofmann F. The biology of cyclic GMP-dependent protein kinases. J Biol Chem. 2005, 280(1):1-4.

Huang Y.J., Maruyama Y., Dvoryanchikov G., Pereira E., Chaudhari N., Roper S.D. The role of pannexin 1 hemichannels in ATP release and cell-cell communication in mouse taste buds. Proc Natl Acad Sci U S A. 2007, 104(15):6436-41.

Humphries R.G., Robertson M.J., Leff P. A novel series of P2T purinoceptor antagonists: definition of the role of ADP in arterial thrombosis. Trends Pharmacol Sci. 1995, 16:179–81.

Idzko M., Ferrari D., Eltzschig H.K. Nucleotide signalling during inflammation. Nature. 2014,509(7500):310-7.

Ingall A.H., Dixon J., Bailey A., Coombs M.E., Cox D., McInally J.I., et al. Antagonists of the platelet P2T receptor: a novel approach to antithrombotic therapy. J Med Chem. 1999, 42:213–20.

Jacob F., Pérez Novo C., Bachert C., Van Crombruggen K. Purinergic signaling in inflammatory cells: P2 receptor expression, functional effects, and modulation of inflammatory responses. Purinergic Signal. 2013, 9(3):285-306.

Jacobson K.A., Ivanov A.A., Castro S., Harden T.K., Ko H. Development of selective agonists and antagonists of P2Y receptors Purinergic Signal. 2009, 5, 75-89.

Jacobson K.A., Jayasekara M.P., Costanzi S. Molecular Structure of P2Y Receptors: Mutagenesis, Modeling, and Chemical Probes. Wiley Interdiscip Rev Membr Transp Signal. 2012, 1(6).

Jankowski V., Tölle M., Vanholder R., Schönfelder G., van der Giet M., Henning L., et al. Uridine adenosine tetraphosphate: a novel endothelium- derived vasoconstrictive factor. Nat Med. 2005, 11(2):223-7.

Jiang Y., Borrelli L., Bacskai B. J., Kanaoka Y., Boyce J. A. P2Y6 receptors require an intact cysteinyl leukotriene synthetic and signaling system to induce survival and activation of mast cells. J. Immunol. 2009, 182:1129-1137.

Jin J., Dasari V.R., Sistare F.D., Kunapuli S.P. Distribution of P2Y receptor subtypes on haematopoietic cells. Br J Pharmacol. 1998, 123(5):789-94.

Joseph S.M., Buchakjian M.R., Dubyak G.R. Colocalization of ATP release sites and ecto-ATPase activity at the extracellular surface of human astrocytes. J Biol Chem. 2003, 278(26):23331-42.

Kalsi K.K., González-Alonso J. Temperature-dependent release of ATP from human erythrocytes: mechanism for the control of local tissue perfusion. Exp Physiol. 2012, 97(3):419-32.

Kang J., Kang N., Lovatt D., Torres A., Zhao Z., Lin J., Nedergaard M. Connexin 43 hemichannels are permeable to ATP. J Neurosci. 2008, 28(18):4702-11.

Kenakin T. Functional selectivity through protean and biased agonism: who steers the ship? Mol Pharmacol. 2007, 72(6):1393-401.

Khakh B.S., North R.A. P2X receptors as cell-surface ATP sensors in health and disease. Nature. 2006, 442(7102):527-32.

Khine A.A., Del Sorbo L., Vaschetto R., Voglis S., Tullis E., Slutsky A.S., et al. Human neutrophil peptides induce interleukin-8 production through the P2Y$_6$ signaling pathway. Blood. 2006, 107(7):2936-42.

Kim S.G., Soltysiak K.A., Gao Z.G., Chang T.S., Chung E., Jacobson K.A. Tumor necrosis factor alpha-induced apoptosis in astrocytes is prevented by the activation of P2Y$_6$, but not P2Y$_4$ nucleotide receptors. Biochem Pharmacol. 2003, 65(6):923-31.

Kim S.G., Gao Z., Soltysiak K.A., Chang T., Brodie C., Jacobson K.A. P2Y$_6$ Nucleotide Receptor Activates PKC to Protect 1321N1 Astrocytoma Cells Against Tumor Necrosis Factor-Induced Apoptosis. Cell Mol Neurobiol. 2003, 23(3):401-18.

King A.E., Ackley M.A., Cass C.E., Young J.D., Baldwin S.A. Nucleoside transporters: from scavengers to novel therapeutic targets. Trends Pharmacol Sci. 2006, 27(8):416-25.

Knight G.E., Bodin P., De Groat W.C., Burnstock G. ATP is released from guinea pig ureter epithelium on distension. Am J Physiol Renal Physiol. 2002, 282(2):F281-8.

Ko H., Carter R.L., Cosyn L., Petrelli R., de Castro S., Besada P., et al. Synthesis and potency of novel uracil nucleotides and derivatives as P2Y$_2$ and P2Y$_6$ receptor agonists. Bioorg Med Chem. 2008, 16(12):6319-32.

Koizumi S., Ohsawa K., Inoue K., Kohsaka S. Purinergic receptors in microglia: functional modal shifts of microglia mediated by P2 and P1 receptors. Glia. 2013, 61(1):47-54.

Korcok J., Raimundo L.N., Du X., Sims S.M., Dixon S.J. P2Y6 nucleotide receptors activate NF-kappaB and increase survival of osteoclasts. J Biol Chem. 2005, 280(17):16909-15.

Kornum B.R., Kawashima M., Faraco J., Lin L., Rico T.J., Hesselson S., et al. Common variants in P2RY11 are associated with narcolepsy. Nat Genet. 2011, 43(1):66-71.

Ku C.J., Karunarathne W., Kenyon S., Root P., Spence D. Fluorescence determination of nitric oxide production in stimulated and activated platelets. Anal Chem. 2007;79(6):2421-6.

Latek D., Modzelewska A., Trzaskowski B., Palczewski K., Filipek S. G protein-coupled receptors--recent advances. Acta Biochim Pol. 2012, 59(4):515-29.

Lazarowski E.R., Homolya L., Boucher R.C., Harden T.K. Identification of an ecto-nucleoside diphosphokinase and its contribution to interconversion of P2 receptor agonists. J Biol Chem. 1997a, 272(33):20402-7.

Lazarowski E.R., Homolya L., Boucher R.C., Harden T.K. Direct demonstration of mechanically induced release of cellular UTP and its implication for uridine nucleotide receptor activation. J Biol Chem. 1997, 272(39):24348-54.

Lazarowski E.R., Boucher R.C., Harden T.K. Constitutive release of ATP and evidence for major contribution of ecto-nucleotide pyrophosphatase and nucleoside diphosphokinase to extracellular nucleotide concentrations.
J Biol Chem. 2000, 275(40):31061-8.

Lefkowitz R.J., Shenoy S.K. Transduction of receptor signals by β-arrestins. Science. 2005, 308(5721):512-7.

Liu H.T., Toychiev A.H., Takahashi N., Sabirov R.Z., Okada Y. Maxi-anion channel as a candidate pathway for osmosensitive ATP release from mouse astrocytes in primary culture. Cell Res. 2008, 18(5):558-65.

Lüthje J., Ogilvie A. The Presence of Diadenosine 5',5'''-P^1,P^3-Triphosphate (Ap_3A) in Human Platelets. Biochem Biophys Res Commun. 1983, 115(1):253-260.

Lüthje J., Ogilvie A. Diadenosine triphosphate (Ap_3A) mediates human platelet aggregation by liberation of ADP. Biochem Biophys Res Commun. 1984, 118(3):704-9.

Major D.T., Fischer B. Molecular recognition in purinergic receptors. 1. A comprehensive computational study of the h-$P2Y_1$-receptor. J Med Chem. 2004a, 47(18):4391-404.

Major D.T., Nahum V., Wang Y., Reiser G., Fischer B. Molecular recognition in purinergic receptors. 2. Diastereoselectivity of the h-$P2Y_1$-receptor. J Med Chem. 2004b, 47(18):4405-16.

Malmsjö M., Hou M., Pendergast W., Erlinge D., Edvinsson L. Potent $P2Y_6$ receptor mediated contractions in human cerebral arteries. BMC Pharmacol. 2003, 3:4.

Mamedova L.K., Joshi B.V., Gao Z., von Kügelgen I., Jacobson K.A. Diisothiocyanate derivatives as potent, insurmountable antagonists of $P2Y_6$ nucleotide receptors. Biochem Pharmacol. 2004, 67(9):1763-70.

Mamedova L.K., Wang R., Besada P., Liang B.T., Jacobson K.A. Attenuation of apoptosis *in vitro* and ischemia/reperfusion injury *in vivo* in mouse skeletal muscle by $P2Y_6$ receptor activation. Pharmacol Res. 2008, 58(3-4):232-9.

Mantovani A., Cassatella M.A., Costantini C., Jaillon S. Neutrophils in the activation and regulation of innate and adaptive immunity. Nat Rev Immunol. 2011, 11(8):519-31.

Makarenkova H.P., Shestopalov V.I. The role of pannexin hemichannels in inflammation and regeneration. Front Physiol. 2014, 5:63.

Maruoka H., Barrett M.O., Ko H., Tosh D.K., Melman A., Burianek L.E., et al. Pyrimidine ribonucleotides with enhanced selectivity as $P2Y_6$ receptor agonists: novel 4-alkyloxyimino, (S)-methanocarba, and 5'-triphosphate γ-ester modifications. J Med Chem. 2010, 53(11):4488-501.

Marteau F., Le Poul E., Communi D., Labouret C., Savi P., Boeynaems J.M., et al. Pharmacological characterization of the human $P2Y_{13}$ receptor. Mol Pharmacol. 2003, 64:104–12.

Meis S., Hamacher A., Hongwiset D., Marzian C., Wiese M., Eckstein N., et al. NF546 [4,4'-(carbonylbis(imino-3,1-phenylene-carbonylimino-3,1-(4-methyl-phenylene)-carbonylimino))-bis(1,3-xylene-α,α'-diphosphonic acid) tetrasodium salt] is a non-nucleotide $P2Y_{11}$ agonist and stimulates release of interleukin-8 from human monocyte-derived dendritic cells. J Pharmacol Exp Ther. 2010, 332(1):238-47.

Moore D.J., Chambers J.K., Wahlin J.P., Tan K.B., Moore G.B., Jenkins O., et al. Expression pattern of human P2Y receptor subtypes: a quantitative reverse transcription-polymerase chain reaction study. Biochim Biophys Acta. 2001, 1521(1-3):107-19.

Moro S., Hoffmann C., Jacobson K.A. Role of the extracellular loops of G protein-coupled receptors in ligand recognition: a molecular modeling study of the human $P2Y_1$ receptor. Biochemistry. 1999, 38(12):3498-507.

Mundell S.J., Luo J., Benovic J.L., Conley P.B., Poole A.W. Distinct clathrin-coated pits sort different G protein-coupled receptor cargo. Traffic. 2006, 7(10):1420-31.

Murthy K.S., Makhlouf G.M. Coexpression of ligand-gated P2X and G protein-coupled P2Y receptors in smooth muscle. Preferential activation of P2Y receptors coupled to phospholipase C (PLC)-β1 via G$\alpha_{q/11}$ and to PLC-β3 via G$\beta\gamma_{i3}$. J Biol Chem. 1998, 273(8):4695-704.

Nahum V., Tulapurkar M., Levesque S.A., Sevigny J., Reiser G., Fischer B. Diadenosine and diuridine poly(borano)phosphate analogues: synthesis, chemical and enzymatic stability, and activity at P2Y$_1$ and P2Y$_2$ receptors. J Med Chem. 2006, 49:1980–90.

Nicholas R.A., Watt W.C., Lazarowski E.R., Li Q., Harden K. Uridine nucleotide selectivity of three phospholipase C-activating P2 receptors: identification of a UDP-selective, a UTP-selective, and an ATP- and UTP-specific receptor. Mol Pharmacol. 1996, 50(2):224-9.

Okada T., Palczewski K. Crystal structure of rhodopsin: implications for vision and beyond. Curr Opin Struct Biol. 2001, 11(4):420-6.

Osipchuk Y., Cahalan M. Cell-to-cell spread of calcium signals mediated by ATP receptors in mast cells. Nature. 1992, 359(6392):241-4.

Ostrom R.S., Gregorian C., Insel P.A. Cellular release of and response to ATP as key determinants of the set-point of signal transduction pathways. J Biol Chem. 2000, 275(16):11735-9.

Palczewski K., Kumasaka T., Hori T., Behnke C.A., Motoshima H., Fox B.A., et al. Crystal structure of rhodopsin: a G protein-coupled receptor. Am J Ophthalmol. 2000, 130(6):865.

Pelegrin P., Surprenant A. Pannexin-1 mediates large pore formation and interleukin-1β release by the ATP-gated P2X$_7$ receptor. EMBO J. 2006, 25(21):5071-82.

Pintor J., Rotllan P., Torres M., Miras-Portugal M.T. Characterization and quantification of diadenosine hexaphosphate in chromaffin cells: granular storage and secretagogue-induced release. Anal Biochem. 1992, 200(2):296-300.

Ralevic V., Burnstock G. Receptors for purines and pyrimidines. Pharmacol Rev. 1998, 50(3):413-92.

Relvas L.J., Bouffioux C., Marcet B., Communi D., Makhoul M., Horckmans M., et al. Extracellular nucleotides and interleukin-8 production by ARPE cells: potential role of danger signals in blood-retinal barrier activation. Invest Ophthalmol Vis Sci. 2009, 50(3):1241-6.

Robson S.C., Sévigny J., Zimmermann H. The E-NTPDase family of ectonucleotidases: Structure function relationships and pathophysiological significance. Purinergic Signal. 2006, 2(2):409-30.

Rodriguez del Castillo A., Torres M., Delicado E.G., Miras-Portugal M.T. Subcellular distribution studies of diadenosine polyphosphates—Ap$_4$A and Ap$_5$A—in bovine adrenal medulla: presence in chromaffin granules.
J Neurochem. 1988, 51(6):1696-703.

Sakaki H., Tsukimoto M., Harada H., Moriyama Y., Kojima S. Autocrine regulation of macrophage activation via exocytosis of ATP and activation of P2Y11 receptor. PLoS One. 2013, 8(4):e59778.

Sassone-Corsi P. The cyclic AMP pathway. Cold Spring Harb Perspect Biol. 2012, 4(12).

Sawada K., Echigo N., Juge N., Miyaji T., Otsuka M., Omote H., et al. Identification of a vesicular nucleotide transporter. Proc Natl Acad Sci U S A. 2008, 105(15):5683-6.

Schlüter H., Offers E., Brüggemann G., van der Giet M., Tepel M., Nordhoff E., et al. Diadenosine phosphates and the physiological control of blood pressure. Nature. 1994, 367(6459):186-8.

Schnurr M., Toy T., Stoitzner P., Cameron P., Shin A., Beecroft T., et al. ATP gradients inhibit the migratory capacity of specific human dendritic cell types: implications for P2Y$_{11}$ receptor signaling. Blood. 2003, 102(2):613-20.

Somers G.R., Hammet F.M.A., Trute L., Southey M.C., Venter D.J. Expression of the P2Y$_6$ purinergic receptor in human T cells infiltrating inflammatory bowel disease. Lab Invest. 1998, 78(11):1375-83.

Sprague R.S., Ellsworth M.L., Stephenson A.H., Lonigro A.J. ATP: the red blood cell link to NO and local control of the pulmonary circulation. Am J Physiol. 1996, 271(6 Pt 2):H2717-22.

Strange P.G. Agonist binding, agonist affinity and agonist efficacy at G protein-coupled receptors. Br J Pharmacol. 2008, 153(7):1353-63.

Suarez-Huerta N., Boeynaems J., Communi D. Cloning, genomic organization, and tissue distribution of human Ssf-1. Biochem Biophys Res Commun. 2000, 275(1):37-42.

Suadicani S.O., Brosnan C.F., Scemes E. P2X$_7$ receptors mediate ATP release and amplification of astrocytic intercellular Ca^{2+} signaling. J Neurosci. 2006, 26(5):1378-85.

Tabas I. Macrophage death and defective inflammation resolution in atherosclerosis. Nat Rev Immunol. 2010, 10(1):36-46.

Taylor A.L., Kudlow B.A., Marrs K.L., Gruenert D.C., Guggino W.B., Schwiebert E.M. Bioluminescence detection of ATP release mechanisms in epithelia. Am J Physiol. 1998, 275:C1391-406.

Tulapurkar M.E., Schäfer R., Hanck T., Flores R.V., Weisman G.A., González F.A., Reiser G. Endocytosis mechanism of P2Y$_2$ nucleotide receptor tagged with green fluorescent protein: clathrin and actin cytoskeleton dependence. Cell Mol Life Sci. 2005, 62(12):1388-99.

Tulapurkar M.E., Laubinger W., Nahum V., Fischer B., Reiser G. Subtype specific internalization of P2Y$_1$ and P2Y$_2$ receptors induced by novel adenosine 5'-O-(1-boranotriphosphate) derivatives. Br J Pharmacol. 2004, 142(5):869-78.

Tulapurkar M.E., Zündorf G., Reiser G. Internalization and desensitization of a green fluorescent protein-tagged P2Y nucleotide receptor are differently controlled by inhibition of calmodulin-dependent protein kinase II. J Neurochem. 2006, 96(3):624-34.

Trautmann A. Extracellular ATP in the immune system: more than just a "danger signal". Sci Signal. 2009, 2(56):pe6.

Ullmann H., Meis S., Hongwiset D., Marzian C., Wiese M., Nickel P., et al. Synthesis and structure-activity relationships of suramin-derived P2Y$_{11}$ receptor antagonists with nanomolar potency. J Med Chem. 2005, 48:7040-8.

Vaughan K.R., Stokes L., Prince L.R., Marriott H.M., Meis S., Kassack M.U., et al. Inhibition of neutrophil apoptosis by ATP is mediated by the P2Y$_{11}$ receptor. J Immunol. 2007, 179(12):8544-53.

Velasquez S., Eugenin E.A. Role of Pannexin-1 hemichannels and purinergic receptors in the pathogenesis of human diseases. Front Physiol. 2014, 5:96.

Vitiello L., Gorini S., Rosano G., la Sala A. Immunoregulation through extracellular nucleotides. Blood. 2012, 120(3):511-8.

Wang L., Ostberg O., Wihlborg A.K., Brogren H., Jern S., Erlinge D. Quantification of ADP and ATP receptor expression in human platelets. J Thromb Haemost. 2003, 1(2):330-6.

Warny M., Aboudola S., Robson S.C., Sévigny J., Communi D., Soltoff S.P., Kelly C.P. P2Y$_6$ nucleotide receptor mediates monocyte interleukin-8 production in response to UDP or lipopolysaccharide. J Biol Chem. 2001, 276(28):26051-6.

Wihlborg A.K., Balogh J., Wang L., Borna C., Dou Y., Joshi B.V., et al. Positive inotropic effects by uridine triphosphate (UTP) and uridine diphosphate (UDP) via P2Y$_2$ and P2Y$_6$ receptors on cardiomyocytes and release of UTP in man during myocardial infarction. Circ Res. 2006, 98(7):970-6.

Wilkin F., Duhant X., Bruyns C., Suarez-Huerta N., Boeynaems J.M., Robaye B. The $P2Y_{11}$ receptor mediates the ATP-induced maturation of human monocyte-derived dendritic cells. J Immunol. 2001, 166(12):7172-7.

Wilkin F., Stordeur P., Goldman M., Boeynaems J.M., Robaye B. Extracellular adenine nucleotides modulate cytokine production by human monocyte-derived dendritic cells: dual effect on IL-12 and stimulation of IL-10. Eur J Immunol. 2002, 32(9):2409-17.

Wolter S., Golombek M., Seifert R. Differential activation of cAMP- and cGMP-dependent protein kinases by cyclic purine and pyrimidine nucleotides. Biochem Biophys Res Commun. 2011, 415(4):563-6.

Wong A.M., Chow A.W., Au S.C., Wong C.C., Ko W.H. Apical versus basolateral $P2Y_6$ receptor-mediated Cl^- secretion in immortalized bronchial epithelia. Am J Respir Cell Mol Biol. 2009, 40(6):733-45.

Yerxa B.R., Sabater J.R., Davis C.W., Stutts M.J., Lang-Furr M., Picher M., et al. Pharmacology of INS37217 [P^1-(uridine 5')-P^4- (2'-deoxycytidine 5')tetraphosphate, tetrasodium salt], a next-generation $P2Y_2$ receptor agonist for the treatment of cystic fibrosis. J Pharmacol Exp Ther. 2002, 302(3):871-80.

Zhang J., Ferguson S.S., Barak L.S., Bodduluri S.R., Laporte S.A., Law P.Y., Caron M.G. Role for G protein-coupled receptor kinase in agonist-specific regulation of μ-opioid receptor responsiveness. Proc Natl Acad Sci U S A. 1998, 95(12):7157-62.

Zhang Z., Chen G., Zhou W., Song A., Xu T., Luo Q., et al. Regulated ATP release from astrocytes through lysosome exocytosis. Nat Cell Biol. 2007, 9(8):945-53.

Zimmermann H. 5'-Nucleotidase - molecular structure and functional aspects. Biochem J. 1992, 285 (Pt 2):345-65.

Zimmermann H. Extracellular metabolism of ATP and other nucleotides. Naunyn Schmiedebergs Arch Pharmacol. 2000, 362(4-5):299-309.

Zylberg J., Ecke D., Fischer B., Reiser G. Structure and ligand-binding site characteristics of the human $P2Y_{11}$ nucleotide receptor deduced from computational modelling and mutational analysis. Biochem J. 2007, 405:277-86.

9. List of publications

Studies on the human P2Y$_6$ receptor:

Ginsburg-Shmuel T., **Haas M.**, Schumann M., Reiser G., Kalid O., Stern N., Fischer B.
5-OMe-UDP is a potent and selective P2Y$_6$-receptor agonist. J Med Chem. 2010,
53(4):1673-85.

Ginsburg-Shmuel T.*, **Haas M.***, Grbic D., Arguin G., Nadel Y., Gendron F.P., Reiser G.*,
Fischer B.* UDP made a highly promising stable, potent, and selective P2Y6-receptor
agonist upon introduction of a boranophosphate moiety. Bioorg Med Chem. 2012,
20(18):5483-95.
*equal contribution, as given in the publication.

Haas M., Ginsburg-Shmuel T., Fischer B., Reiser G.
5-OMe-uridine-5'-O-(α-boranodiphosphate), a novel nucleotide derivative highly active at the
human P2Y$_6$ receptor protects against death-receptor mediated glial apoptosis. Neurosci
Lett. 2014, 578C:80-84. Data not included in this thesis.

Study on antagonists of phosphodiesterases (comparative analysis):

Eliahu S., Lecka J., Reiser G., **Haas M.**, Bigonnesse F., Lévesque S.A., Pelletier J., Sévigny
J., Fischer B. Diadenosine 5',5''-(boranated)polyphosphonate analogues as selective
nucleotide pyrophosphatase/phosphodiesterase inhibitors. J Med Chem. 2010, 53(24):8485-
97. Data not included in this thesis.

Studies on the human P2Y$_{11}$ receptor:

Haas M., Ben-Moshe I., Fischer B., Reiser G. S*p*-2-propylthio-ATP-α-B and S*p*-2-propylthio-
ATP-α-B,β-γ-dichloromethylene are novel potent and specific agonists of the human P2Y$_{11}$
receptor. Biochem Pharmacol. 2013, 86(5):645-55.

Haas M., Shaaban A., Reiser G. Alanine-(87)-threonine polymorphism impairs signaling and
internalization of the human P2Y$_{11}$ receptor, when co-expressed with the P2Y$_1$ receptor.
J Neurochem. 2014, 129(4):602-13.

10. Curriculum vitae

Persönliche Daten :

Name: Michael Haas

Wohnort: Gerhart-Hauptmann-Straße 1, 39108 Magdeburg

Geboren am: 13.12.1979 in Mittweida, Sachsen

Staatsangehörigkeit: Deutsch

Familienstand: verheiratet

Kinder: Benedikt Haas, geboren am 13.11.2011

Lebenslauf:

September 1992 bis Juli 1999	Besuch des Johannes-Kepler-Gymnasiums in Chemnitz und Abschluss mit dem Abitur.
Juli 1999 bis April 2000	Grundwehrdienst in Cham und Regensburg.
Oktober 2000 bis September 2002	Vier Semester Studium der Soziologie (Diplom) an der Technischen Universität Chemnitz.
Oktober 2002 bis Januar 2008	Studium der Biologie an der Justus-Liebig-Universität Gießen. Abschluss mit einem Diplom in Biologie.
Mai 2008 bis September 2014	Doktorand (Biologie) am Institut für Neurobiochemie der Medizinischen Fakultät der Otto-von-Guericke-Universität Magdeburg.
Ab Oktober 2014	Angestellter der Santis GmbH.

Magdeburg, 30. September 2014

Michael Haas

11. Selbstständigkeitserklärung

Michael Haas, Gerhart-Hauptmann-Strasse 1, 39108 Magdeburg

Hiermit erkläre ich, dass ich die von mir eingereichte Dissertation zum Thema

„Analysis of functional impairments of the human $P2Y_{11}$ nucleotide receptor with the Alanine-87-Threonine mutation, and development of novel agonists specific for the human $P2Y_{11}$ and $P2Y_6$ receptors"

selbstständig verfasst, nicht bereits als Dissertation verwendet und die benutzten Hilfsmittel und Quellen vollständig angegeben habe.

Weiterhin erkläre ich, dass ich weder diese noch eine andere Arbeit zur Erlangung des akademischen Grades doctor rerum naturalium (Dr. rer. nat.) an anderen Einrichtungen eingereicht habe.

Magdeburg, 30. September 2014

Michael Haas